To the Graduate Council:

I am submitting herewith a dissertation written by John Addison Benek, entitled "The Effects of Periodic Free Stream Disturbances on the Flat Plate Boundary Layer." I recommend that it be accepted in partial fulfillment of the requirements for the degree of Doctor of Philosophy, with a major in Aerospace Engineering.

James R. Maus

James R. Maus, Major Professor

We have read this dissertation
and recommend its acceptance:

Frank G. Collins

Ying-chu Lin Wu

Walter Frost

Kenneth R. Kunkle

Accepted for the Council:

Hilton A. Smith

Vice Chancellor
Graduate Studies and Research

E

# THE EFFECTS OF PERIODIC FREE STREAM DISTURBANCES ON THE FLAT PLATE BOUNDARY LAYER

A Dissertation

Presented for the

Doctor of Philosophy

Degree

The University of Tennessee

John Addison Benek

December 1975

1266915

ACKNOWLEDGEMENTS

I should like to take this opportunity to recognize the outstanding assistance provided me by Ms. J. W. Iannuzzi in the development of the computer program used to make the computations for this paper. Without her adroit technical advice the maturation of the computer program would have taken far longer and been much more difficult.

The contribution of Dr. M. D. High to the present work also requires recognition. He provided the necessary discussion and technical advice required to develop the analytical model. His high standard of technical excellence supplied the impetus required to carry this investigation to its final completion.

I would also like to acknowledge the assistance of Dr. E. F. Kurtz who kindly furnished me with results of his computations quoted in this work.

ABSTRACT

The growth of perturbations to the boundary layer induced by a periodic wave disturbance in the far field is examined. The equations of motion for the perturbation are reduced to a nonhomogeneous Orr-Sommerfeld equation which is solved in terms of the eigenfunctions of the homogeneous equation. Computations of the root mean square fluctuating velocity at constant fraction of the boundary layer thickness indicate higher amplitudes at lower Reynolds numbers than that expected without the presence of the free stream disturbance. It is suggested that the presence of the disturbance in the free stream may induce a transition to turbulence at a lower value of Reynolds number than the unforced case.

## PREFACE

The work reported herein was conducted by the Arnold Engineering Development (AEDC), Air Force Systems Command (AFSC), under Program Element 65807F. The results of the investigation were obtained by ARO, Inc. (a subsidiary of Sverdrup & Parcel and Associates, Inc.), contract operator of AEDC, AFSC, Arnold Air Force Station, Tennessee, under ARO Project Numbers P32A-31B and P32A-29B. The author of this report is John A. Benek, ARO, Inc. The investigation was completed on April 1, 1975, and the manuscript was submitted for publication on July 15, 1975.

TABLE OF CONTENTS


| SECTION | | PAGE |
|---|---|---|
| I. | INTRODUCTION | 1 |
| | Background | 1 |
| | Treatment of Free Stream Disturbances with Linear Stability Theory | 3 |
| II. | ANALYSIS | 6 |
| | Mathematical Model | 6 |
| | The Nonhomogeneous Problem | 9 |
| | The Eigenvalue Problem | 15 |
| | Elimination of the Overdeterminancy | 25 |
| | The Adjoint Problem | 32 |
| | Numerical Solution | 36 |
| | Auxiliary Functions | 41 |
| III. | RESULTS AND DISCUSSION | 43 |
| | Comparisons with Classical Stability Theory | 43 |
| | Computations of the Forced Problem | 48 |
| IV. | CONCLUSIONS AND RECOMMENDATIONS | 61 |
| | Conclusions | 61 |
| | Recommendations | 63 |
| BIBLIOGRAPHY | | 64 |
| APPENDICES | | 69 |
| A. | ILLUSTRATIONS | 70 |

SECTION PAGE

B. THE PARALLEL FLOW APPROXIMATION . . . . . 129

C. THE ORTHOGONALITY RELATION . . . . . 134

D. SPECIAL PROPERTIES OF CHEBYSHEV EXPANSION . . . . 138

E. THE ADJOINT OPERATOR . . . . . 144

F. SOME PROPERTIES OF THE GENERAL ALGEBRAIC EIGEN-
VALUE PROBLEM: $\det (A - \lambda B) = 0$ . . . . . 146

VITA . . . . . 153

LIST OF FIGURES


| FIGURE | | PAGE |
|---|---|---|
| 1. | Chebyshev Approximation of the Zeroth Order Blasius Profiles for the Parallel Flow Assumption | 71 |
| 2. | Improved Chebyshev Approximation of the Zeroth Order Profiles in the Reduced Interval | 73 |
| 3. | Neutral Curves for the Blasius Velocity Profile. | 75 |
| 4. | Amplification Factor, amp*, as a Function of Wave Number | 77 |
| 5. | Computations of the Streamfunction for the Sample Cases of Kurtz (Ref. 26) | 80 |
| 6. | Calculations of the Adjoint Conjugate Streamfunctions for the Three Sample Cases of Kurtz. | 83 |
| 7. | Comparison of Theory with rms Velocity Profiles of Schubauer and Skramstad (Ref. 1) | 86 |
| 8. | Comparison of Theory with rms Velocity Profiles of Ross, et al. (Ref. 29) | 87 |
| 9. | The Reynolds Stress Distribution Across the Boundary Layer for the Three Sample Cases of Kurtz | 90 |
| 10. | The Higher Eigenfunctions | 91 |
| 11. | The Higher Adjoint Streamfunction | 95 |

FIGURE PAGE

12. Variation of Root Mean Square Fluctuating Velocity with Increasing Streamwise Distance at Several Points in the Layer . . . . . 99

13. Comparison of Forced and Unforced Growth Rates . 101

14. Reynolds Stress as a Function of Streamline Distance . . . . . 103

15. Development of the rms Velocity Profiles at $\omega^*/R_\delta^* = 62 \times 10^{-6}$ with $R_\delta^*$ . . . . . 105

16. Development of the Reynolds Stress Profiles at $\omega^*/R_\delta^* = 62 \times 10^{-6}$ with $R_\delta^*$ . . . . . 111

17. Composite Velocity Profiles for $\omega^*/R_\delta^* = 62 \times 10^{-6}$ and $\varepsilon = .01$ . . . . . 117

18. Composite Velocity Profiles for $\omega^*/R_\delta^* = 83.5 \times 10^{-6}$ and $\varepsilon = .01$ . . . . . 120

19. Composite Velocity Profiles for $\omega^*/R_\delta^* = 62 \times 10^{-6}$ and $\varepsilon = .001$ . . . . . 123

20. Composite Velocity Profiles for $\omega^*/R_\delta^* = 83.5 \times 10^{-6}$ and $\varepsilon = .001$ . . . . . 126

## NOMENCLATURE

| | |
|---|---|
| $D$ | Differential operator, $d/dy$ |
| $d$ | Characteristic length, taken as $y_\infty$ |
| $F$ | Function satisfying the nonhomogeneous boundary conditions of Eqns. (5b) |
| $i$ | $\sqrt{-1}$ |
| $L$ | General Orr-Sommerfeld operator (see Eqns. (8)) |
| $\hat{L}$ | General adjoint Orr-Sommerfeld operator (see Eqn. (D-1)) |
| $\ell_j$ | $(j = 1,---,4)$ functions arising from the derivatives of $T_n^*$. They are defined in Eqn. (C-4) |
| $M$ | Order of the largest Chebyshev polynomial in the approximation of the velocity and vorticity components appearing in the Operators $L$ and $\hat{L}$ |
| $N$ | Order of the largest Chebyshev polynomial in the approximation of $\phi, \chi$ |
| $p$ | Static pressure |
| $R$ | Reynolds number, $u_\infty d/\nu$ |
| $T_n^*$ | $n^{th}$ shifted Chebyshev polynomial of the first kind |
| $t$ | Temporal variable |
| $U_\infty$ | Free-stream (far field) mean velocity |
| $u$ | Velocity component parallel to x axis (see Figure 1) |
| $u_{rms}$ | Root-mean-square of the fluctuating velocity |

| | |
|---|---|
| $\vec{V}$ | Velocity vector |
| v | Velocity component parallel to y axis (see Figure 1) |
| x | Spatial coordinate, for the cases of Blasius flow x is parallel to the wall (see Figure 1) |
| y | Spatial coordinate, for the case of Blasius flow y is perpendicular to the wall (see Figure 1) |
| $y_\infty$ | Value of y defining the interval over which the Chebyshev approximation is to be made |
| z | Vorticity, $\partial u/\partial y - \partial v/\partial x$ |
| $\alpha$ | Dimensionless wave number (see Eqn. (18)) |
| $\delta$ | Boundary layer thickness |
| $\delta^*$ | Displacement thickness |
| $\varepsilon$ | Small parameter indicating the magnitude of the free-stream velocity perturbation |
| $\lambda$ | Eigenvalue of the Orr-Sommerfeld operator $L$ |
| $\mu$ | Eigenvalue of $\hat{L}^*$ |
| $\sigma$ | Number of periods over which rms values are computed |
| $\tau_m$ | Lanczos' Taus (see discussion Section II) |
| $\phi$ | Function containing the y dependence of the perturbation stream function $\psi$ |
| $\chi$ | Function adjoint to $\tilde{\phi}$ |
| $\psi$ | Stream function |

$\psi^H$ Homogeneous part of the perturbation stream function, $\psi$

$\omega$ Dimensionless frequency of the free-stream modulation

$\nabla$ Two-dimensional del operator

$\nabla^2$ Laplacian operator

$\nabla^4$ Biharmonic operator

SUPERSCRIPTS (except as noted)

$\hat{}$ The adjoint

$\sim$ Eigenfunction

$*$ Conjugate

MATHEMATICAL OPERATIONS

$\langle f,g \rangle \equiv \int f^*(\Gamma)\, g(\Gamma)\, d\Gamma$, the inner product

$||f|| \equiv \langle f,f \rangle^{1/2}$, the norm

SUBSCRIPTS

r Real part

i Imaginary part

x,y,t Differentiation with respect to indicated variable

# I. INTRODUCTION

## Background

The effect of free-stream disturbances on the location of the onset of transition of the laminar boundary layer to turbulent flow is well established in the literature. The best known experiments demonstrating this effect are those conducted by Schubauer and Skramstad (1)[1]. They demonstrated that the transition Reynolds number, $R_T$, on a flat plate decreased when the ratio of the root mean square of the fluctuating velocity to the mean free-stream velocity, $u'/u_\infty$, increased beyond 0.08%. For $u'/u_\infty < 0.08\%$ they found $R_T \sim 2.86 \times 10^6$. The magnitude of $u'/u_\infty$ was varied by changing the screen arrangement in the wind tunnel stilling chamber. At the lowest value of $u'/u_\infty \sim 0.05\%$, the velocity fluctuations were found to be of the magnitude expected for the acoustic level of 100 db (Ref. = .00022 dyn/cm$^2$) which was measured at this condition.

The measurements of Reference (1) and the inference that the acoustic disturbances could be influencing the measurements of transition location stimulated several subsequent studies at lower noise levels. The most notable

---

[1]Numbers in parentheses refer to similarly numbered references in the bibliography.

of these studies are those by De Mitz and Casarella (2); Wells (3); and Spangler and Wells (4). De Mitz and Casarella recently obtained $R_T \sim 2.86 \times 10^6$ on a flat plate with $u'/u_\infty < 0.08\%$ and an acoustic level of 90 db. Wells (3) and Spangler and Wells (4) conducted a series of experiments in a boundary layer channel and found $R_T > 5 \times 10^6$ with $u'/u_\infty < 0.08\%$ and an acoustic level of 85 db. In addition, they established that the frequency of an acoustic disturbance, as well as its magnitude, has a great affect on the $R_T$ variation with $u'/u_\infty$. The results of these experiments indicate that something is indeed influencing the data.

There have been several efforts to develop empirical correlations between free-stream disturbances and their effect on boundary layer development as characterized by transition location. The most widely accepted is the correlation of Pate and Schueler (5) and Pate (6) which relates the end of transition on cones and hollow cylinders in supersonic flow to acoustic radiation from wind tunnel wall turbulent boundary layer. While this correlation remains implicit, an explicit relation is given by Benek and High (7) where free-stream disturbances are related through Liepmann's hypothesis (i.e., a critical ratio of inertial to viscous stresses) to $R_T$. However, the relation of Reference (7) has only been verified for cones and Mach numbers below 1.2.

While no general theory has been established to compute the transition process, a great deal of insight has been obtained from the classical stability theory. The stability theory studies the growth of small disturbances in the boundary layer with the implication that once these disturbances obtain a sufficient magnitude they initiate the transition process. It would be most instructive, therefore, to examine the body of literature dealing with stability theory to determine its applicability in the case where free-stream disturbances are present.

## Treatment of Free Stream Disturbances with Linear Stability Theory

There has been some effort to apply the linear stability theory to the case of flows with disturbances in the free stream. Werle, et al. (8) consider a flow with secondary vorticity. They employ what is essentially a double perturbation scheme. The secondary vorticity, $0(1/\sqrt{R})$, is included through the van Dyke second order boundary layer theory and then the stability of the modified flow is examined. If $\varepsilon$ represents the magnitude of the stability perturbation, the solutions, which correspond to $0(\varepsilon) + 0(\varepsilon/\sqrt{R})$ only, show that for the Falkner-Skan family of velocity profiles the stability may either be increased or decreased depending upon the orientation of the assumed two-dimensional vorticity. The drawback to the analysis is

that the vorticity parameter employed bears little resemblance to the usual experimental quantity $u'/u_\infty$. Therefore, it is difficult to verify the predicted shifts in stability with existing experimental data.

Another approach to the case of disturbances in the free stream has been taken by Criminale (9,10). He develops a nonhomogeneous Orr-Sommerfeld equation. However, the forcing term is not rigorously derived but is added to the usual Orr-Sommerfeld equation and is taken to be zero in the boundary layer and nonzero far away from the body. Such a development allows the usual homogeneous boundary conditions to be applied at the wall and infinitely far from it. A matching procedure is then required to join Green's function solutions obtained in the boundary layer and free streams. These solutions are difficult to interpret because of the lack of rigor with which the forcing term is introduced and will not be considered here.

Mack (11) investigates the case of radiation from supersonic, turbulent, wind tunnel wall, boundary layers. His solutions employ right running wave solutions as the forcing term. This solution corresponds to an incoming acoustic disturbance when the phase speed has the appropriate relation to the free-stream Mach number. Although Mack does not explicitly state the formalism required to obtain the form of the solutions presented in Reference (11), it can

easily be shown to be a special case of that employed in the next section. The computational results for a flat plate show that for acoustically irradiated flow all frequencies are amplified in a region near the leading edge. This finding is supported by experiments conducted by Kendall (12), although only qualitatively. In light of the success experienced by Mack (11), it would appear that a properly formulated forced stability analysis is adequate to describe the essential features of the response of a laminar flow to free-stream disturbances.

## II. ANALYSIS

### Mathematical Model

Consider the two-dimensional flow of an incompressible, Newtonian fluid over a body submersed in it. Such a fluid model is governed by the Navier-Stokes equations:

$$\text{Continuity:} \quad \vec{\nabla} \cdot \vec{V} = 0$$

$$\text{Momentum:} \quad \frac{\partial}{\partial t} \vec{V} + \vec{V} \cdot \vec{\nabla}\vec{V} = - \vec{\nabla} p + R^{-1} \nabla^2 \vec{V} \qquad (1)$$

Equations (1) have been nondimensionalized as follows: the velocity with the free-stream speed, $U_\infty$; the spatial coordinates with the characteristic length, d; the temporal coordinate with the characteristic time, $\tau = U_\infty/d$; and the pressure with the characteristic pressure, $\rho U_\infty^2$. The nondimensional quantity $U_\infty d/\nu = R$, is the characteristic Reynolds number. The specification of the physical and nondimensional variables will be left to a later section.

Equations (1) may be reduced to a single scalar equation in one variable by introduction of the stream function, $\psi$. The stream function, $\psi$, is defined by

$$u(x,y,t) = \partial/\partial y \; \psi(x,y,t), \quad -v(x,y,t) = \partial/\partial x \; \psi(x,y,t)$$

and will identically satisfy the continuity equation. Substitution of $\psi$ into Eqn. (1) and elimination of the pressure gradient terms by cross differentiation yields, after some rearrangement

$$\left( \frac{\partial}{\partial t} + \psi_y(x,y,t) \frac{\partial}{\partial x} - \psi_x(x,y,t) \frac{\partial}{\partial y} - R^{-1}\nabla^2 \right) \nabla^2 \psi(x,y,t) = 0 \qquad (2)$$

Consider the free-stream velocity fluctuation as being small compared to the mean flow. If, in addition, the disturbance can be described as a plane wave moving in the flow direction, then away from the body the stream function, $\psi$, has the form

$$\psi(x,y,t) = y \left( 1 + \varepsilon\, e^{i(\alpha x - \omega t)} \right), \quad \varepsilon << 1$$

Because $\varepsilon$ is taken to be much less than one, solutions to Eqn. (2) can be sought in the form

$$\psi(x,y,t) = \sum_k \varepsilon^k \overset{(k)}{\psi}(x,y,t) e^{ik(\alpha x - \omega t)}$$

and in particular

$$\psi(x,y,t) = \overset{(0)}{\psi}(x,y) + \varepsilon \overset{(1)}{\psi}(x,y) e^{i(\alpha x - \omega t)} + O(\varepsilon^2) \qquad (3)$$

Substitution of $\psi$ into Eqn. (2) and separation of the coefficients of $\varepsilon^k$ gives for $\varepsilon^\circ$

$$\left( \psi_y^{(0)} \frac{\partial}{\partial x} - \psi_x^{(0)} \frac{\partial}{\partial y} - R^{-1} \nabla^2 \right) \nabla^2 \psi^{(0)} = 0 \qquad (4)$$

subject to the boundary conditions

$$\psi_x^{(0)}(x,0) = \psi_y^{(0)}(x,0) = 0 \quad \text{(no slip)}$$

$$\psi_x(x,\infty) \to 0, \quad \psi_y^{(0)}(x,\infty) \to 1$$

and for $\epsilon^1$

$$\left[\left(\psi_y^{(0)} \frac{\partial}{\partial x} - \psi_x^{(0)} \frac{\partial}{\partial y} - R^{-1} \nabla^2 - i\omega\right)\nabla^2 + \frac{\partial}{\partial x}\left(\nabla^2 \psi^{(0)}\right)\frac{\partial}{\partial y} - \frac{\partial}{\partial y}\left(\nabla^2 \psi^{(0)}\right)\frac{\partial}{\partial x}\right] \cdot \left(\psi^{(1)} e^{i\alpha x}\right) e^{-i\omega t} = 0 \tag{5}$$

Note that the time dependence separates out of Eqn. (5) as the variable coefficients do not depend on t. The boundary conditions for the separated equation are

$$\left(\psi^{(1)}(x,0) e^{i\alpha x}\right)_x = \psi_y^{(1)}(x,0) = 0$$

$$\left(\psi^{(1)}(x,\infty) e^{i\alpha x}\right)_x \sim \text{periodic in } x \quad \psi_y^{(1)}(x,\infty) \to 1$$

and as $x \to \pm \infty$ $\psi \to$ periodic. The periodicity condition on the x derivative as $y \to \infty$ is assured by the form taken for the solution, and thus, this boundary condition is effectively removed. The necessity of such a condition will be made apparent in the next section.

Equation (4) represents the mean flow over a flat

plate and Eqn. (5) represents the perturbation flow. Consider, for example, the case of flow over a semi-infinite flat plate; the high Reynolds number approximation to Eqns. (4) for this case is the well known Blasius function. In the subsequent treatment $\psi^{(0)}$ and its derivatives shall be assumed to be specified from the appropriate derivatives of the Blasius function.

The Nonhomogeneous Problem

Examination of Eqns. (5) reveals a homogeneous equation with nonhomogeneous boundary conditions. It is through these nonhomogeneous boundary conditions that the free-stream disturbance enters the formulation. It is not convenient to solve such a system and, therefore, a transformation of the form

$$\psi^{(1)} e^{i\alpha x} = \psi^{(H)} e^{i\alpha x} + F\, e^{i\alpha x} \tag{6}$$

is proposed where $\psi^{(H)} e^{i\alpha x}$ satisfies homogeneous boundary conditions and $F\, e^{i\alpha x}$ satisfies the nonhomogeneous conditions. Substitution of Eqn. (6) into Eqn. (5) yields a more convenient boundary value problem, namely

$$\left[\left(\psi_y^{(0)}\frac{\partial}{\partial x} - \psi_x^{(0)}\frac{\partial}{\partial y} - R^{-1}\nabla^2 - i\omega\right)\nabla^2 + \frac{\partial}{\partial x}\left(\nabla^2\psi^{(0)}\right)\frac{\partial}{\partial y} - \frac{\partial}{\partial y}\left(\nabla^2\psi^{(0)}\right)\frac{\partial}{\partial x}\right]\left(\psi^{(H)}e^{i\alpha x}\right)$$

$$= -\left[\left(\psi_y^{(0)}\frac{\partial}{\partial x} - \psi_x^{(0)}\frac{\partial}{\partial y} - R^{-1}\nabla^2 - i\omega\right)\nabla^2 + \frac{\partial}{\partial x}\left(\nabla^2\psi^{(0)}\right)\frac{\partial}{\partial y} - \frac{\partial}{\partial y}\left(\nabla^2\psi^{(0)}\right)\frac{\partial}{\partial x}\right]\left(F\,e^{i\alpha x}\right) \qquad (7)$$

and

$$\left(\psi^{(H)}e^{i\alpha x}\right)_x = \psi_y^{(H)}e^{i\alpha x} = 0 \text{ at } y = 0 \text{ and as } y \to \infty$$

and

$$\left(F(x,0)e^{i\alpha x}\right)_x = 0,\ F_y(x,0) = 0,\ F_y(x,\infty) \to 1$$

Equation (7) in $\psi^{(H)}$ is nonhomogeneous with homogeneous boundary conditions and F is arbitrary as long as it satisfies the boundary conditions of Eqns. (7). Boundary value problems of the form of Eqn. (7) may be solved by expansion of the dependent variable (i.e., $\psi^{(H)}e^{i\alpha x}$) in terms of the eigenfunctions, $\tilde{\psi}_j e^{i\alpha x}$, of the operator, which in this case is

$$L(x,y) = \left[\left(\psi_y^{(0)} \frac{\partial}{\partial x} - \psi_x^{(0)} \frac{\partial}{\partial y} - R^{-1}\right)\nabla^2\right] + \frac{\partial}{\partial x}\left(\nabla^2 \psi^{(0)}\right)\frac{\partial}{\partial y} - \frac{\partial}{\partial y}\left(\nabla^2 \psi^{(0)}\right)\frac{\partial}{\partial x} - i\lambda\nabla^2 \qquad (8)$$

or more briefly

$$L(x,y) = L(x,y) - i\lambda\nabla^2.$$

The notation $L(x,y)$ and $L(x,y)$ is used to indicate that the operators $L$ and L involve terms which depend upon x and y. The operator of Eqn. (8) is reducible to the classical Orr-Sommerfeld operator by application of the parallel flow approximations, i.e. $\frac{\partial}{\partial x}\psi^{(0)} = 0$, $\psi^{(0)} = \psi^{(0)}(y)$

$$\left[\left(\psi_y^{(0)} \frac{\partial}{\partial x} - R^{-1}\right)\nabla^2 - \psi_{yyy}^{(0)} \frac{\partial}{\partial x}\right] - i\lambda\nabla^2 . \qquad (8a)$$

The operator defined by Eqn. (8) involves partial derivatives to the fourth order and has variable coefficients. Solution of Eqn. (7) with this general operator can be expected to be extremely incommodious. Therefore, simplifications are necessary to reduce the effort required to obtain solutions. As a stability type formulation is sought, consider that the variable coefficients involved in Eqn. (8) are calculated locally, say at $x = x_o$. In this case $L(x,y)$ becomes separable and solutions of the form $\psi^{(H)}(x,y)e^{i\alpha x} = \phi^{(H)}(y)e^{i\alpha x}$ become admissible if F is also chosen to be separable. Denote the local approximation by

$$L(\alpha,y) = L(\alpha,y) - i\lambda \nabla^2$$

$$= \left[\left(u^{(0)} i\alpha + v^{(0)} \frac{\partial}{\partial y}\right) - R^{-1} (D^2-\alpha^2)\right] (D^2-\alpha^2)$$

$$+ z_x^{(0)} D - i\alpha z_y^{(0)} - i\lambda (D^2-\alpha^2) \qquad (8b)$$

where $u^{(0)}$, $v^{(0)}$, $z^{(0)}$ are $\psi_y^{(0)}$, $-\psi_x^{(0)}$, $\nabla^2\psi^{(0)}$, respectively, evaluated at $x = x_o$, and where $D = d/dy$. Equation (7) is now

$$L(\alpha,y)\ \phi^{(H)}(y) = -\ L(\alpha,y)\ F(y) \qquad (7a)$$

and $\phi^{(H)}(y)$ can be expanded in terms of the eigenfunctions of $L(\alpha,y)$. If the eigenvalue spectrum of $L(\alpha,y)$ is assumed to be discrete and the corresponding eigenfunctions are assumed to form a complete set, then $\phi^{(H)}(y)$ has the representation

$$\phi^{(H)} = \sum_j C_j \tilde{\phi}_j \qquad (9)$$

where $\tilde{\phi}_j$ are solutions of $L(\alpha,y)\ \tilde{\phi}_j = 0$ corresponding to $\lambda_j$.

The extent to which the "local" and parallel flow assumptions effect the validity of the solution is currently the subject of a great deal of investigation. A brief summary of this aspect of the theory is given in Appendix B. For the present purpose, it is assumed that the form of the operator given by Eqn. (8b) is adequate.

Once a suitable form for F(y) has been found, solutions to Eqn. (7a) are obtained by substituting Eqn. (9) into Eqn. (7a) to obtain

$$\sum_j C_j \left[ L(\alpha,y) - i\omega \, (D^2-\alpha^2) \right] \tilde{\phi}_j = - L(\alpha,y)F$$

From Appendix C, Eqn. (C-3a) it can be seen that

$$L(\alpha,y) \, \tilde{\phi}_j = i \, \lambda_j \, (D^2-\alpha^2) \, \tilde{\phi}_j$$

Hence,

$$\sum_j i \, C_j \, (\lambda_j-\omega) \, (D^2-\alpha^2) \, \tilde{\phi}_j = - L(\alpha,y)F \tag{10}$$

Because $L(\alpha,y)$ is a nonhermitian operator, the sequence $\{\tilde{\phi}_j\}$ are not mutually orthogonal. It is shown in Appendix C that the sequences $\{\tilde{\phi}_j\}$ and $\{\tilde{\chi}_j\}$ form a binormal system, where $\tilde{\chi}_j$ is the adjoint stream function. Therefore, form the inner product of $\tilde{\chi}_k$ with Eqn. (10)

$$\sum_j i \, C_j (\lambda_j-\omega) \langle \tilde{\chi}_k, (D^2-\alpha^2) \tilde{\phi}_j \rangle$$

$$= \langle \tilde{\chi}_k, - L(\alpha,y)F \rangle \tag{11}$$

and finally by using Eqn. (C-6), Eqn. (11) reduces to

$$C_j = \frac{-i \langle \tilde{\chi}_j - L(\alpha,y)F \rangle}{(\lambda_j-\omega) \langle \tilde{\chi}_j, \nabla^2 \tilde{\phi}_j \rangle} \tag{12}$$

This leaves the specification of F to complete the formulation. Inspection of the conditions on F given by

Eqn. (7) shows a suitable choice which insures separation of Eqn. (7) is

$$F(y) = \ell n \left[ \cosh (y) \right] \tag{13}$$

The complete solution for the perturbation stream function $\psi^{(1)}$ (Eqn. (5)), is given at $x_o$ by

$$\psi^{(1)} \sum_j C_j \tilde{\phi}_j e^{i(\alpha x)} + F e^{i(\alpha x)} \tag{14}$$

with the $\tilde{\phi}_j$ defined by $L(\alpha,y)\ \tilde{\phi}_j = 0$, the $C_j$ by Eqn. (11) and F by Eqn. (13).

Examination of Eqn. (14) indicates that as $y \to \infty$

$$\psi^{(1)} \to F(\infty) \exp \left[ i(\alpha x - \omega t) \right]$$

and Eqn. (13) shows that $F(\infty)$ is unbounded. It is necessary, therefore, to insure that this asymptotic variation of $\psi^{(1)}$ satisfies the "local" form of Eqn. (5). Thus, examine

$$\lim_{y \to \infty} L(\alpha,y)\ \psi^{(1)} = (i\alpha - i\omega)\ (-\alpha^2 F(\infty)) = 0$$

where the exact conditions $v^{(0)}(\infty) \to 0$, $z^{(0)}(\infty) \to 0$, are assumed to apply. In addition, the viscous terms $R^{-1} \nabla^4 \psi^{(1)} \to 0$ and $u^{(0)}(\infty) \to 1$ have also been assumed to hold. Since $F(\infty)$ is unbounded, it is necessary that

$$i(\alpha-\omega) = i\ \alpha(1 - \omega/\alpha) = 0 \tag{15}$$

Now, the ratio $\omega/\alpha$ is $C_{ph}$, the phase velocity of the wave. Thus, the present formulation requires that the phase

velocity of the free-stream wave be equal to the free-stream velocity for solutions.

The restriction on the free-stream wave imposed by Eqn. (15) precludes several types of disturbances from this analysis. Most notable among those excluded types are acoustic disturbances. However, it is not difficult to imagine velocity disturbances convecting in the free stream at the free-stream velocity. Therefore, the formulation presented here has not limited itself to a nonrealizable class of flows.

The Eigenvalue Problem

In order to perform the expansion indicated by Eqn. (9) it is necessary to obtain solutions to $L(\alpha,y)\tilde{\phi} = 0$, i.e.

$$\left\{\left[i\alpha u^{(0)} + v^{(0)} D - R^{-1} (D^2-\alpha^2)\right](D^2-\alpha^2) + z_x^{(0)} D - i\alpha z_y^{(0)} - i\lambda (D^2-\alpha^2)\right\}\tilde{\phi} = 0$$

subject to

$$\tilde{\phi}(0) = \tilde{\phi}_y(0) = 0 \quad \tilde{\phi}(\infty) = \tilde{\phi}_y(\infty) = 0 \qquad (16)$$

Although Eqn. (16) is an ordinary differential equation, it is not possible to obtain an exact analytical solution and, as a result, there has been a considerable amount of work done on the asymptotic theory (see e.g. Lin (13) or Mack (14)). Mack recommends in (14) that a direct numerical treatment be made of Eqn. (16) to effect accurate solutions.

Rather than employ finite differences on Eqn. (16), it is possible to facilitate the computations by expanding $\tilde{\phi}$ as

$$\tilde{\phi} = \sum_{n} a_n f_n (y)$$

where the $\{f_n\}$ are an orthogonal set in the interval of definition. The choice of $f_n$ may be made from two basic groups of functions: (1) those bearing a close resemblance to solutions of the Orr-Sommerfeld equation and (2) those providing outstanding accuracy in the domain of the independent variable. An example of this first group is given by Grosh and Salwen (15) who employ generalized Chandrasekhar-Reid functions to the case of plane poiseuille flow.

The recent work of Orszag (16,17) falls in the domain of the second group. He recommends use of Chebyshev polynomials as expansion functions because they provide infinite order accuracy for infinitely differentiable functions such as $\tilde{\phi}$ which satisfy a linear ordinary differential operator with polynomial coefficients. (Such a case for the Orr-Sommerfeld operator is plane Poiseuille flow where $\psi^{(0)} = y - 1/3\ y^3$.) Infinite order means that the truncation error decreases faster than any power of (1/N), where N is the number of terms in the expansion. This compares with $0(|\Delta x|^{+n})$ for finite difference methods where $\Delta x$

is the mesh size and n is some positive number. The generalized Chaudrasekhar-Reid functions used in (10) give a truncation error of $0(N^{-5})$. In Reference (16) Orszag considers plane Poiseuille flow and with a 25-term expansion and obtains accuracies of 1 part in $10^8$ for the eigenvalues. In general, it is not possible to infer the same high accuracy with operators having nonpolynomial coefficients. However, the Chebyshev approximation to $\tilde{\phi}$ will be utilized here on the assumption that they will provide greater accuracy than the finite difference methods.

Application of the Chebyshev polynomials which are defined in the interval $[0,1]$ to an infinite interval requires some deliberation. While the transform of $(0,\infty)$ to $[0,1]$ is not possible with a linear transform, any finite interval may be so transformed. Noting that if a finite difference approach were used, the infinite interval could only be approximated over a finite sub-interval; it is, therefore, reasonable to consider the same sub-interval but use the expansion procedure instead of the differences.

Approximation on a subinterval, say $y \in [0,y_\infty]$, requires some modifications to the formulation, namely: (1) transform of $(0,y_\infty)$ to $[0,1]$, (2) identification of the characteristic length with $y_\infty$ for the flat plate case, and (3) redefinition of the boundary conditions. The first two conditions are easily met but the reformulation of the outer

boundary conditions requires a more detailed treatment. Discussion of this point will be delayed to later in this section.

The function $\tilde{\phi}(y)$ may be expressed in terms of the Chebyshev polynomials as

$$\tilde{\phi}(y) \quad \sum_{n=0}^{N} a_n T_n^*(y) \tag{17a}$$

where the $T_n^*$ are the shifted Chebyshev polynomials of the first kind which are defined on $\left[0,1\right]$. The finite summation indicated in Eqn. (17a) is in anticipation of a later requirement. As the $T_n^*$ do not have a closed representation for their derivatives, it is necessary to expand each derivative in its own series (see Fox (18) and Parker (19)), i.e.

$$\frac{\partial^m}{\partial y^m} \quad \sum_{n=0}^{N-m} a_n^{(m)} T_n^*, \; m = 1,2,\text{----} \tag{17b}$$

It is then possible to eliminate the $a_n^{(m)}$ in terms of the $a_n$. These relations are developed in Appendix D. Because the coefficients in $L(\alpha,y)$ depend upon y it is also necessary to have the expansions

$$u^{(0)}(y) = \sum_{m=0}^{M} u_m T_m^*, \qquad z_x^{(0)} = \sum_{m=0}^{M} z_{x_m} T_m^*$$

$$v^{(0)}(y) = \sum_{m=0}^{M} v_m T_n^*, \qquad z_y^{(0)} = \sum_{m=0}^{M} z_{y_m} T_m^* \tag{18}$$

where in general $M \neq N$ and where the coefficients have the general form, e.g.

$$b_m = \langle b(y), T_m^* \sqrt{y-y^2} \rangle \Big/ ||T_m^*||^2$$

These coefficients are readily evaluated since the b(y) are known functions.

Substitution of Eqns. (17) and (18) into Eqn. (16) yields

$$i\alpha \sum_{m=0}^{M} u_m T_m^* \sum_{n=0}^{N-2} a_n^{(2)} T_n^* - i\alpha^3 \sum_{m=0}^{M} u_m T_m^* \sum_{n=0}^{N} a_n T_n^*$$

$$+ \sum_{m=0}^{M} v_m T_m^* \sum_{n=0}^{N-3} a_n^{(3)} T_n^* - \alpha^2 \sum_{m=0}^{M} v_m T_m^* \sum_{n=0}^{N-1} a_n^{(1)} T_n^*$$

$$- R^{-1} \left[ \sum_{n=0}^{N-4} a_n^{(4)} T_n^* - 2 \sum_{n=0}^{N-2} a_n^{(2)} + \alpha^4 \sum_{n=0}^{N} a_n T_n^* \right]$$

$$+ \sum_{m=0}^{M} z_{x_m} T_m^* \sum_{n=0}^{N-1} a_n^{(1)} T_n^* - i\alpha \sum_{m=0}^{M} z_{y_m} T_m^* \sum_{m=0}^{N} a_n T_n^*$$

$$- i\lambda \left[ \sum_{n=0}^{N-2} a_n^{(2)} T_n^* - \alpha^2 \sum_{n=0}^{N} a_n T_n^* \right] = 0$$

The $a_n^{(j)}$ terms are written in terms of the $a_n$ using Eqns. (D-3), and the product terms $T_m^* T_n^*$, arising from the convection terms, are removed using Eqns. (D-6 and D-7). The above becomes after some additional rearrangement:

$$\sum_{n=0}^{N+M} \Bigg\{ \frac{-i\alpha^3}{2\gamma_n} \sum_{\substack{|m| \le N \\ |n-m| \le M}} \bar{u}_{n-m} \bar{a}_n$$

$$+ \frac{i\alpha}{2\gamma_n} \sum_{k=0}^{N} a_k \sum_{\substack{|m| \le k-2,2 \\ |n-m| \le M}} \bar{\gamma}_m \; \bar{u}_{n-m} \; {}_2(kgm)$$

$$- \frac{\alpha^2}{2\gamma_n} \sum_{k=1}^{N} a_k \sum_{\substack{|m| \le k-1,2 \\ |n-m| \le M}} \bar{\gamma}_m \; \bar{v}_{n-m} \; \ell_1(k)$$

$$+ \frac{1}{2\gamma_n} \sum_{k=3}^{N} a_k \sum_{\substack{|m| \le k-3,2 \\ |n-m| \le M}} \bar{\gamma}_m \; \bar{v}_{n-m} \; \ell_3(k,m)$$

$$+ \frac{1}{2\gamma_n} \sum_{k=1}^{N} a_k \sum_{\substack{|m| \le k-1,2 \\ |n-m| \le M}} \bar{\gamma}_n \; \bar{z}_{x_{n-m}} \; \ell_1(k)$$

$$\frac{i\alpha}{2\gamma_n} \sum_{\substack{|m| \le N \\ |n-m| \le M}} \bar{z}_{y_{n-m}} \; \bar{a}_m \Bigg\} \; T_n^*$$

$$+ \sum_{n=0}^{N} \Bigg\{ R^{-1} \left[ \alpha^4 \; a_n - 2\alpha^2 \sum_{k=n+2,2}^{N} \ell_2(n,k) a_k + \sum_{k=n+4,2}^{N} \ell_4(n,k) \; a_k \right]$$

$$- i\lambda \left[ - \alpha^2 a_n + \sum_{k=n+2,2}^{N} \ell_2(n,k)\ a_k \right] \Bigg\} T_n^* = 0 \qquad (19)$$

The summation notation $k = n+j,2$ means $k = n+j,\ n+j+2,\ n+j+4$, etc. The functions $\ell_j(n,k)$ arise from the elimination of the $a_n^{(m)}$ in terms of the $a_n$ and are defined in Eqns. (D-4). The constants $\gamma_j$ are such that $\gamma_o = 2$, $\gamma_j = 1$, $j > 0$. The overscore indicates $\overline{a}_m = \gamma_{|m|}\ a_{|m|}$ and $\overline{\gamma}_m = \gamma_{|m|}$.

Clearly, the coefficients of $T_n^*$ of Eqn. (19) must be zero if solutions exist. After some rearrangement this coefficient may be written as

$$\Bigg\{ \frac{-2\gamma_n}{R} \alpha^4 a_n - i\alpha^3 \sum_{\substack{|m| \le N \\ |n-m| \le M}} \overline{u}_{n-m}\ \overline{a}_m$$

$$- \alpha^2 \left[ \sum_{k=1}^{N} \left( \sum_{\substack{|m| \le k-1,2 \\ |n-m| \le M}} \overline{\gamma}_m \overline{v}_{n-m} \ell_1(k) \right) a_k \right.$$

$$\left. - \frac{4}{R} \sum_{k=n+2,2}^{N} \ell_2(k,n)\, a_k \right] + i\alpha \left[ \sum_{k=2}^{N} \left( \sum_{|m| \le k-2,2} \overline{\gamma}_m\ \overline{u}_{n-m}\ \ell_2\ (k,m) \right) a_k \right.$$

$$\left. - \sum_{\substack{|m| \le N \\ |n-m| \le M}} \overline{z} y_{n-m}\ \overline{a}_m \right] + \left[ \sum_{k=3}^{N} \left( \sum_{\substack{|m| \le k-3,2 \\ |n-m| \le M}} \overline{\gamma}_m\ \overline{v}_{n-m}\ \ell_3\ (k,m) \right) a_k \right] \Bigg\}$$

$$+ \sum_{k=1}^{N} \left( \sum_{\substack{|m| \leq k-1,2 \\ |n-m| \leq M}} \bar{\gamma}_m \bar{z}^{x_{n-m}} \ell_1(k) \right) a_k - \frac{2}{R} \sum_{k=n+4,2}^{N} \ell_4(k,n)\ a_k \Bigg] \Bigg\}$$

$$- 2i\lambda \left\{ -\alpha^2 \gamma_n\ a_n + \sum_{k=n+2,2}^{N} \ell_2(k,n)\ a_k \right\} = 0$$

$$n = 0,1,2,\ldots,\ N+M \qquad (20)$$

Equation (20) represents a system of N+M+1 algebraic equations in N+1 unknowns. An additional four equations will be added to this system from the boundary conditions to yield a surfeit of M+4 equations. However, before further discussion of the overdeterminancy, the boundary conditions will be considered.

At $y = 0$, the conditions on $\tilde{\phi}$ are

$$\tilde{\phi}(0) = 0 \quad \text{and} \quad \tilde{\phi}_y(0) = 0$$

These conditions expressed in terms of the Chebyshev expansion are

$$\sum_{n=0}^{N} a_n\ T_n^*(0) = 0 \qquad (21a)$$

and

$$\sum_{n=0}^{N-1} \frac{1}{\gamma_n} \left( \sum_{m=n+1,2}^{N} \ell_1(m)\ a_m \right) T_n^*(0) = 0 \qquad (21b)$$

The condition as $y \to \infty$ will be approximated on the finite interval $\left[0,1\right]$ by the appropriate asymptotic form for

large y. The asymptote is found by taking the limit of Eqn. (16) as $y \to \infty$ to yield

$$i(\alpha-\lambda)\ (D^2 - \alpha^2)\ \tilde{\phi} = 0$$

It has been established that $\alpha = \omega$, but, in general, $\omega \neq \lambda$, implying $\alpha \neq \lambda$. Thus, as $y \to \infty$, it is necessary that

$$(D^2 - \alpha^2)\ \tilde{\phi} = 0$$

The only solution of the above which satisfies the boundary as $y \to \infty$ is

$$\tilde{\phi} \sim \exp\ (-\alpha y)$$

This last expression gives the behavior of $\tilde{\phi}$ for large values of y and may be used as an appropriate boundary condition at $y = y_\infty$ when $y_\infty$ is chosen sufficiently large that the asymptotic condition appertains.

The boundary condition at $y_\infty$ can now be found. Since $\tilde{\phi}$ is analytic, it has a Taylor's series expansion. Therefore, expand $\tilde{\phi}$ about $y_e$ where $y_e$ is such that $y_e < y_\infty$ and $\tilde{\phi}(y_e) = p \exp\ (-\alpha y_e)$ is valid where p is the constant of proportionality. The Taylor's series is then

$$\tilde{\phi}(y) = \tilde{\phi}(y_e) + \tilde{\phi}_y(y_e)(y-y_e) + \tilde{\phi}_{yy}(y_e)(y-y_e)^2/2! + \text{---}$$

$$= p\ e^{-\alpha y_e} - \alpha p e^{-\alpha y_e}(y-y_e) + \alpha^2 p\ e^{-\alpha y_e}(y-y_e)^2/2! + \text{---}$$

$$= p\ e^{-\alpha y_e}\left[1 - \alpha(y-y_e) + \alpha^2\ (y-y_e)^2/2! + \text{---}\right]$$

The terms in brackets can be recognized as the expansion of $\exp\left[-\alpha(y-y_e)\right]$, hence

$$\tilde{\phi}(y) = \tilde{\phi}(y_e)\ \exp\left[-\alpha(y-y_e)\right]$$

and the appropriate homogeneous boundary condition at $y = y_\infty$ is

$$\tilde{\phi}(y_\infty) - \tilde{\phi}(y_e)\ \exp\left[-\alpha(y_\infty - y_e)\right] = 0 \qquad (22a)$$

and similarly

$$\tilde{\phi}_y(y_\infty) - \tilde{\phi}_y(y_e)\ \exp\left[-\alpha(y_\infty - y_e)\right] = 0 \qquad (22b)$$

Equations (22) must be normalized to the interval $[0,1]$ by normalizing y with $y_\infty$. The condition at $y_\infty = 1$ in the normalized coordinates may be expanded in the Chebyshev series, thus

$$\tilde{\phi}(1) - \tilde{\phi}(y_e)\ \exp\left[-\alpha(1 - y_e)\right] = 0$$

becomes

$$\sum_{n=0}^{N} a_n \left\{ T_n^*(1) - T_n^*(y_e)\ \exp\left[-\alpha(1-y_e)\right] \right\} = 0 \qquad (23a)$$

and

$$\tilde{\phi}_y(1) - \tilde{\phi}_y(y_e)\ \exp\left[-\alpha(1 - y_e)\right] = 0$$

becomes

$$\sum_{n=0}^{N-1} \frac{1}{\gamma_n} \left( \sum_{m=n+1}^{N} \ell_1(m)\, a_m \right) \left\{ T_n^*(1) - T_n^*(y_e)\ \exp\left[-\alpha(1-y_e)\right] \right\} = 0 \qquad (23b)$$

Equations (21) and (23) form the boundary conditions at $y = 0$ and $y = 1$, respectively.

Elimination of the Overdeterminancy

The algebraic system formed by Eqns. (20), (21), and (23) is overdetermined as it consists of N+M+5 equations in N+1 unknowns. In general, such a system has no solutions. However, if the Lanczos Tau method is employed, M+4 additional unknowns may be added to this system and solutions can be obtained. (This is the reason for the finite number of terms in the expansion of $\tilde{\phi}$ noted earlier.)

Before discussion of the Tau method as applied to the present formulation, it will be pedagogical to consider the method as applied to a one-dimensional operator, $O$, having constant coefficients and order M. The appropriate boundary value problem has the form

$$Of = 0$$

subject to

$$B_M f = 0$$

where $B_M f = 0$ are the set of M boundary conditions. We know from preceding discussions of the theory of orthogonal functions that f may be expanded as

$$f = \sum^{\infty} e_n g_n$$

where the $g_n$ are a set of orthogonal functions and the $e_n$ are determined by

$$e_n = \langle f, g_n \rangle / ||g_n||^2$$

The difficulty associated with the above procedure is that the $e_n$ must be determined from a set of integral equations, which are either unavailable (i.e., f unknown) or require a numerical integration. It would be more convenient from a computational point of view to have an alternate technique from which the $e_n$ may be determined or accurately approximated. Therefore, consider that f is approximated by a finite expansion (i.e., an extrapolating series, see Lanczo (20)),

$$f \simeq \sum_{n=0}^{N} e_n g_n + \eta$$

where $\eta$ represents the error due to the truncation. The boundary value problem is then of the perturbed form

$$Of = \sum_{n=0}^{N} e_n \, Og_n + \varepsilon_N = 0$$

and the boundary conditions are taken in the form

$$B_M f = \sum_{n=0}^{N} e_n B_M g_n = 0$$

The error term $\varepsilon_N$ has been added so that the equality can be applied. In this form the boundary value problem consists of N+M+1 equations in N+1 unknowns. Thus, a surfeit of M equations is obtained.

The essence of the Tau method is to add additional unknowns (in this case M unknowns) by expansion of the error

term in an interpolation expansion (see (20)) of the form

$$\varepsilon_N = \sum_{m=0}^{M-1} \tau_m \, h_m$$

The $e_n$ may be obtained from recurrance relations such as Eqn. (20) where the last M relations are unfulfilled. Therefore, it is desirable to have these last M equations equal to an error term or terms, depending upon the choice of the $h_m$ (e.g., if the $h_m$ are taken to be the $g_n$ then only one error term, $\tau_i$, will appear in each of the last M equations). As long as the $h_m$ may be related to the $g_n$, i.e. $h_n = h_n(g_n)$, m = 0, 1, 2, ...,M, they are arbitrary. However, if the additional requirement that the error be spread evenly over the domain of the independent variable, then it can be shown that the optimum choice for the $h_m$ on a finite interval is the Chebyshev polynomials. (This assumes the $g_n$ have been chosen to be representable as polynomials.)

In summary, then the Lanczos Tau method provides exact solutions to the perturbed system

$$O\left[\sum_{n=0}^{N} e_n \, g_n\right] = -\varepsilon_N = -\sum_{m=0}^{M-1} \tau_m \, h_m$$

The values of the $e_n$ can be obtained algebraicly and the associated $\tau_m$ can be used to obtain an estimate of the error involved in the approximation. Note that as more and more terms are taken (i.e., $N \to \infty$) the number of $\tau_m$ remains constant and are always associated with the last M equations.

Thus, the $\tau_m$ change for each degree of approximation considered.

Application of the $\tau$ method to Eqn. (20) requires that a new right hand side be added of the form

$$\sum_{m=0}^{M+3} \tau_m T_m^{*}{}_{+N-2}$$

where the $\tau_m$ are associated with the last M+4 equations of Eqn. (20). Equations (20), (21), and (23) with the addition of the $\tau$ terms can be written in matrix form as

$$\left[\left(-R^{-1}\,\alpha^4 P - i\alpha^3 B_o + \alpha^2 B_1 + i\alpha B_2 - B_3\right) - i\lambda\left(B_4 - \alpha^2 P\right)\right] A = 0$$

or

$$\left[\left(-\alpha^3 B_o + \alpha B_2\right) + i\left(\alpha^4 P - \alpha^2 R B_1 + R B_3\right)\right] A = \lambda\left[R\left(B_4 - \alpha^2 P\right)\right] A \qquad (24)$$

where A is the vector of unknowns containing the N+1, $a_n$ and the M+4, $\tau_m$ as elements. The elements of the coefficient matrices are indicated in Table I. Equation (24) represents a general, complex, algebraic eigenvalue problem of the form

$$(S - \lambda T)A = 0 \qquad (25)$$

with the characteristic equation

TABLE I

THE COEFFICIENT MATRICES OF THE GENERAL ORR-SOMMERFELD OPERATOR, $L(\alpha,y)$

| | | |
|---|---|---|
| $(B_o)_{n,m} =$ | $\begin{cases} \bar{u}_{n-m}\ \bar{\gamma}_m \\ \lvert m\rvert \le N \\ \lvert n-m\rvert \le M \\ o \quad \text{otherwise} \end{cases}$ | $n \le M+N$ |
| $(B_1)_{n,m} =$ | $\begin{cases} -\sum \bar{\gamma}_k\ \bar{v}_{n-k}\ \ell_1(m) \\ \lvert k\rvert \le m-1,2 \\ \lvert n-k\rvert \le M \\ o \quad \text{otherwise} \end{cases}$ | $n \le M+N-1$<br>$1 \le m \le N$ |
| $+$ | $\begin{cases} -\ 4/R\ \ell_2(m,n) \\ o \quad \text{otherwise} \end{cases}$ | $n \le N-2$<br>$n+2,2 \le m \le N$ |
| $(B_2)_{n,m} =$ | $\begin{cases} \sum \bar{\gamma}_k\ \bar{u}_{n-k}\ \ell_2(m,k) \\ \lvert k\rvert \le m-2,2 \\ \lvert n-k\rvert \le M \\ o \quad \text{otherwise} \end{cases}$ | $n \le M+N-2$<br>$2 \le m \le N$ |
| $-$ | $\begin{cases} \sum \bar{\gamma}_m\ \bar{z}_{y_{n-m}} \\ \lvert m\rvert \le N \\ \lvert n-m\rvert \le M \\ o \quad \text{otherwise} \end{cases}$ | $n \le N+M$ |

TABLE I (continued)

$$
(B_3)_{n,m} = \begin{cases} \sum \bar{\gamma}_k \, \bar{v}_{n-k} \, \ell_3(m,k) & n \le N+M-3 \\ |k| \le m-3,2 & 3 \le m \le N \\ |n-m| \le M & \\ o \quad \text{otherwise} & \end{cases}
$$

$$
+ \begin{cases} \sum \bar{\gamma}_m \, \bar{z}x_{n-m} \, \ell_1(m) & n \le N+M-1 \\ |k| \le m-1,2 & 1 \le m \le N \\ |n-k| \le M & \\ o \quad \text{otherwise} & \end{cases}
$$

$$
- \begin{cases} 2/R \quad \ell_4(m,n) & n \le N-4 \\ o \quad \text{otherwise} & n+4,\ 2 \le m \le N \end{cases}
$$

$$
+ \begin{cases} \delta_{n-4,m} & m > N \\ o \quad \text{otherwise} & \end{cases}
$$

$$
+ \begin{cases} T_m^*(0) & n = N+M+1,\ m \le N \end{cases}
$$

$$
+ \begin{cases} \ell_1(m) \sum_{k=K(m),2}^{m-1} \frac{1}{\gamma_k} T_k^*(0) & n=N+M+2 \quad 1 \le m \le N \\ & K(j)=2\left[j/2\right]_I - (j-1) \end{cases}
$$

$$
+ \begin{cases} \left[T_n^*(1) - T_n^*(y_e) e^{-\alpha(1-y_e)}\right] & n=N+M+3 \quad m \le N \end{cases}
$$

$$
+ \begin{cases} \ell_1(m) \sum_{k=K(m),2}^{m-1} \frac{1}{\gamma_k} & n=N+M+4,\ 1 \le m \le N \\ \left[T_n^*(1) - T_n^*(1) e^{-\alpha(1-y_e)}\right] & K(j)=2\left[j/2\right]_I - (j-1) \end{cases}
$$

TABLE I (continued)

| | | |
|---|---|---|
| $(B_4)_{n,m} =$ | $2\ \ell_2\ (n,m)$ | $n \leq N-2, n+2, 2 \leq m \leq N$ |
| | o otherwise | |
| $(P)_{n,m} =$ | $2\ \gamma_n\ \ \delta_{n,m}$ | $n \leq N$ |
| | o otherwise | |

$$\det (S - \lambda T) = 0 \tag{25a}$$

Because the four boundary conditions (Eqns. (21) and (23)) are contained in matrix $B_3$, the remaining matrices will have zero elements in their last four rows. The matrix, T, will be singular. Reference to Table I indicates that the rank of T will be considerably less than its order. Therefore, the reduction to the standard form $(S - \lambda I)$ is precluded. Solution techniques for this type of eigenvalue problem (Eqn. (25)) is discussed later.

The Adjoint Problem

The adjoint conjugate eigenfunctions appear in the inner products which define the expansion coefficients, $c_j$ (Eqn. (12)) of the nonhomogeneous streamfunction $\phi^{(H)}$ (Eqn. (9). Therefore, it will be necessary to obtain solutions for $\tilde{\chi}_j^*$ in an appropriate Chebyshev expansion. In order to accomplish this, consider the adjoint operator, $\hat{L}$, which is given in Appendix E, Eqn. (E-4) to be:

$$\hat{L}(x,y) = - \left( u^{(0)} \frac{\partial}{\partial x} + v^{(0)} \frac{\partial}{\partial y} \right) \nabla^2$$

$$- 2 \left[ u_x^{(0)} \frac{\partial^2}{\partial x^2} + \hat{z}^{(0)} \frac{\partial^2}{\partial x \partial y} + v_y^{(0)} \frac{\partial^2}{\partial y^2} \right]$$

$$- R^{-1} \nabla^4 + i \mu^* \nabla^2$$

where $\hat{z}^{(0)} = u_y^{(0)} + v_x^{(0)}$.

The analysis requires that the "local" adjoint conjugate form $\hat{L}^*(\alpha,y)$ be employed in the calculations. Hence, applying the "local" approximation and taking conjugates of the above leads to the adjoint conjugate problem

$$\hat{L}^*(\alpha,y)\tilde{\chi}^* = \Big[ -R^{-1}\alpha^4 - i\alpha^3 u^{(0)} + \alpha^2 \left(v^{(0)} D + 2u_x^{(0)} + 2R^{-1} D^2\right) + i\alpha\left(u^{(0)} D^2 + 2\hat{z}^{(0)} D\right) - \left(v^{(0)} D^3 + 2v_y^{(0)} D^2 - R^{-1} D^4\right) - i\lambda \left(D^2-\alpha^2\right)\Big] \tilde{\chi}^* = 0 \qquad (26)$$

The adjoint conjugate streamfunction, $\hat{\chi}^*$, and the coefficients of $\hat{L}^*$ may be expanded in Chebyshev series, i.e.

$$\tilde{\chi}^* = \sum_{n=0}^{N} \hat{a}_n^* T_n^* \qquad u_x^{(0)} = \sum_{m=0}^{M} u_{x_m} T_m^*$$

$$u^{(0)} = \sum_{m=0}^{M} u_m T_m^* \qquad v_y^{(0)} = \sum_{m=0}^{M} v_{y_m} T_m^* \qquad (26a)$$

$$v^{(0)} = \sum_{m=0}^{M} v_m T_m^* \qquad \hat{z}^{(0)} = \sum_{m=0}^{M} \hat{z}_m T_m^*$$

and $$D^m \tilde{\chi}^* = \sum_{m=0}^{N-M} \hat{a}_n^{*(m)} T_n^*$$

Substitution of Eqns. (26a) into Eqn. (26) and use of Eqns. (D-3) to replace the $\hat{a}_n^{*(m)}$ in terms of $\hat{a}_m^*$ and Eqns. (D-6) and (D-7) to remove the product terms $T_m^* T_n^*$ gives the

coefficient of $T_n^*$ to be

$$-2\,R^{-1}\,\gamma_n\,\alpha^4\,\hat{a}_n^* - i\,\alpha^3 \sum_{\substack{|m| \le N \\ |n-m| \le M}} \bar{u}_{n-m}\,\bar{\hat{a}}_m^*$$

$$+ \alpha^2\left[\sum_{k=1}^{N} \bar{\hat{a}}_k^* \left(\sum_{\substack{|m| \le k-1,2 \\ |n-m| \le M}} \bar{\gamma}_m\,\bar{v}_{n-m}\,\ell_1(k)\right) + 2 \sum_{\substack{|m| \le N \\ |n-m| \le M}} \bar{u}_{x_{n-m}}\,\bar{\hat{a}}_m^*\right.$$

$$\left. + 4R^{-1} \sum_{m=n+2,2}^{N} \ell_2(n,m)\,\hat{a}_m^*\right] + i\alpha\left[\sum_{k=2}^{N} \hat{a}_k^* \left(\sum_{\substack{|m| \le k-2,2 \\ |n-m| \le M}} \bar{\gamma}_m\,\bar{u}_{n-m}\ell_2(k,m)\right)\right.$$

$$\left. + 2 \sum_{k=1}^{N} \bar{\hat{a}}_k^* \left(\sum_{\substack{|m| \le k-1,2 \\ |n-m| \le M}} \bar{\gamma}_m\,\bar{\hat{z}}_{n-m}\ell_1(m)\right)\right] - \left[\sum_{k=3}^{N} \hat{a}_k^* \left(\sum_{\substack{|m| \le k-3,2 \\ |n-m| \le M}} \bar{\gamma}_m\,\bar{v}_{n-m}\ell_3(k,m)\right)\right.$$

$$\left. + 2 \sum_{k=2}^{N} \hat{a}_k^* \left(\sum_{\substack{|m| \le k-2,2 \\ |n-m| \le M}} \bar{\gamma}_m\,\bar{v}_{y_{n-m}}\ell_2(k,m)\right) + 2R^{-1} \sum_{m=n+4,2}^{N} \ell_4(n,m)\,\hat{a}_m^*\right]$$

$$- 2i\,\lambda\left[\sum_{m=n+2,2}^{N} \ell_2(m,n)\,\hat{a}_n^* - \gamma_n\,\alpha^2\,\hat{a}_n^*\right] = 0 \qquad (26b)$$

The boundary conditions have the same form as Eqns. (22) and (23). Hence, after reduction to the finite interval $[0,1]$ and

substitution of the Chebyshev expansion for $\hat{\chi}^*$, the boundary conditions are

$$\hat{\chi}^*(0) = \sum_{n=0}^{N} \hat{a}_n^* \, T_n^*(0) = 0$$

$$\hat{\chi}_y^*(0) = \sum_{n=0}^{N-1} \left( \sum_{m=n+1,2}^{N} \ell_1(m) \, \hat{a}_m^* \right) T_n^*(0) = 0$$

$$\hat{\chi}^*(1) = \sum_{n=0}^{N} \hat{a}_n^* \left\{ T_n^*(1) - T_n^*(y_e) \exp\left[-\alpha(1-y_e)\right] \right\} = 0 \qquad (27)$$

$$\hat{\chi}_y^*(1) = \sum_{n=0}^{N-1} \frac{1}{\gamma_n} \left( \sum_{m=n+1,2}^{N} \ell_1(m) \, \hat{a}_m \right)$$

$$\left\{ T_n^*(1) - T_n^*(y_e) \exp -\left[\alpha(1-y_e)\right] \right\} = 0$$

The system of algebraic equations given by Eqns. (27) requires the addition of the M+4, $\tau_m$ error terms from the Lanczos Tau method. Equation (27) then has the form

$$\left[ -R^{-1} \alpha^4 \hat{P} - i\alpha^3 \hat{B}_o + \alpha^2 \hat{B}_1 + i\alpha \hat{B}_2 - \hat{B}_3 - i\lambda\left(\hat{B}_4 - \alpha^2 \hat{P}\right) \right] A = 0$$

or

$$\left[ \left( -\alpha^3 \hat{B}_o + \alpha B_2 \right) + i\left( \alpha^4 \hat{P} - \alpha^2 R\hat{B}_1 + R\hat{B}_3 \right) - \lambda\left(\hat{B}_4 - \alpha^2 \hat{P}\right) \right] A = 0 \qquad (28)$$

where the elements of the coefficient matrices are given in Table II. Equation (28) has the general form

$$(\hat{S} - \lambda\hat{T})\ \hat{A} = 0.$$

Numerical Solution

It has been shown in the preceding sections that a solution of the nonhomogeneous problem may be obtained by an expansion in the binormal system formed by the eigenfunctions and the adjoint eigenfunctions. A direct analytical solution for these functions is not attempted but rather a solution of their algebraic analog as given in Eqns. (24) and (28). The algebraic equations form a general complex eigenvalue of the form of Eqn. (24), i.e.

$$\det (S - \lambda T) = 0 \qquad (25a)$$

where T has rank much less than its order.

Solution of the general eigenvalue problem posed by Eqn. (25a) is accomplished by reducing the matrices, S and T, to an equivalent system $\overline{S}$ and $\overline{T}$. The algorithm employed to achieve this end was developed by Gray and Helgason (21) and is discussed in detailed in Appendix F. The equivalent system has the form

$$\det (\overline{S} - \lambda\overline{T}) = 0$$

where $\overline{T}$ is diagonal and has rank equal to its order which is less than the order of S and T. Therefore, multiplication by $\overline{T}^{-1}$ reduces Eqn. (25a) to the standard form

TABLE II

THE MATRIX COEFFICIENTS OF $\hat{L}^*(\alpha,y)$

$$(\hat{B}_o)_{n,m} = \begin{cases} \bar{\gamma}_m \, \bar{u}_{n-m} & n = N+M, \ |m| \le N, \ |n-m| \le M \\ o \quad \text{otherwise} \end{cases}$$

$$(\hat{B}_1)_{n,m} = \begin{cases} \sum \bar{\gamma}_k \, \bar{v}_{n-k} \, \ell_1(k) \\ |k| \le m-1,2 \\ |n-k| \le M & n \le N+M-1 \\ o \quad \text{otherwise} \end{cases}$$

$$+ \begin{cases} 2 \, \bar{\gamma}_m \, \bar{u}_{x_{n-m}} & n = N+M, \ |m| \le N, \ |n-m| \le M \\ o \quad \text{otherwise} \end{cases}$$

$$\begin{cases} 4/R \, \ell_2(n,m) & n = N-2 \\ o \quad \text{otherwise} & 2+n, \ 2 \le m \le N \end{cases}$$

$$(\hat{B}_2)_{n,m} = \begin{cases} \sum \bar{\gamma}_k \, \bar{u}_{n-k} \, \ell_2(m,k) \\ |k| \le m-2,2 \\ |n-m| \le M & n \le N+M-2 \\ o \quad \text{otherwise} \end{cases}$$

$$+ \begin{cases} \sum \bar{\gamma}_k \, \bar{\tilde{z}}_{n-k} \, \ell_1(k) \\ |k| \le m-1,2 \\ |n-k| \le M & n \le N+M-1 \\ o \quad \text{otherwise} \end{cases}$$

TABLE II (continued)

$$(\hat{B}_3)_{n,m} = \begin{cases} \sum \bar{\gamma}_k \, \bar{v}_{n-k} \, \ell_3(m,k) & n \leq N+M-3 \\ |k| \leq m-3,2 & \\ |n-m| \leq M & \\ o \quad \text{otherwise} & \end{cases}$$

$$+ \begin{cases} 2 \sum \bar{\gamma}_k \, \bar{v}y_{n-k} \, \ell_2(k,m) & n \leq N+M-2 \\ |k| \leq m-2,2 & \\ |n-k| \leq M & \\ o \quad \text{otherwise} & \end{cases}$$

$$+ \begin{cases} 2/R \, \ell_4(n,m) & n \leq N-4 \\ & n+4, \; 2 \leq m \leq N \\ o \quad \text{otherwise} & \end{cases}$$

for $m > N$ and $n > M+N$ $(\hat{B}_3)_{n,m} = (B_3)_{n,m}$

$$(\hat{B}_4)_{n,m} = \begin{cases} 2 \, \ell_2(n,m) & n \leq N-2 \\ & n+2,2 \leq m \leq N \\ o \quad \text{otherwise} & \end{cases}$$

$$(P)_{n,m} = \begin{cases} -2 \, \gamma_n \, \delta_{n,m} & n \leq N \\ o \quad \text{otherwise} & \end{cases}$$

where $\delta_{n,m}$ is the Kronecker delta, i.e.

$$\delta_{m,n} = \begin{cases} 1, & m = n \\ 0, & m \neq n \end{cases}$$

$$\det (\tilde{\tilde{S}} - \lambda I) = 0$$

where $\tilde{\tilde{S}} = \bar{T}^{-1} \bar{S}$.

The eigenvalues of Eqn. (29) are determined by implementation of the QR algorithm developed by Francis (23) for complex matrices. As the QR algorithm preserves the similarity of Hessenberg matrices, $\tilde{\tilde{S}}$ is reduced to almost triangular form (Hessenberg) by similarity transforms according to a procedure developed by Wilkinson (23). Reduction to Hessenberg form has the additional advantage of requiring fewer arithmetic operations to determine the eigenvalues.

The QR algorithm is based upon the theorem of matrix theory which states:

> TH. Every square matrix A over the complex field may be reduced by a unitary transformation to an upper triangular matrix with the characteristic values on the diagonal.

If $\tilde{\tilde{S}}_T$ is the desired triangular form, then the theorem indicates there exists a transform matrix U such that

$$\tilde{\tilde{S}}_T = U^H S U, \; U^H U = I$$

where the superscript H indicates the conjugate transpose. The mechanics of the QR algorithm are based upon an iterative decomposition of $\tilde{\tilde{S}}$ into the product of a unitary matrix, Q, and an upper triangular matrix, R, i.e.

$$\tilde{S} = QR$$

The $k^{th}$ iteration is then

$$\tilde{S}^{(k)} = Q^{(k)} \; R^{(k)}$$

and

$$\tilde{S}^{(k+1)} = R^{(k)} \; Q^{(k)}$$

or in similarity form the above is equivalent to

$$\tilde{S}^{(k+1)} = Q^{(k)H} \; Q^{(k-1)H} \; \ldots \; Q^{(1)H} \; \tilde{S} \; Q^{(1)} \; Q^{(2)} \; \ldots \; Q^{(k)}$$

Francis (22) demonstrates that as $K \to \infty$, $S^{(k)}$ tends to $S_T$, an upper triangular matrix whose diagonal elements are the eigenvalues.

Once the eigenvalues are computed the eigenvectors may be evaluated. This is accomplished by implementing the inverse iteration scheme of Osborne (24) for the general complex eigenvalue problem of Eqn. (24). The iteration procedure is for the $i^{th}$ iteration

$$(S - \lambda T)E_{i+1} = -T \; A_i$$

$$A_{i+1} = E_i / \max_i (E_i).$$

The adjoint problem is treated in an identical manner to the above. However, since the adjoint conjugate problem has identical eigenvalues to Eqn. (24) (see Appendix C), they need to be determined only once. The adjoint conjugate eigenvectors are computed using the Osborne algorithms.

Auxiliary Functions

After the series coefficients $a_n$ and $\hat{a}_n^*$ have been evaluated, several additional parameters of theoretical and experimental interest may be evaluated. For example, the forced instantaneous velocity profile may be obtained from

$$u^{(1)}(x_o,y,t) = \text{Real}\,(\psi_y^{(1)})$$

$$= \text{Real}\left\{ \sum_j^J C_j \sum_{n=0}^{N-1} \left( \sum_{m=n+1,2}^{N} \ell_1(m)\, a_m \right) T_n^* \, e^{i\alpha x_o - i\omega t} + F_y \, e^{(i\alpha x_o - i\omega t)} \right\} \tag{30}$$

The usually measured experimental quantity is the rms fluctuating velocity, $\overline{u^{(1)}}$, evaluated at a constant value of $y/\delta^* = \eta_o$. If this value of $\overline{u^{(1)}}$ is designated as $u_{rms}$, the amplitude function, it may be evalued as

$$\overline{u^{(1)}}(x_o,y,t) = \left[ \frac{1}{\gamma} \int_o^{\gamma} \left( u^{(1)}(x_o,y,t) \right)^2 dt \right]^{1/2} \tag{31}$$

or

$$u_{rms} = \overline{u^{(1)}}(x_o, \eta_o, t) \tag{31a}$$

where $\gamma$ is the time interval over which the average is to be taken, say $\gamma = 2\pi\sigma/\omega$, where $\sigma$ is an integer. The corresponding result for the classical, unforced case is not as precise due to the indeterminancy arising from the eigenvalue problem, i.e. $\overline{u^{(1)}}$ unforced can only be determined to a constant of

proportionality. Unfortunately, this constant of proportionality is a function of $x_o$. Therefore, for comparison purposes only, the approximate relation

$$\ell n \left( \frac{A}{A_o} \right) = \int_{R_{\delta_o^*}}^{R_{\delta^*}} \frac{\lambda_i \alpha}{\lambda_r} \, dR_{\delta^*} \tag{32}$$

is employed to give the local total amplification (e.g. see Mack (14), for a detailed discussion of this point).

The local, instantaneous, Reynolds stress distribution through the boundary layer can be obtained from

$$\begin{aligned} u^{(1)} v^{(1)} (x_o, y, t) &= \text{Real} \left\{ \psi_y^{(1)} \right\} \text{Real} \left\{ - i\alpha \, \psi_x^{(1)} \right\} \\ &= \text{Real} \left\{ \sum_{j=1}^{J} C_j \left( \sum_{n=0}^{N-1} \sum_{m=n+1,2}^{N} \ell_1(m) \, a_m \right) T_n^* \, e^{i(\alpha x_o - \omega t)} \right. \\ &\quad \left. + F_y \, e^{i(\alpha x_o - \omega t)} \right\} \text{Real} \left\{ -i\alpha \sum_{j=1}^{J} C_j \sum_{n=0}^{N} a_n T_n^* \, e^{i(\alpha x_o - \omega t)} \right. \\ &\quad \left. - i\alpha \, F \, e^{i(\alpha x_o - \omega t)} \right\} \end{aligned} \tag{33}$$

The average value of the Reynolds stress is then

$$\overline{uv} \, (x_o, y) = \frac{1}{\gamma} \int_o^{\gamma} u^{(1)} \, v^{(1)} \, (x_o, y, t) \, dt. \tag{34}$$

# III. RESULTS AND DISCUSSION

## Comparisons with Classical Stability Theory

Several comparisons are made in this section between calculations based on the present formulation with other well established solutions of the Orr-Sommerfeld equation and with experimental data where it is available. These comparisons are restricted to flow over a flat plate as the computations are based upon profiles obtained from the Blasius function. Appropriately, then, the first matter to be considered is the representation of the derivatives of the Blasius function as a series of Chebyshev polynomials.

The effect of the number of terms (M+1) (see Eqn. 18)) required to approximate the velocity and vorticity profiles for the parallel flow approximation is shown in Figure 1 (all figures are in Appendix A). The velocity profile is well represented with ten terms in the expansion, but the vorticity profile is not. Numerical experimentation has revealed that as many as twenty terms will not remove the oscillations about zero when $y/y_\infty > 0.65$. An excellent approximation can be obtained if the interval $0,y_\infty$ is reduced from the value $\eta_\infty = 11$ in Figure 1 to $\eta_\infty = 7.2$ in Figure 2. Here, $\eta$ is the similarity variable of the Blasius equation, i.e., $\eta = y/\sqrt{Rex}/x$. Figure 2 illustrates the improvement in the representation of the velocity and

vorticity profiles with the ten-term expansion in the smaller interval over the approximation in the larger interval. It was subsequently determined that this reduction in the value of $y_\infty$ had no effect upon the eigenvalue computations, and hence, is utilized throughout the remaining computations.

It has become customary to prevent boundary layer stability calculations and data normalized with the local displacement thickness, $\delta^*$, where $\delta^* = 1.7208x/\sqrt{R_x}$ and where $R_x$ is the Reynolds number based upon the distance from the leading edge. Therefore, the results of this investigation will be presented in a similar manner. In order to emphasize this change of characteristic length to $\delta^*$, the parameters R, $\alpha$, $\omega$, etc., will be designated as $R_{\delta^*}$, $\delta^*$, $\omega^*$, etc., in the remainder of the discussion.

Computations of the neutral stability curves based on Eqn. (8a) and defined by $\alpha^*$ vs $R_{\delta^*}$ and $\omega^*/R_{\delta^*}$ vs $R_{\delta^*}$ are exhibited in Figure 3. The data of Schubauer and Skramstad (1) are shown for reference. The effect of the non-parallel flow terms, Eqn. (8), on the calculation of the neutral stability curve is also illustrated. The major effect of the additional terms appears to be limited to $R_{\delta^*} < 600$. The non-parallel flow solution of Barry and Ross (25) is presented in Figure 3b. Good agreement is evidenced between their results and those obtained from Eqn. (8).

The numerical computations of the neutral curve obtained by Kurtz (26) are also included in Figure 3. He utilized a finite difference approximation of the Orr-Sommerfeld equation accurate to $h^4$, where h is the increment size. He obtained solutions for a 40 point mesh with asymptotic boundary conditions imposed at $\eta = 7.2$. Kurtz made his calculations before the advent of the matrix of algorithms used in this work. He was forced by obtain eigenvalues by tedious mappings of the values of the finite difference analog of the determinant $|S - \lambda T|$ in the complex plane for varying values of $\lambda$. The present computations of the neutral curve, $\alpha^*$ $(R_{\delta^*})$, Figure 3a, agrees quite well with the results of Kurtz. However, a disparity is evident between the two calculations for $R_{\delta^*} < 650$ in Figure 3b. Whether this disagreement is a result of increased accuracy of the present computations or some deficiency in them could not be ascertained as these results were obtained at the maximum limit of available computer storage. Because of the good agreement obtained with the non-parallel flow and the results of Barry and Ross, the disparity with Kurtz is assumed to be due to an increase in accuracy with the present formulation.

The temporal growth of the disturbance in the boundary layer is governed by the imaginary part of $\lambda^*$, i.e., $\lambda_{i^*}$. It is usual to represent the amplification implied by $\lambda_{i^*}$ in

the parameter, amp = $\lambda_i/\alpha$. Figure 4 shows the variation of amp with $\alpha$ at several values of $R_{\delta*}$. For comparison the data of Schubauer and Skramstad (1) and the computations of Kurtz (26) are also displayed. In addition, Figure 4a includes a computation for non-parallel flow effects which are shown to be small for this value of $R_{\delta*}$ (= 630). Agreement between the theoretical predictions is noted to be better than the agreement with the data.

Calculation of the normalized eigenfunction

$$\phi_1(y)/\max_y \left[\text{Real } (\phi_1)\right]$$

are illustrated in Figure 5. The calculations were made for the three sample cases evaluated by Kurtz (26). His calculations are given for comparison. Figure 5c also includes the computations of Jordinson (27). In general, the real parts of the eigenfunctions compare quite favorably and are identical for the present formulation and that of Jordinson in Figure 5c. The imaginary part of the eigenfunction indicates considerable variation between the solutions. It should be noted that the scale of the imaginary parts is magnified by a factor of ten in the figure. Therefore, these differences are really quite small and are no cause for concern regarding the accuracy of the calculations.

The adjoint conjugate stream function is required in the formulation of the inner products such as $< \hat{\chi}_j, \mathcal{L} F >$.

Computations of the normalized adjoint conjugate stream function

$$\hat{\chi}_1^*(y)/\max_y \left[\text{Real } (\tilde{\chi}_1^*)\right]$$

are illustrated in Figure 6. The normalized $\tilde{\chi}_1^*$ of Figure 6 correspond to the three sample cases of Kurtz shown in Figure 5. There are few computations of $\tilde{\chi}^*$ in the literature; and therefore, Figure 6 includes only the results of the present formulation. The profiles of Figure 6 are in qualitative agreement with a similar calculation of Ling and Reynolds (28).

Figures 7 and 8 illustrate comparisons of theoretical predictions of the rms values of the perturbation velocity, $u^{(1)}$, and the experimentally measured values of Schubauer and Skramstad (1) and Ross, et al. (29). The data are displayed in a form similar to that given in (1). The theoretical curves were obtained as follows: First, the Orr-Sommerfeld equation was solved and the $a_n^{(1)}$ were obtained. The rms perturbation velocity, $\overline{u^{(1)}}$, was then obtained from Eqns. (30) and (31) by setting J = 1, F = 0, and the exponentials in x equal to zero. This procedure left the constant $c_1$ unspecified. In this case $c_1$ corresponds to the undetermined constant of proportionality necessarily associated with eigen solutions. A value was assigned to $c_1$ by equating the areas under the $\overline{u^{(1)}}$ profiles and a similar curve through the data. Agreement between

experiment and theory is observed to be quite good.

Calculations of the Reynolds stress, $\overline{u^{(1)}v^{(1)}}$, across the boundary is illustrated in Figure 9 for the three sample cases of Kurtz given in Figure 5. The computations were made from Eqns. (33) and (34) with $J = 1$, $F \equiv 0$, and the exponentials in x equal to 0. These results are in qualitative agreement with similar computations of Jordinson (28).

Computations of the Forced Problem

The adequacy of the present formulation employing a Chebyshev polynomial expansion rather than finite differences has been demonstrated in the previous section for the case of the classical computations of the Orr-Sommerfeld equation. In this section the solutions of the forced problem, i.e. flow will small disturbances in the free stream, will be discussed.

It is necessary to establish that the higher eigenvalues and eigenfunctions are sufficiently well approximated before considering the forced solutions. Table III demonstrates the convergence of eigenvalues for two values of $R_{\delta*}$, specifically 850 and 1900, for increasing $N + 1$. The table demonstrates that there are 19 eigenvalues converged to five significant figures at $R_{\delta*} = 850$ and six at $R_{\delta*} = 1900$. The convergence at the higher $R_{\delta*}$ reflects the usual difficulties associated with computations involving branch II of the neutral stability curve. The calculations for the data of Table III

TABLE III

EIGENVALUE CONVERGENCE CHECK

| Eigenvalue Number | No. of Terms in Series | Value | |
|---|---|---|---|
| | CASE I: $R_{\delta^*} = 850$, $\alpha = .1606$ | | |
| $\lambda_1$ | 25 | $.13162 \times 10^{-1}$ | $-.50316 \times 10^{-2}i$ |
| | 30 | $.13162 \times 10^{-1}$ | $-.50896 \times 10^{-2}i$ |
| | 35 | $.13162 \times 10^{-1}$ | $-.50896 \times 10^{-2}i$ |
| | 40 | $.13162 \times 10^{-1}$ | $-.50892 \times 10^{-2}i$ |
| | 45 | $.13162 \times 10^{-1}$ | $-.50892 \times 10^{-2}i$ |
| | 52 | $.13162 \times 10^{-1}$ | $-.50892 \times 10^{-2}i$ |
| $\lambda_2$ | 25 | $.28715 \times 10^{-1}$ | $-.18947 \times 10^{-1}i$ |
| | 30 | $.28715 \times 10^{-1}$ | $-.18947 \times 10^{-1}i$ |
| | 35 | $.28715 \times 10^{-1}$ | $-.18947 \times 10^{-1}i$ |
| | 40 | $.28715 \times 10^{-1}$ | $-.18947 \times 10^{-1}i$ |
| | 45 | $.28715 \times 10^{-1}$ | $-.18947 \times 10^{-1}i$ |
| | 52 | $.28715 \times 10^{-1}$ | $-.18947 \times 10^{-1}i$ |
| $\lambda_3$ | 25 | $.39939 \times 10^{-1}$ | $-.20960 \times 10^{-1}i$ |
| | 30 | $.39939 \times 10^{-1}$ | $-.20960 \times 10^{-1}i$ |
| | 35 | $.39939 \times 10^{-1}$ | $-.20960 \times 10^{-1}i$ |
| | 40 | $.39939 \times 10^{-1}$ | $-.20960 \times 10^{-1}i$ |
| | 45 | $.39939 \times 10^{-1}$ | $-.20960 \times 10^{-1}i$ |
| | 52 | $.20960 \times 10^{-1}$ | $-.30960 \times 10^{-1}i$ |
| $\lambda_4$ | 25 | $.47812 \times 10^{-1}$ | $-.79371 \times 10^{-2}i$ |
| | 30 | $.47812 \times 10^{-1}$ | $-.79371 \times 10^{-2}i$ |
| | 35 | $.47812 \times 10^{-1}$ | $-.79371 \times 10^{-2}i$ |
| | 40 | $.47812 \times 10^{-1}$ | $-.79371 \times 10^{-2}i$ |
| | 45 | $.47812 \times 10^{-1}$ | $-.79371 \times 10^{-2}i$ |
| | 52 | $.47812 \times 10^{-1}$ | $-.79371 \times 10^{-2}i$ |
| $\lambda_5$ | 25 | $.42044 \times 10^{-1}$ | $-.25262 \times 10^{-1}i$ |
| | 30 | $.42044 \times 10^{-1}$ | $-.25262 \times 10^{-1}i$ |
| | 35 | $.42044 \times 10^{-1}$ | $-.25262 \times 10^{-1}i$ |
| | 40 | $.42044 \times 10^{-1}$ | $-.25262 \times 10^{-1}i$ |
| | 45 | $.42044 \times 10^{-1}$ | $-.25262 \times 10^{-1}i$ |
| | 52 | $.42044 \times 10^{-1}$ | $-.25262 \times 10^{-1}i$ |
| $\lambda_6$ | 25 | $.48236 \times 10^{-1}$ | $-.10540 \times 10^{-1}i$ |
| | 30 | $.48236 \times 10^{-1}$ | $-.10540 \times 10^{-1}i$ |
| | 35 | $.48326 \times 10^{-1}$ | $-.10540 \times 10^{-1}i$ |
| | 40 | $.48326 \times 10^{-1}$ | $-.10540 \times 10^{-1}i$ |
| | 45 | $.48326 \times 10^{-1}$ | $-.10540 \times 10^{-1}i$ |
| | 52 | $.48326 \times 10^{-1}$ | $-.10540 \times 10^{-1}i$ |

TABLE III (continued)

| Eigenvalue Number | No. of Terms in Series | Value | |
|---|---|---|---|
| $\lambda_7$ | 25 | $.39135 \times 10^{-1}$ | $-.39281 \times 10^{-1}i$ |
| | 30 | $.39135 \times 10^{-1}$ | $-.39274 \times 10^{-1}i$ |
| | 35 | $.39135 \times 10^{-1}$ | $-.39274 \times 10^{-1}i$ |
| | 40 | $.39135 \times 10^{-1}$ | $-.39274 \times 10^{-1}i$ |
| | 45 | $.39135 \times 10^{-1}$ | $-.39274 \times 10^{-1}i$ |
| | 52 | $.39135 \times 10^{-1}$ | $-.39274 \times 10^{-1}i$ |
| $\lambda_8$ | 25 | $.40755 \times 10^{-1}$ | $-.44613 \times 10^{-1}i$ |
| | 30 | $.40767 \times 10^{-1}$ | $-.44623 \times 10^{-1}i$ |
| | 35 | $.40767 \times 10^{-1}$ | $-.44623 \times 10^{-1}i$ |
| | 40 | $.40767 \times 10^{-1}$ | $-.44623 \times 10^{-1}i$ |
| | 45 | $.40767 \times 10^{-1}$ | $-.44623 \times 10^{-1}i$ |
| | 52 | $.40767 \times 10^{-1}$ | $-.44623 \times 10^{-1}i$ |
| $\lambda_9$ | 25 | $.39502 \times 10^{-1}$ | $-.63639 \times 10^{-1}i$ |
| | 30 | $.39309 \times 10^{-1}$ | $-.63846 \times 10^{-1}i$ |
| | 35 | $.39309 \times 10^{-1}$ | $-.63846 \times 10^{-1}i$ |
| | 40 | $.39309 \times 10^{-1}$ | $-.63846 \times 10^{-1}i$ |
| | 45 | $.39309 \times 10^{-1}$ | $-.63846 \times 10^{-1}i$ |
| | 52 | $.39309 \times 10^{-1}$ | $-.63846 \times 10^{-1}i$ |
| * | | | |
| CASE II: $R_{\delta^*} = 1900$, $\alpha = .3588$ | | | |
| $\lambda_1$ | 25 | $.31897 \times 10^{-1}$ | $-.44428 \times 10^{-3}i$ |
| | 30 | $.31897 \times 10^{-1}$ | $-.44398 \times 10^{-3}i$ |
| | 35 | $.31897 \times 10^{-1}$ | $-.44399 \times 10^{-3}i$ |
| | 40 | $.31897 \times 10^{-1}$ | $-.44399 \times 10^{-3}i$ |
| | 45 | $.31897 \times 10^{-1}$ | $-.44399 \times 10^{-3}i$ |
| | 52 | $.31897 \times 10^{-1}$ | $-.44399 \times 10^{-3}i$ |
| $\lambda_2$ | 25 | $.35267 \times 10^{-1}$ | $-.30407 \times 10^{-1}i$ |
| | 30 | $.34487 \times 10^{-1}$ | $-.30247 \times 10^{-1}i$ |
| | 35 | $.34501 \times 10^{-1}$ | $-.30237 \times 10^{-1}i$ |
| | 40 | $.34501 \times 10^{-1}$ | $-.30237 \times 10^{-1}i$ |
| | 45 | $.34501 \times 10^{-1}$ | $-.30237 \times 10^{-1}i$ |
| | 52 | $.34501 \times 10^{-1}$ | $-.30237 \times 10^{-1}i$ |

TABLE III (continued)

| Eigenvalue Number | No. of Terms in Series | Value | |
|---|---|---|---|
| $\lambda_3$ | 25 | $.43178 \times 10^{-1}$ | $-.41521 \times 10^{-1}i$ |
| | 30 | $.59435 \times 10^{-1}$ | $-.29475 \times 10^{-1}i$ |
| | 35 | $.59050 \times 10^{-1}$ | $-.29579 \times 10^{-1}i$ |
| | 40 | $.59048 \times 10^{-1}$ | $-.29576 \times 10^{-1}i$ |
| | 45 | $.59048 \times 10^{-1}$ | $-.29576 \times 10^{-1}i$ |
| | 52 | $.59048 \times 10^{-1}$ | $-.29576 \times 10^{-1}i$ |
| $\lambda_4$ | 25 | $.58481 \times 10^{-1}$ | $-.25202 \times 10^{-1}i$ |
| | 30 | $.60689 \times 10^{-1}$ | $-.41572 \times 10^{-1}i$ |
| | 35 | $.71697 \times 10^{-1}$ | $-.44018 \times 10^{-1}i$ |
| | 40 | $.72317 \times 10^{-1}$ | $-.43105 \times 10^{-1}i$ |
| | 45 | $.72317 \times 10^{-1}$ | $-.43101 \times 10^{-1}i$ |
| | 52 | $.72317 \times 10^{-1}$ | $-.43101 \times 10^{-1}i$ |
| $\lambda_5$ | 25 | $.74630 \times 10^{-1}$ | $-.24125 \times 10^{-1}i$ |
| | 30 | $.77070 \times 10^{-1}$ | $-.33249 \times 10^{-1}i$ |
| | 35 | $.79999 \times 10^{-1}$ | $-.44965 \times 10^{-1}i$ |
| | 40 | $.88919 \times 10^{-1}$ | $-.44128 \times 10^{-1}i$ |
| | 45 | $.88873 \times 10^{-1}$ | $-.44130 \times 10^{-1}i$ |
| | 52 | $.88873 \times 10^{-1}$ | $-.44130 \times 10^{-1}i$ |
| $\lambda_6$ | 25 | $.90504 \times 10^{-1}$ | $-.21969 \times 10^{-1}i$ |
| | 30 | $.48580 \times 10^{-1}$ | $-.70107 \times 10^{-1}i$ |
| | 35 | $.65821 \times 10^{-1}$ | $-.70933 \times 10^{-1}i$ |
| | 40 | $.94543 \times 10^{-1}$ | $-.40933 \times 10^{-1}i$ |
| | 45 | $.94543 \times 10^{-1}$ | $-.40926 \times 10^{-1}i$ |
| | 52 | $.94543 \times 10^{-1}$ | $-.40926 \times 10^{-1}i$ |

*This table has not been completed. The convergence of eigenvalues continued for this to $\lambda_{19}$, i.e. $\lambda_{20}$ was the first eigenvalue to be unconverged.

have to be extended to N + 1 = 52 for reasons that will be discussed later in this section. However, at present it suffices to indicate that a number of converged eigenvalues are available for the forced computations.

The higher eigenfunctions and adjoint conjugate eigenfunctions are also required by the solution procedure expressed in Eqn. (9). Because the higher eigenfunctions are not presently found in the literature, the first four eigenfunctions are presented for purposes of illustration in Figure 10 for the case of $R_{\delta^*}$ or $\alpha = 0.186$. The increasing complexity of the higher modes is demonstrated by the appearance of the "kink" in the second eigenfunction which becomes more pronounced in the third and fourth modes. Several numerical experiments have been undertaken to ensure that these "kinks" are not numerical in origin. Corresponding results for the first four adjoint conjugate eigenfunctions are given in Figure 11. In all cases the eigenfunctions have been normalized with the maximum real part. The increasing magnitude of the imaginary part of the higher modes is evident in the figures. This indicates a phase shift in the boundary layer much different from the approximate $\pi/2$ shift for the least stable mode.

Figure 11d illustrates the difficulty which limits the number of terms that can be taken in the eigenfunction expansion of Eqn. (10). It is observed that $\tilde{\chi}_4^*$ does not

satisfy the boundary conditions at y = 0. This is thought to imply that the eigenvalue computed from the Chebyshev expansion of Eqn. (16) is not an eigenvalue of the Chebyshev expansion of Eqn. (26). Appendix C shows that the eigenvalues of these two equations must be identical; therefore, the numerical approximation becomes suspect. It was for this reason that the computer program was extended to N + 1 = 52 terms. Subsequent numerical experiments revealed that increasing N + 1 did not relieve the problem. The Osborne inverse iteration technique (24) was employed to compute both the eigenvectors and the eigenvalues using the QR results as starting values. It was found that the QR values were accurate to at least one part in $10^8$. However, the adjoint conjugate eigenvalues were found to become altered from the QR values from the Orr-Sommerfeld equation.

It has subsequently been determined that the disagreement experienced in the two computations of the eigenvalues stems from the failure to accumulate the vector inner products involved in the matrix operations to a sufficiently high precision and as a result round-off error is limiting computational accuracy. (For a more complete discussion of these phenomena, see Wilkinson (23).) Unfortunately, nothing could be done to remedy this situation as all the computations presented here were performed in the IBM double precision arithmetic (64 bits per word) and no extended precision option

was available to the author.

With this limitation in mind, the following criterion was established to determine when the computed eigenvalues were no longer sufficiently in agreement to allow accurate evaluations:

1. Both spectra of the Orr-Sommerfeld and its adjoint operators were computed using the Osborne inverse iteration procedure to update the QR values.

2. The moduli were checked for error and when

$$e_i = \frac{|\lambda_i| - |\mu_i|}{|\lambda_i|} > .01$$

$$i = J + 1$$

that is, when the discrepancy in the computed eigenvalues becomes greater than 1% the expansion is truncated.

It remained, then, to assure that the truncated series of eigenfunctions provided sufficient accuracy. This was accomplished by comparing computations made with J and J + 1 terms. In general, for J + 1, $e_i \leq .05$. The comparisons showed very little change in the computed magnitudes of $u_{rms}$, $\overline{u^{(1)}v^{(1)}}$, etc. regardless of the value found for J. Hence, the solutions which will be presented here are assumed to be accurate in the sense that they accurately represent trends of the forced solutions while the exact magnitudes are open to some question.

A standard computation of interest in stability theory is the determination of the amplitude or growth rate of disturbances in the boundary layer. Figure 12 illustrates the results of calculations that may be utilized to determine this information for the forced case. The curves in Figure 12 are values of $u_{rms}$ determined from Eqn. (31) at constant fractions of the boundary-layer thickness, $y/\delta$, at two values of $\omega^*/R_{\delta^*}$. One difference with the classical stability results is evident immediately. The variation of $u_{rms}$ with $R_{\delta^*}$ depends upon $y/\delta$. Thus, experiments with free-stream disturbances of the form modeled here must be made with care to accurately define growth rates. The largest growth appears to be confined to the region $0.2 \leq y/\delta \leq 0.6$ in the boundary layer. The number of terms, J, in the eigen expansions are indicated in Figure 12 where they change. Jumps associated with the shifts are noted to be real in the sense they are present to the same extent when J + 1 terms are considered. Comparison of Figures 12a and b illustrates the dependency of the growth of the disturbances on the frequency parameter, $\omega^*/R_{\delta^*}$.

The amplification function $\ell n\ A/A_o$ is shown in Figure 13 for $y/\delta = 0.2$ and 0.4 for the conditions of Figure 12. The classical variation of $\ell n\ A/A_o$ with $R_{\delta^*}$ as approximated by Eqn. (32) is shown in the figure for comparison. The computations of Figure 12 have been normalized with the value at the neutral stability curve, i.e. $u_{rms}$ (940) and $u_{rms}$ (770) for

$\omega^*/R_{\delta^*} = 62 \times 10^{-6}$ and $83.5 \times 10^{-6}$, respectively. This was done so that the growth of the respective disturbances could be compared from the reference point downstream (i.e. $R_{\delta^*} \rightarrow \infty$). It can be seen from Figure 13 that initially the forced disturbances grow more rapidly than the unforced case. Depending upon the value of $\omega^*/R_{\delta^*}$, the forced case may subsequently grow less rapidly or more rapidly than the unforced case. This implies that if transition depends upon the disturbances reaching a critical amplitude, it should be possible to retard this growth at certain frequencies and, hence, possibly postpone transition. Alternately, there should be frequencies with which the boundary can be perturbed without seriously affecting the transition. This latter effect is, in fact, observed in the experiments of Spangler and Wells (4) although their disturbances were acoustic in nature. The sudden dips evidenced in Figures 12 and 13 will be explained later.

The data of Erens and Chasteau (30) are included in Figure 13 for comparison. These data were obtained at $y/\delta = 0.2$ on a flat plate which was subjected to a free-stream turbulence level of $u'/u_\infty = 0.4\%$. A narrow band filter was used to determine the growth of disturbances at a given frequency from the hot wire signal. It was noted that the disturbances in the boundary layer at given frequency were approximately 10 times the level in the free stream. Because the minima of

the data for the two values of the frequency parameter $\omega^*/R_{\delta^*}$ were not available, some liberty was taken in their normalization in Figure 13. The data for $\omega^*/R_{\delta^*} = 62 \times 10^{-6}$ do not follow the trends of either the forced or unforced cases; whereas, at $\omega^*/R_{\delta^*} = 83.5 \times 10^{-6}$ the data follow the forced expectation. The extent to which this agreement is fortuitous cannot be ascertained because the nature of the disturbances was not extensively documented. Therefore, at best the comparisons are speculative and inconclusive.

Figure 14 shows development of the Reynolds stress corresponding to the conditions of Figure 12. The largest variations are found in the region $0.2 \leq y/\delta \leq 0.8$ of the boundary layer and, thus, appear to extend over a greater fraction of $\delta$ than the major velocity fluctuations. The growth rates are observed to be very sensitive to the frequency parameter, $\omega^*/R_{\delta^*}$. The variations in one part of the boundary layer appear to have little influence on the adjacent part of the layer. Based on the discussion of (14), if $\overline{u^{(1)}v^{(1)}} < 0$ is interpreted as a production term which adds energy to the disturbance and $\overline{u^{(1)}v^{(1)}} > 0$ as a dissipation of energy in the disturbance, (as here, $\partial u^\circ/\partial y > 0$), then we observe that a given $y/\delta$ can switch rapidly between dissipation and production as $R_{\delta^*}$ increases. Finally, it is noted that the Reynolds stresses extended further into the free stream than the velocity perturbation but because of the

smallness of $\partial u^{\circ}/\partial y$ they add little energy to the perturbation from the free stream. Figures 12, 13, and 14 indicate that the strongest interaction of the flow with the free-stream disturbance occurs in the inner one-half or two-thirds of the boundary layer.

More insight into the interaction of the mean flow with the free-stream disturbances can be obtained from consideration of the perturbation profiles. The development of the root-mean-square velocity profiles, $u_{rms}$ with $R_{\delta *}$, is illustrated in Figure 15. The most obvious feature is the increasing complexity of the profiles with increasing $R_{\delta *}$. The increasing number of peaks in the profiles suggest the cause of the dips observed in the curves of Figures 12 and 13, i.e. the dips occur when one of the valleys between peaks occurs at a given value of $y/\delta$. This separation of the $u_{rms}$ profile into several peaks indicates that energy is being concentrated in discrete portions of the boundary layer. The peak of largest magnitude can be observed to move toward the wall as $R_{\delta *}$ increases. The closer to the wall it moves the bigger a fraction of the composite flow it will become; and hence, the more likely it will cause distortion of the mean profile. The magnitude of this largest peak is 10 to 20 times the free-stream value; a condition consistent with the observations of Erens and Chasteau (30). It is also noted that a maximum magnitude is reached and then the magnitude of

the profile begins to decrease with $R_{\delta*}$. Finally, the perturbation is observed to be confined to a smaller fraction of $\delta$ as $R_{\delta*}$ increases.

The Reynolds stress profiles $\overline{u^{(1)}v^{(1)}}$ computed from Eqn. (34) and corresponding to the $u_{rms}$ profiles of Figure 15 are given in Figure 16. The fluctuations in $\overline{u^{(1)}v^{(1)}}$ can be seen to increase and to contain a greater positive part with $R_{\delta*}$ increasing. The largest magnitude of $\overline{u^{(1)}v^{(1)}}$ is positive indicating a strong dissipation in portions of the boundary. This is the mechanism by which the energy of the perturbation becomes partitioned in the layer. The positive fluctuations of $\overline{u^{(1)}v^{(1)}}$ are seen to correspond to valleys in the $u_{rms}$ profiles and the negative fluctuations to peaks in $u_{rms}$. Similarly to the $u_{rms}$ variations, the maximum fluctuations in $\overline{u^{(1)}v^{(1)}}$ tend to move closer to the wall and are confined to a smaller fraction of $\delta$ with $R_{\delta*}$ increasing.

The effects of the interaction with the free-stream disturbance on the mean profile is illustrated in Figures 17 through 20 which displays the composite parallel velocity profiles, $u = u^{\circ} + \varepsilon u_{rms}$. Profiles are given in Figures 17 and 18 for $\varepsilon = .01$ and in Figures 19 and 20 for $\varepsilon = .001$ at $\omega^*/R_{\delta*} = 62 \times 10^{-6}$ and $83.5 \times 10^{-6}$, respectively. Clearly, the effects of the perturbations depend strongly upon $\varepsilon$ and $\omega^*/R_{\delta*}$ where deviations of up to 18% in the mean profiles are observed. The shapes observed in Figures 17c and 18a, for

example, are similar to those expected in transitional flow. Certainly, such profiles containing inflection points are very unstable and cannot be supported for long; however, it is questionable whether the liner perturbation analysis employed here remains valid. The lower values of $\varepsilon$(= .001) do not produce such drastic changes in profile shape as $\varepsilon$ = .01, but rather the effects are postponed until larger $R_{\delta*}$ (large $u_{rms}$ peaks) and tend to produce "lumps" on the basic profile. These effects are clearly dependent upon $\varepsilon$ and $\omega^*/R_{\delta*}$ and tend to reflect similar effects of frequency and disturbance magnitude observed in the experiments of Spangler and Wells (4). Perhaps with a certain amount of audacity, a transition correlation reflecting these effects on transition can be built up from a basis in the present computations.

# IV. CONCLUSIONS AND RECOMMENDATIONS

## Conclusions

In the previous sections, the local approximation to the general Orr-Sommerfeld equation has been considered and was found to compare favorably with other more general approximations. The numerical solution of the model equation employed an expansion of the dependent variable in a finite series of shifted Chebyshev polynomials of the first kind rather than the usual finite difference approach. Solutions based upon this technique were found to be highly accurate and easily obtainable. The higher temporal eigenvalues and eigenfunctions have been obtained utilizing the QR matrix algorithm of Francis. It was assumed that these eigenfunctions corresponded to a discrete, single valued spectrum of the operator $L(\alpha,y)$ and the eigenfunctions form a complete set for the range of $L(\alpha,y)$. The forced problem corresponding to a traveling wave in the free stream was then expanded in the binormal system of eigenfunctions and adjoint conjugate eigenfunctions. Unfortunately, the lack of experimental data precludes assessment of the adequacy of the model.

Based upon the discussion of Section III, the following conclusions may be obtained:

1. Accurate solutions of the Orr-Sommerfeld Equation may be obtained by expansion of the dependent variables

in a series of Chebyshev polynomials. Use of the expansion is straightforward and requires no involved difference schemes (e.g. see Kurtz (26)).

2. Use of the QR algorithm removes the necessity for iteration or serves to provide an excellent first approximation to the eigenvalues. It has the additional advantage of providing several of the higher order eigenvalues simultaneously.

3. Accuracy of the higher eigenvalues can be checked by comparison with the adjoint conjugate eigenvalues computed in a similar manner. This can be extremely important in detailed investigation of the spectrum of the Orr-Sommerfeld Operator.

4. The amplitude function or growth rate of the forced case is dependent upon the y coordinate; whereas, the unforced case is independent of y. The amplitude in the forced case can exceed those expected in the unforced case and may even show amplification in regions where the unforced case is damped.

5. The Reynolds stresses provide the mechanism by which the energy of the forced disturbances become partitioned into discrete layers within the boundary layer.

6. The behavior of sinusoidal disturbances moving at the free-stream velocity has similar qualitative frequency and amplitude dependent effects on the composite velocity

profiles as acoustic disturbances have upon transition data of Spangler and Wells (4).

Recommendations

1. The vector inner products associated with the matrix operations should be accumulated in extended precision so that a larger number of terms can be taken in the eigenfunction expansion.

2. The model should be extended to include three-dimensional disturbances.

3. A model which would accommodate acoustic disturbances would provide a better opportunity for comparison with experiment as well as provide insight into an important aerodynamic phenomenon.

# BIBLIOGRAPHY

## BIBLIOGRAPHY


1. Schubauer, G. B. and Skramstad, H. K. "Laminar Boundary Layer Oscillations and Transition on a Flat Plate." NACA Report No. 909, 1948.

2. DeMitz, F. C. and Casarella, M. J. "An Experimental Study of the Intermittent Properties of the Boundary Layer Pressure Field During Transition on a Flat Plate." Naval Ship Research and Development Center, Report No. 4140, November, 1973.

3. Wells, C. S. "Effects of Freestream Turbulence on Boundary Layer Transition," AIAA Journal, 5:172-174, January, 1967.

4. Spangler, J. G. and Wells, C. S. "Effects of Free Stream Disturbances on Boundary Layer Transition," AIAA Journal, 6:543-545, March, 1968.

5. Pate, S. R. and Schueler, C. J. "Radiated Aerodynamic Noise Effects on Boundary Layer Transition in Supersonic and Hypersonic Wind Tunnels," AIAA Journal, 7:450-457, March, 1968.

6. Pate, S. R. "Induced Boundary Layer Transition at Supersonic Speeds: Combined Effects of Roughness and Free Stream Disturbances." AIAA Paper No. 70-586, AIAA 5th Aerospace Testing Conference, Tullahoma, Tennessee, May, 1970.

7. Benek, J. A. and High, M. D. "Transition Prediction Technique," AIAA Journal, 12:1425-1427, October, 1974.

8. Werle, M. J., Mook, D. T., and Tang, H. "Effect of Free Stream Vorticity on Boundary-Layer Stability," VPI-E-72-2 (PB 209 707) College of Engineering, Virginia Polytechnic Institute and State University, Blacksburg, Virginia, February, 1972.

9. Criminale, W. O. "Interaction of the Laminar Boundary Layer with Free Stream Turbulence," Physics of Fluids Supplement, (1967), S101-S107.

10. Criminale, W. O. "On Structure of the Laminar Boundary Layer in the Presence of a Fluctuating Free Stream," IUTAM Symposium on Unsteady Boundary Layers, Quebec, Canada, May, 1971.

11. Mack, L. M. "Progress in Compressible Boundary Layer Stability Computations," Proceedings, Boundary Layer Transition Workshop, W. D. McCauley, editor. Vol. 4. Aerospace Report TDR 0172, 1971.

12. Kendal, J. M. "Wind Tunnel Experiments Relating to Supersonic and Hypersonic Boundary Layer Transition." AIAA Paper No. 73-133, AIAA Aerospace Sciences Meeting, Washington, D. C., January, 1974.

13. Lin, C. C. The Theory of Hydrodynamic Stability. Cambridge, Massachusetts: Cambridge University Press, 1966.

14. Mack, L. M. "Boundary Layer Stability Theory," JPL Report No. 900-277, Rev. A, Jet Propulsion Laboratory, Pasadena, California, November, 1969.

15. Grosh, C. E. and Salwen, H. "The Stability of Steady and Time-Dependent Plane Poiseuille Flow," J. Fluid Mech., Part I, 34: 171-206, 1968.

16. Orszag, S. A. "Accurate Solution of the Orr-Sommerfeld Stability Equation," J. Fluid Mech., Part IV, 50: 689-703, 1971.

17. Orszag, S. A. and Israeli, M. "Numerical Simulation of Viscous Incompressible Flows," Annual Reviews of Fluid Mechanics, Vol. 6, Palo Alto, California: Annual Reviews, Inc., 1974. p. 281.

18. Fox, L. "Chebyshev Methods for Ordinary Differential Equations," Computer Journal, 4:318-331, 1962.

19. Fox, L. and Parker, I. B. Chebyshev Polynomials in Numerical Analysis. New York: Oxford University Press, 1968.

20. Lanczos, C. "Trigonometric Interpolation of Empirical and Analytical Functions," Journal of Mathematics and Physics, 17:123-199, 1938.

21. Gary, J. and Helgason, R. "A Matrix Method for Ordinary Differential Eigenvalue Problems," Journal of Computational Physics, 5:169-187, 1970.

22. Francis, J. G. F. "The QR Transform: A Unitary Analogue to the L. R. Transformation - Parts I and II," Computer Journal, 4:265-271 and 4:332-345, 1962.

23. Wilkinson, J. H. The Algebraic Eigenvalue Problem. New York: Oxford University Press, 1965.

24. Osborne, M. R. "A New Method for the Solution of Eigenvalue Problems," Computer Journal, 7:228-232, 1964.

25. Barry, M. D. J. and Ross, M. A. S. "The Flat Plate Boundary Layer, Part 2. The Effect of Increasing Thickness on Stability," J. of Fluid Mech., Part IV, 43:813-818, 1970.

26. Kurtz, E. F. and Crandall, S. H. "Computer-Aided Analysis of Hydrodynamic Stability," J. of Mathematical Physics, 41:264-279, 1962.

27. Jordinson, R. "The Flat Plate Boundary Layer. Part 1. Numerical Integration of the Orr-Sommerfeld Equation," J. of Fluid Mech., Part IV, 43:801-811, 1970.

28. Ling, C. H. and Reynolds, W. C. "Non-Parallel Flow Corrections for the Stability of Shear Flows," J. of Fluid Mech., Part III, 59:571-591, 1975.

29. Ross, J. A., Barnes, F. H., and Burns, J. G. "The Flat Plate Boundary Layer. Part 3. Comparison of Theory with Experiment," J. of Fluid Mech., Part IV, 43: 819-832, 1970.

30. Erens, P. J. and Chasteau, V. A. L. "Laminar Boundary Layer Response to Freestream Disturbances," AIAA Journal, 12:93-94, January, 1974.

31. Reid, W. H. "The Stability of Parallel Flows," Basic Developments in Fluid Dynamics, M. Holt, editor. Vol. I, New York: Academic Press, 1962. Pp. 249-307.

32. Wazzan, A. R., Taghavi, H., and Keltner, G. "Effect of Boundary Layer Growth on Stability of Incompressible Flat Plate Boundary Layer with Pressure Gradient," Physics of Fluids, 17:1655-1660, September, 1974.

33. Gaster, M. "On the Effects of Boundary Layer Growth on Flow Stability," J. of Fluid Mech., Part III, 66: 465-480, 1974.

34. Bouthier, M. "Stabilete Lineaire des Ecoulements Presque Paralleles, Partie I," Journal de Mechanique, 11: 599-621, December, 1972.

35. Bouthier, M. "Stabilete Lineaire des Ecoulements Presque Paralleles, Part II. La Couche Limite de Blasius," Journal de Mechanique, 12:75-95, January, 1973.

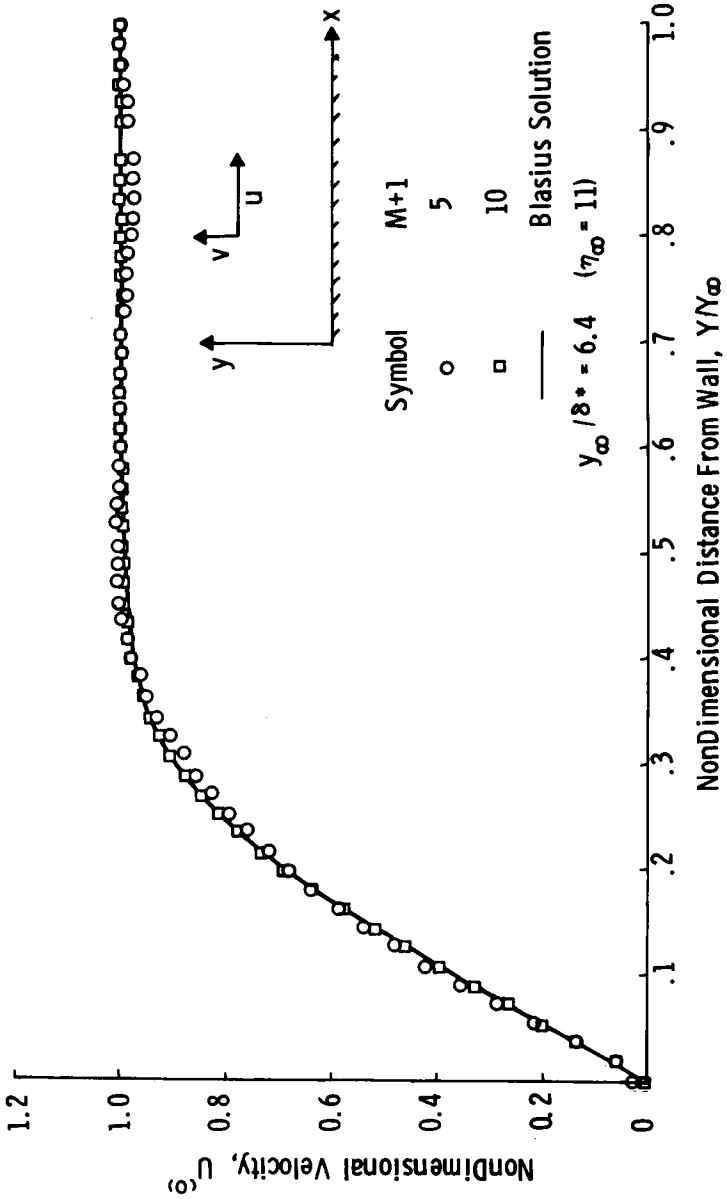
36. Morse, P. M. and Feshbach, H. Methods of Theoretical Physics. New York: McGraw-Hill Book Company, 1953.

37. Collitaz, L. Functional Analysis and Numerical Mathematics. New York: Academic Press, 1966.

# APPENDICES

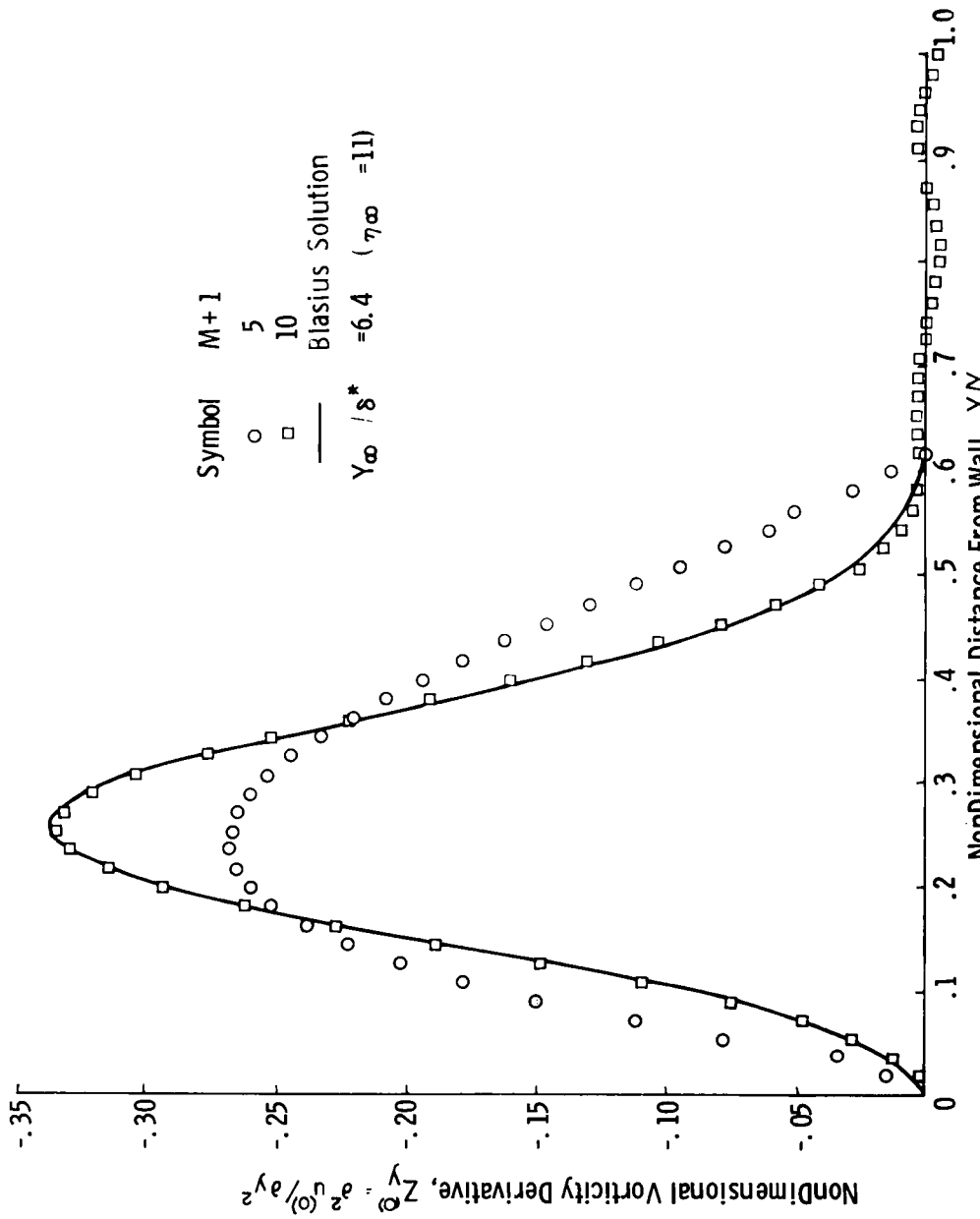
# APPENDIX A

# ILLUSTRATIONS



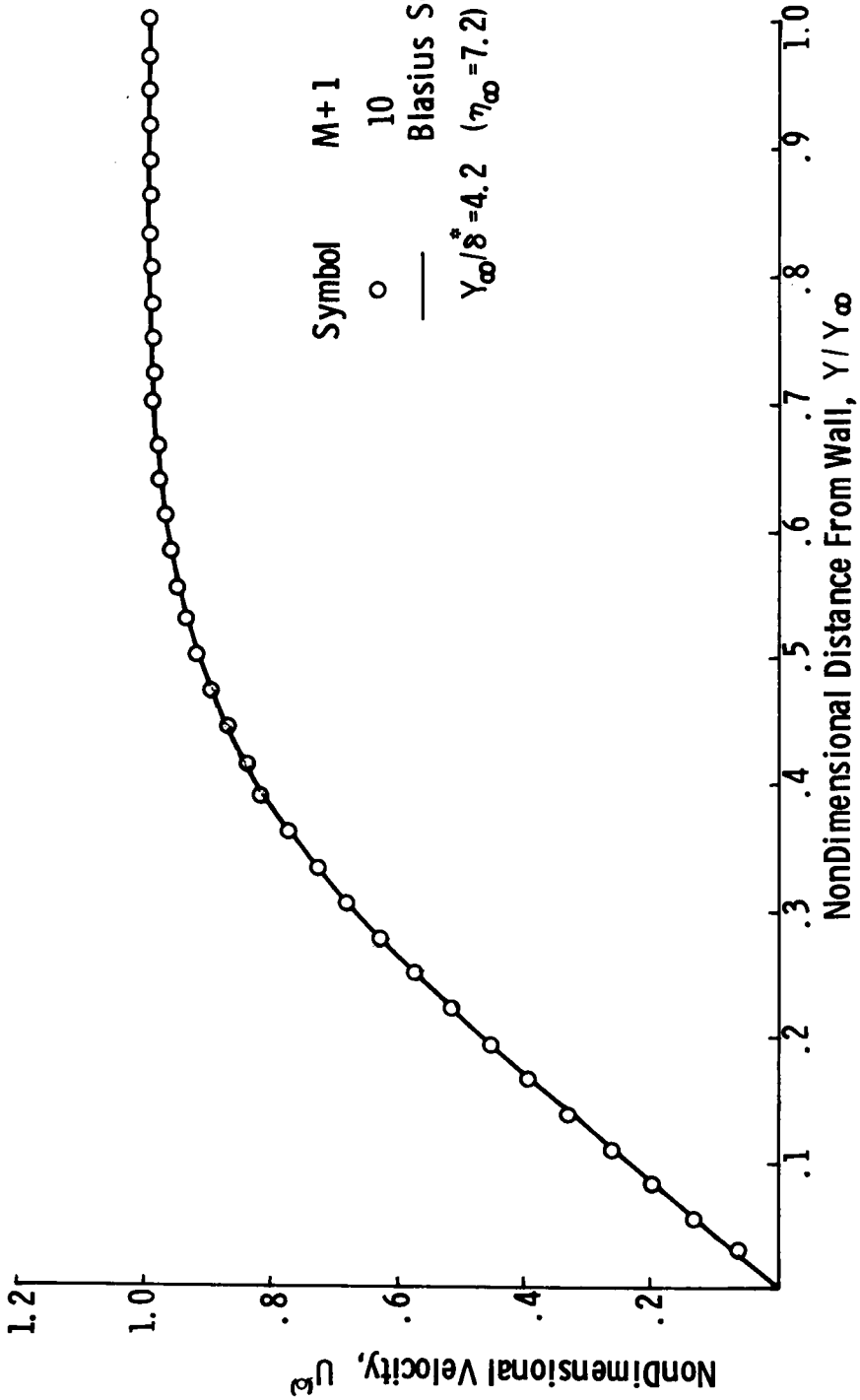

a. Velocity Profile

Figure 1. Chebyshev approximation of the zeroth order Blasius profiles for the parallel flow assumption.



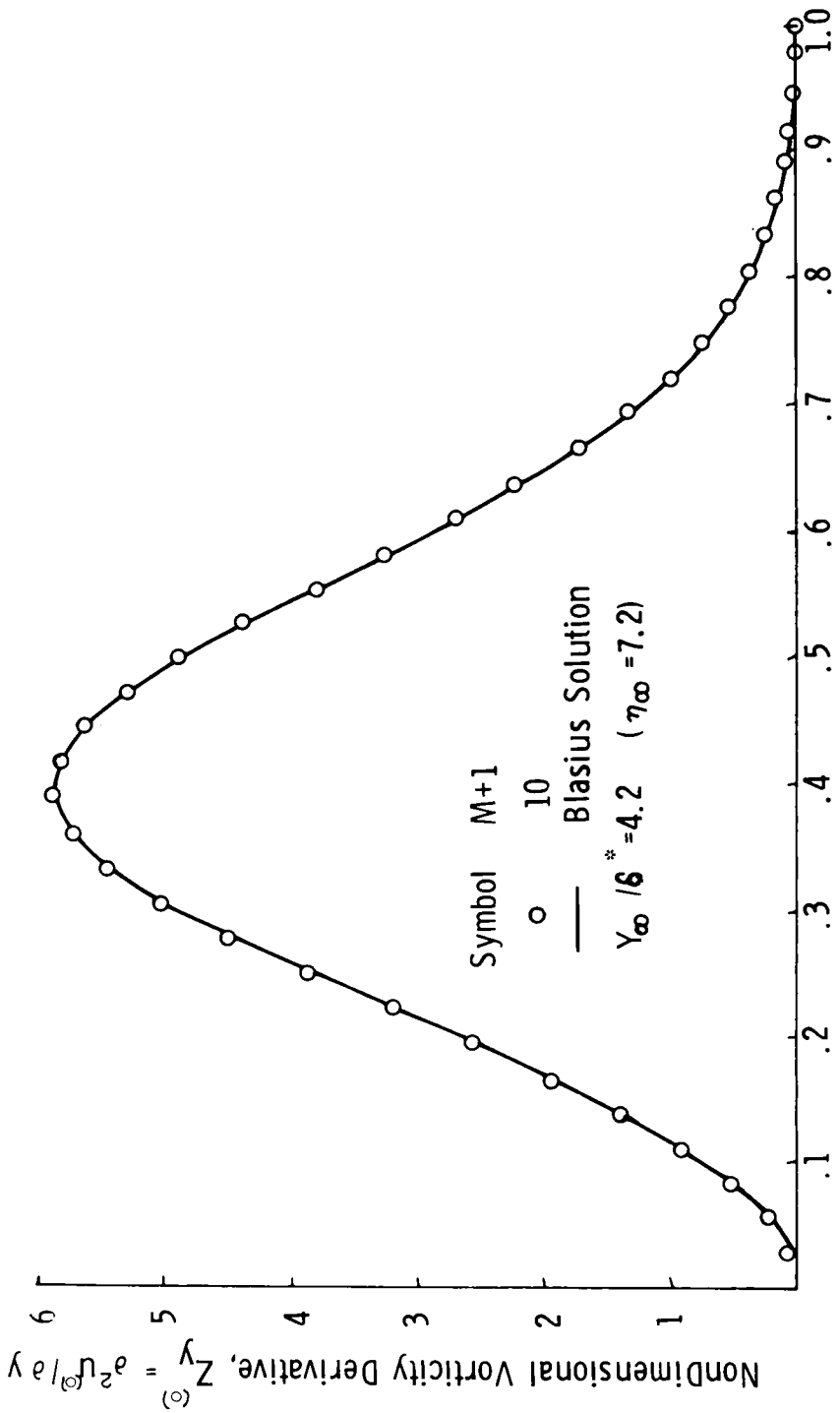

b. Vorticity Derivative Profile

Figure 1. (continued)



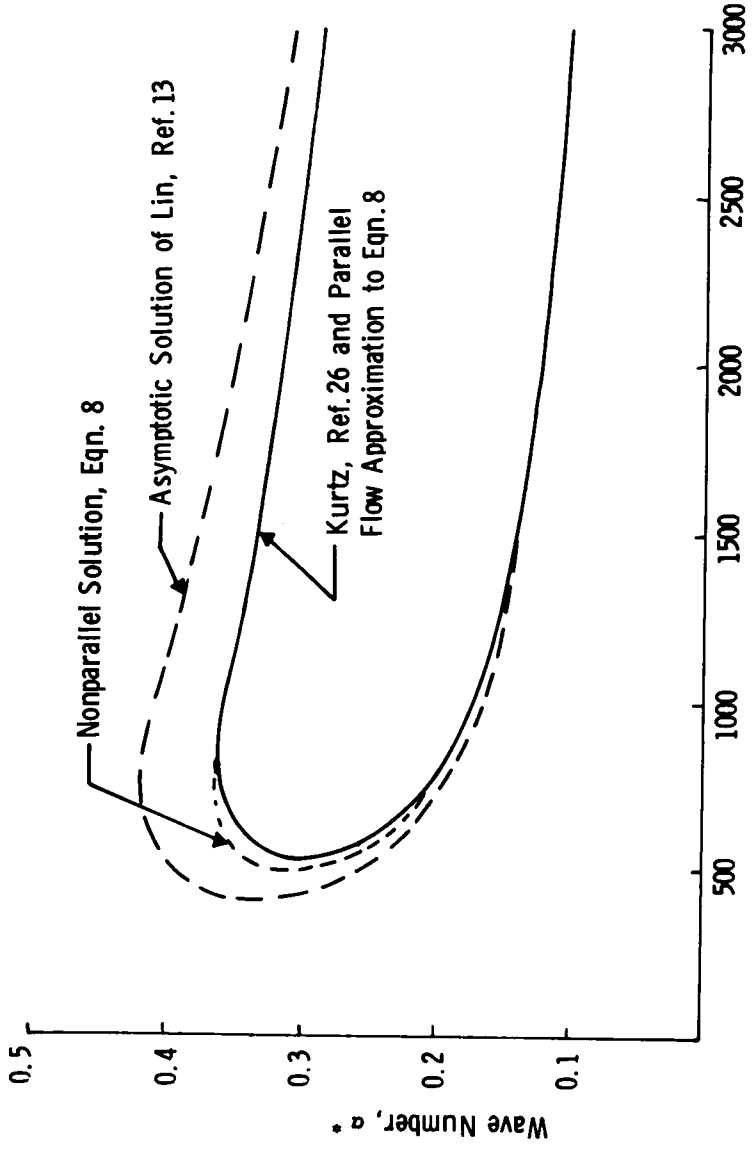

a. Velocity Profile

Figure 2. Improved Chebyshev approximation of the zeroth order profiles in the reduced interval.



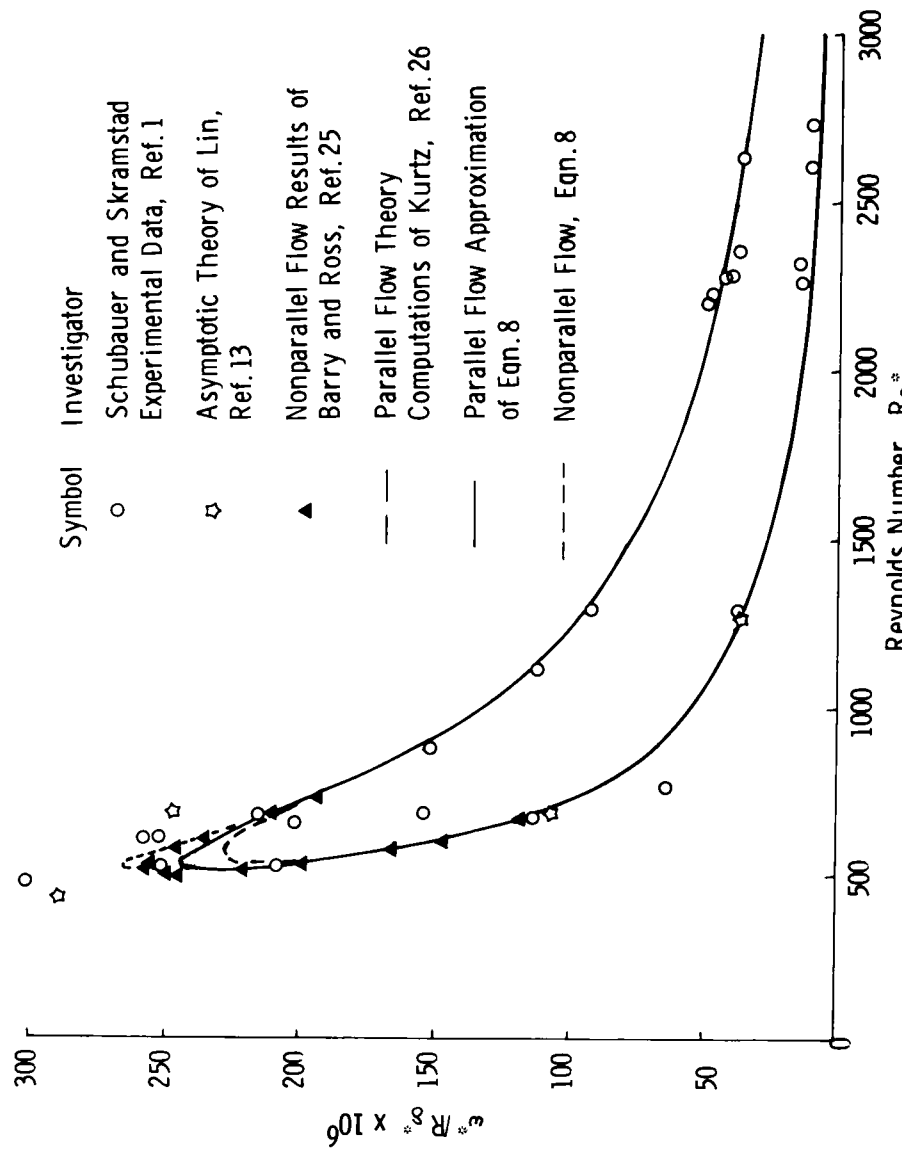

b. Vorticity Derivative Profile

Figure 2. (continued)



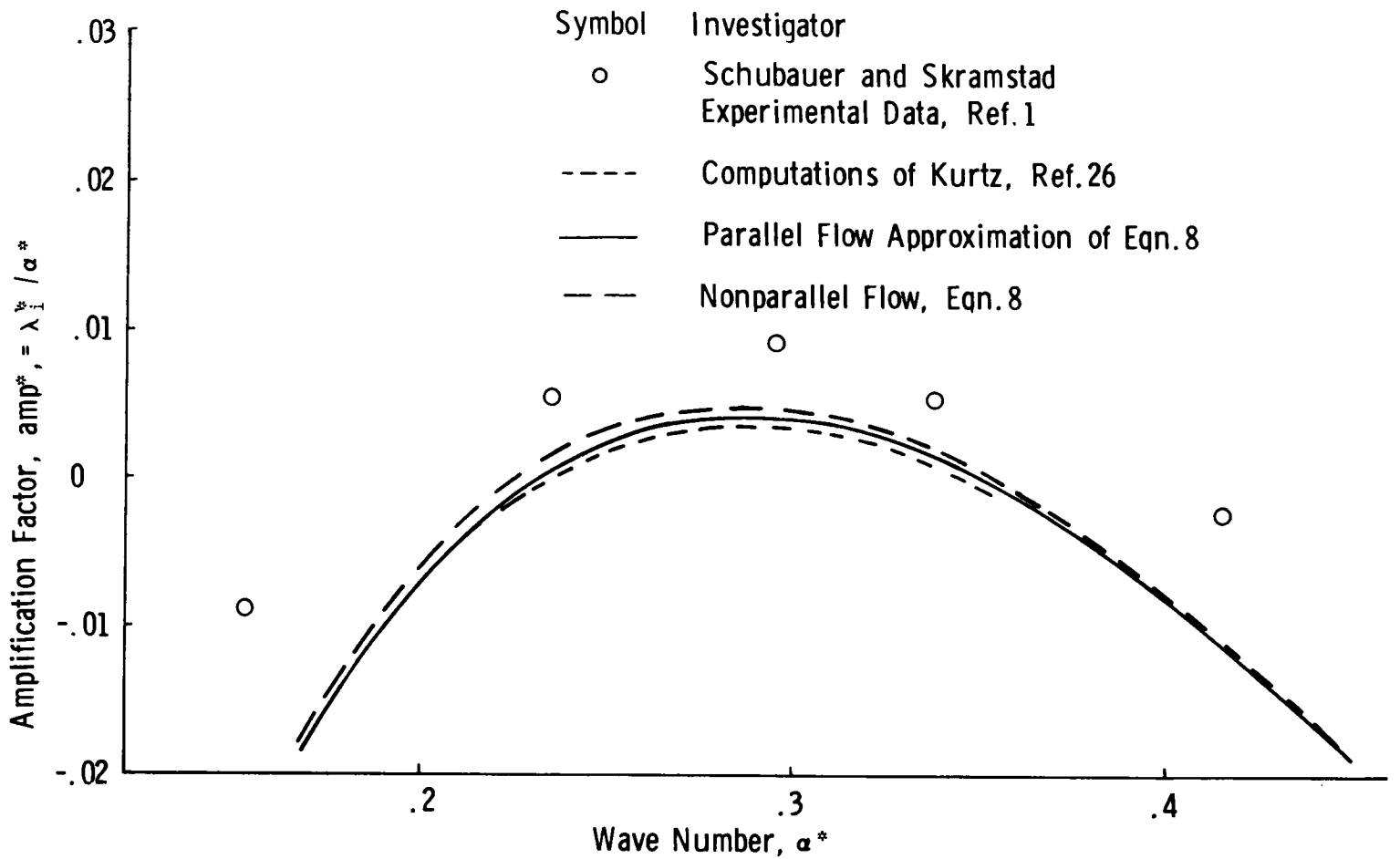

a. Neutral Curve in $\alpha^*$, $R_{\delta^*}$ Plane

Figure 3. Neutral curves for the Blasius velocity profile.



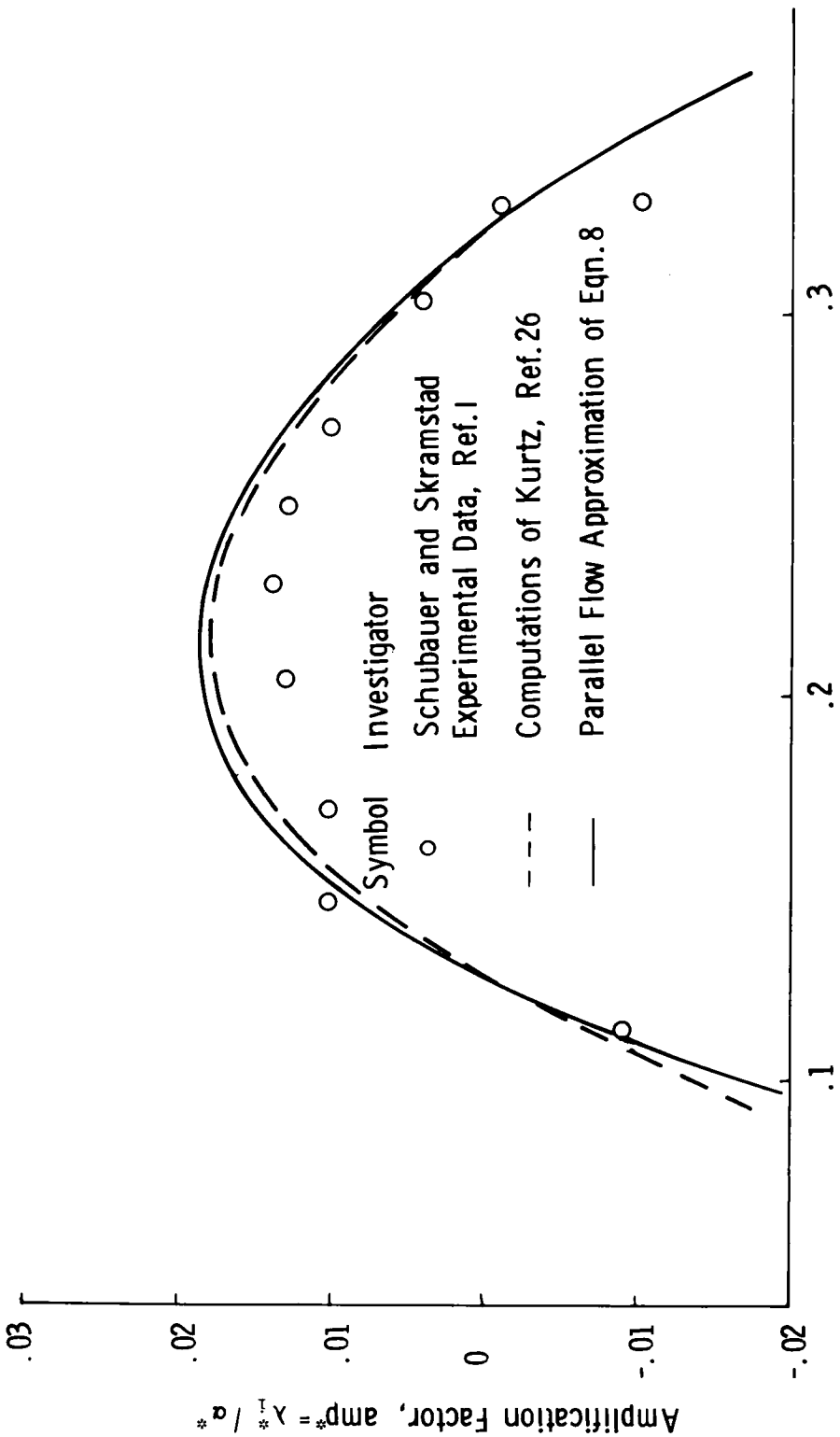

b. Neutral Curve in the $\omega^*/R_{\delta^*}$, $R_{\delta^*}$ Plane

Figure 3. (continued)



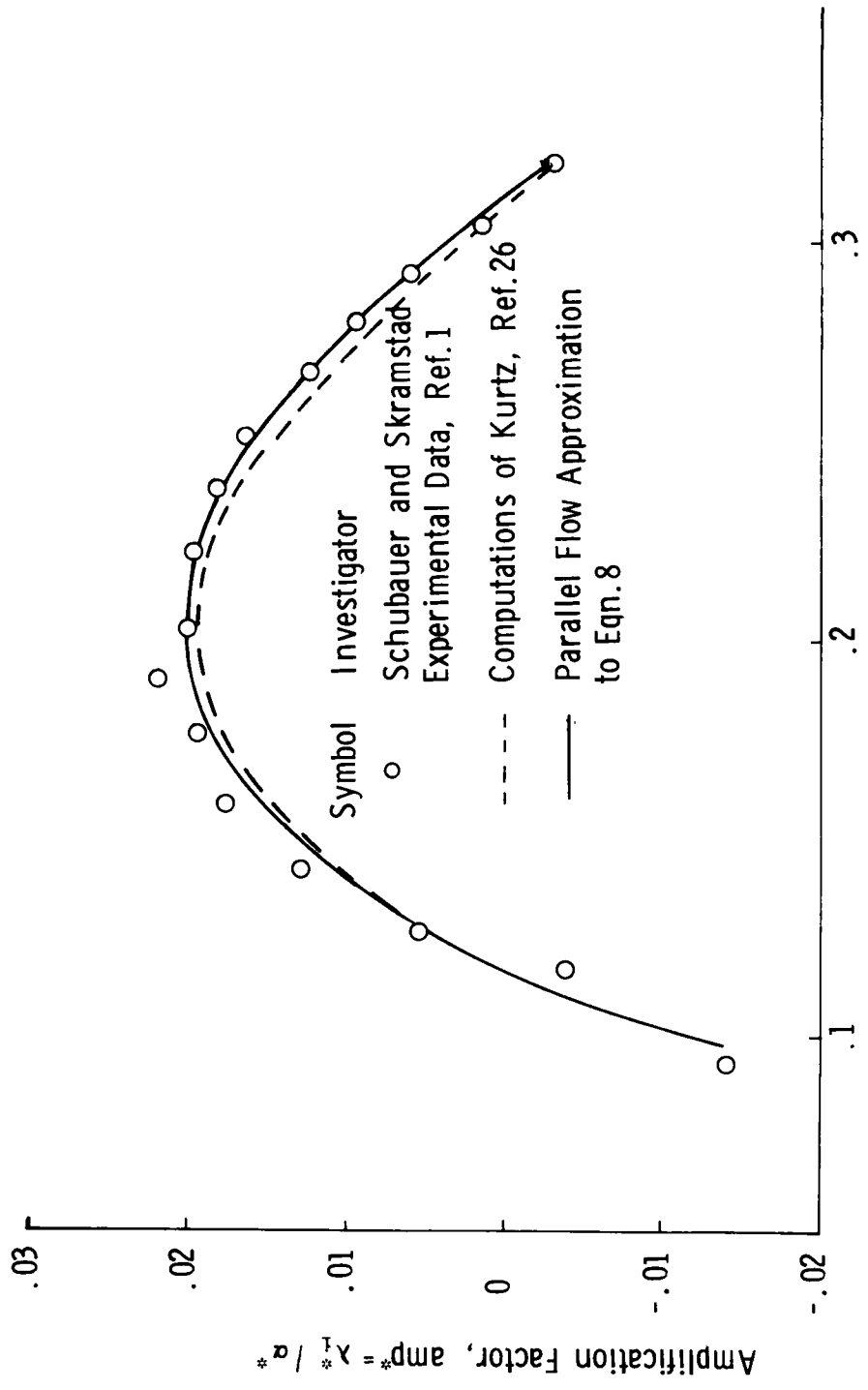

a. $R_{\delta^*} = 630$

Figure 4. Amplification factor, amp*, as a function of wave number.



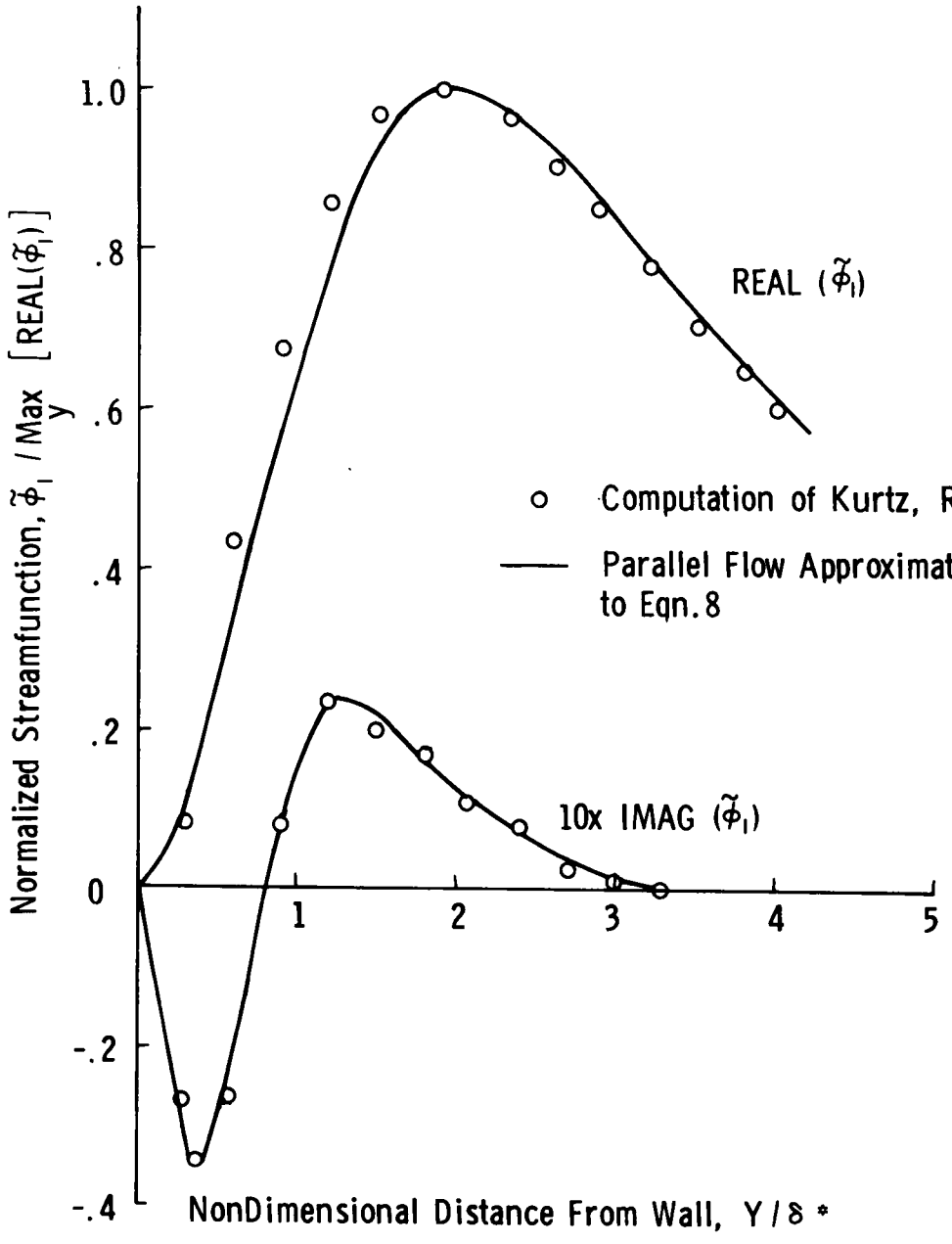

b. $R_{\delta^*} = 1840$

Figure 4. (continued)



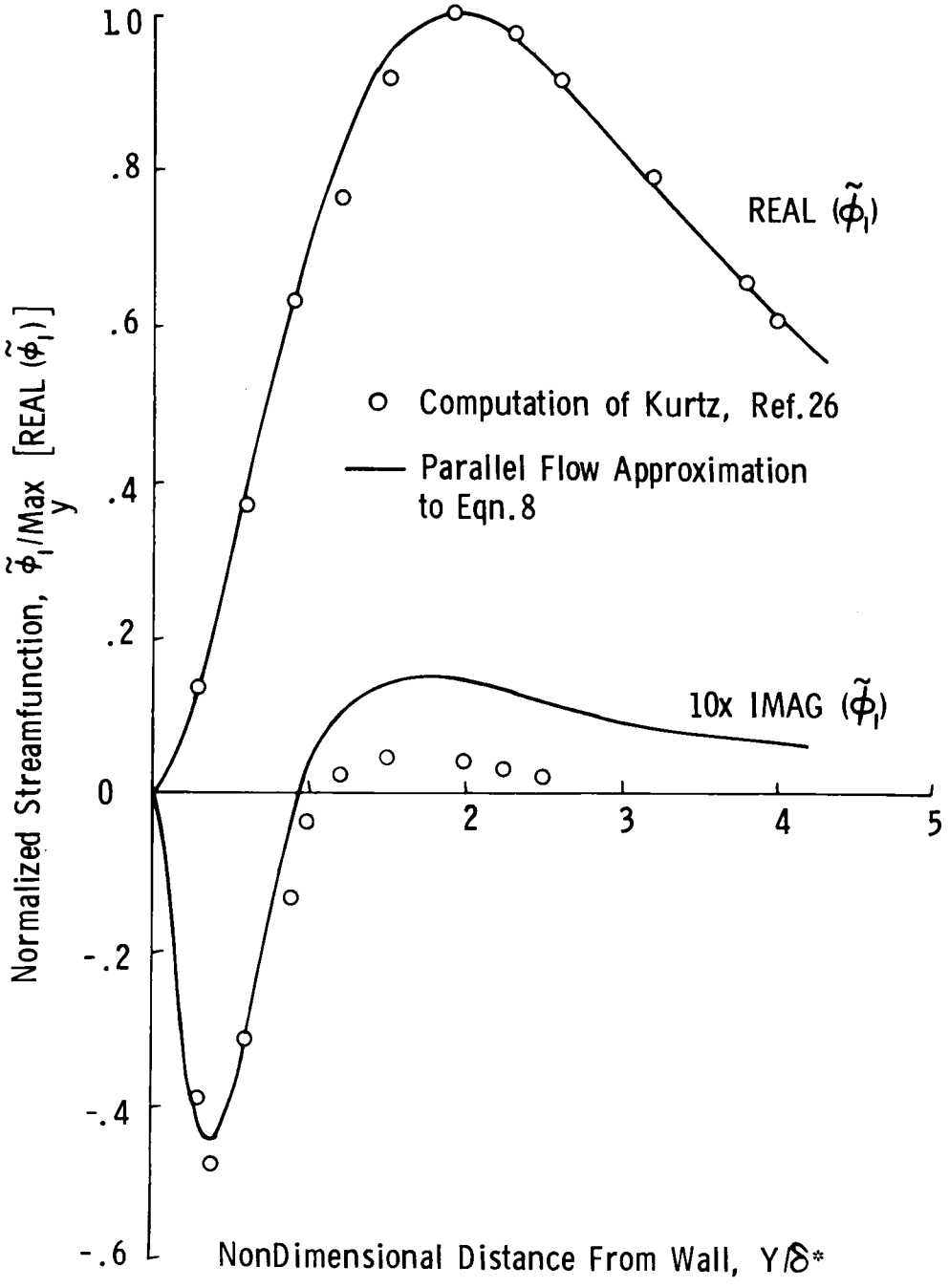

c. $R_{\delta^*}$ = 2200

Figure 4. (continued)



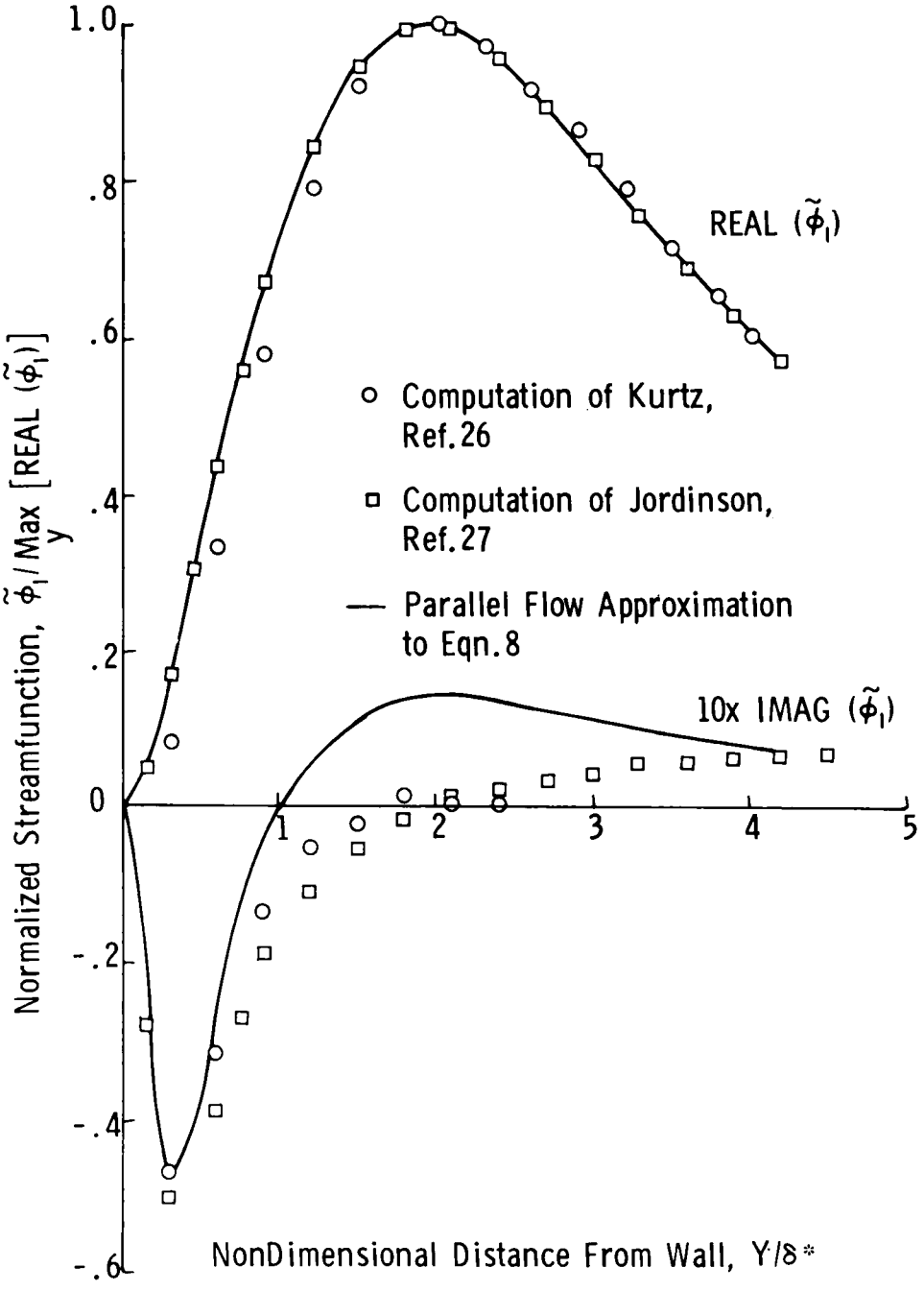

a. $\alpha^* = .308$, $R_{\delta^*} = 336$

Figure 5. Computations of the streamfunction for the sample cases of Kurtz (Ref. 26).



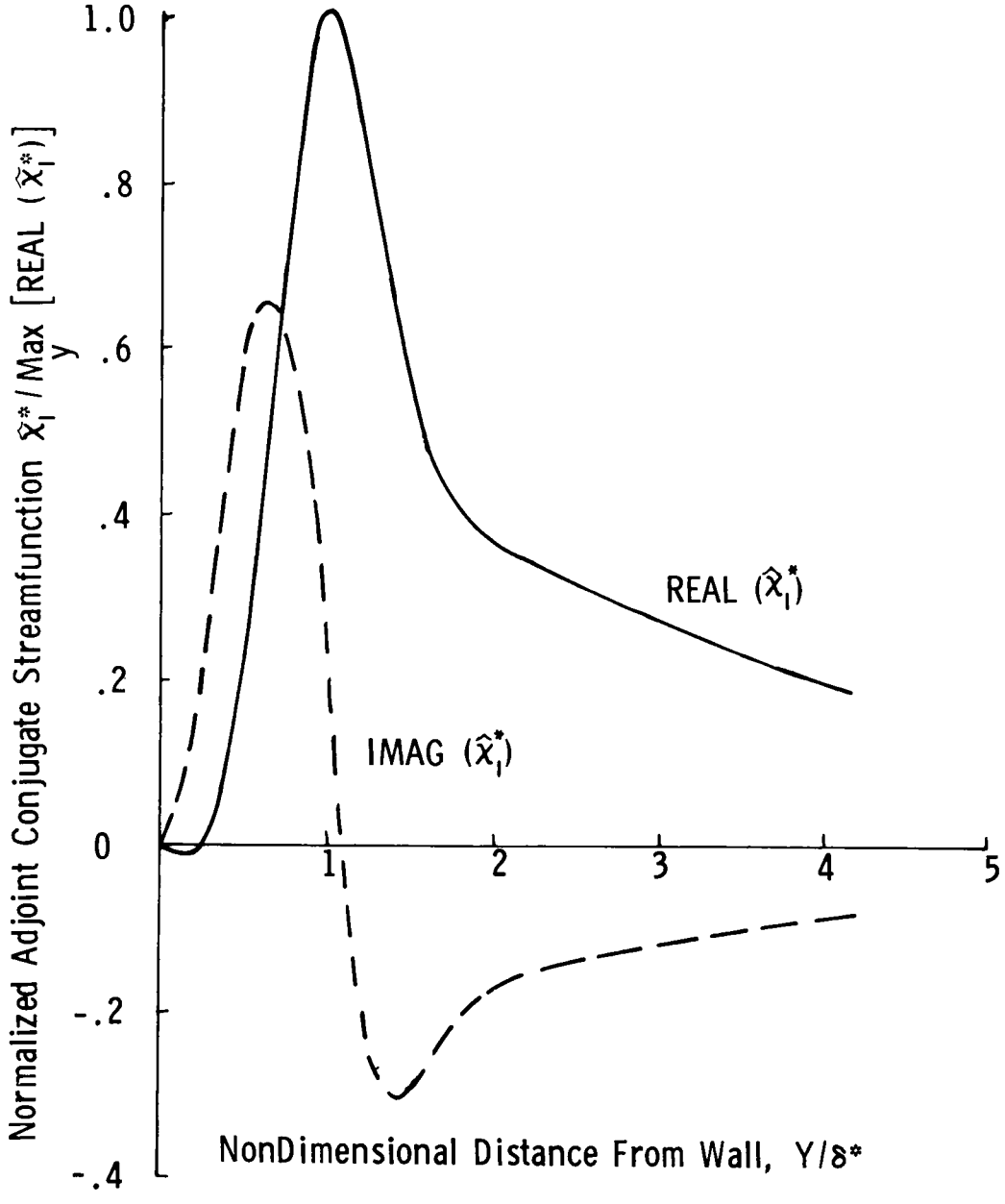

b. $\alpha^* = .308$, $R_{\delta^*} = 598$

Figure 5. (continued)



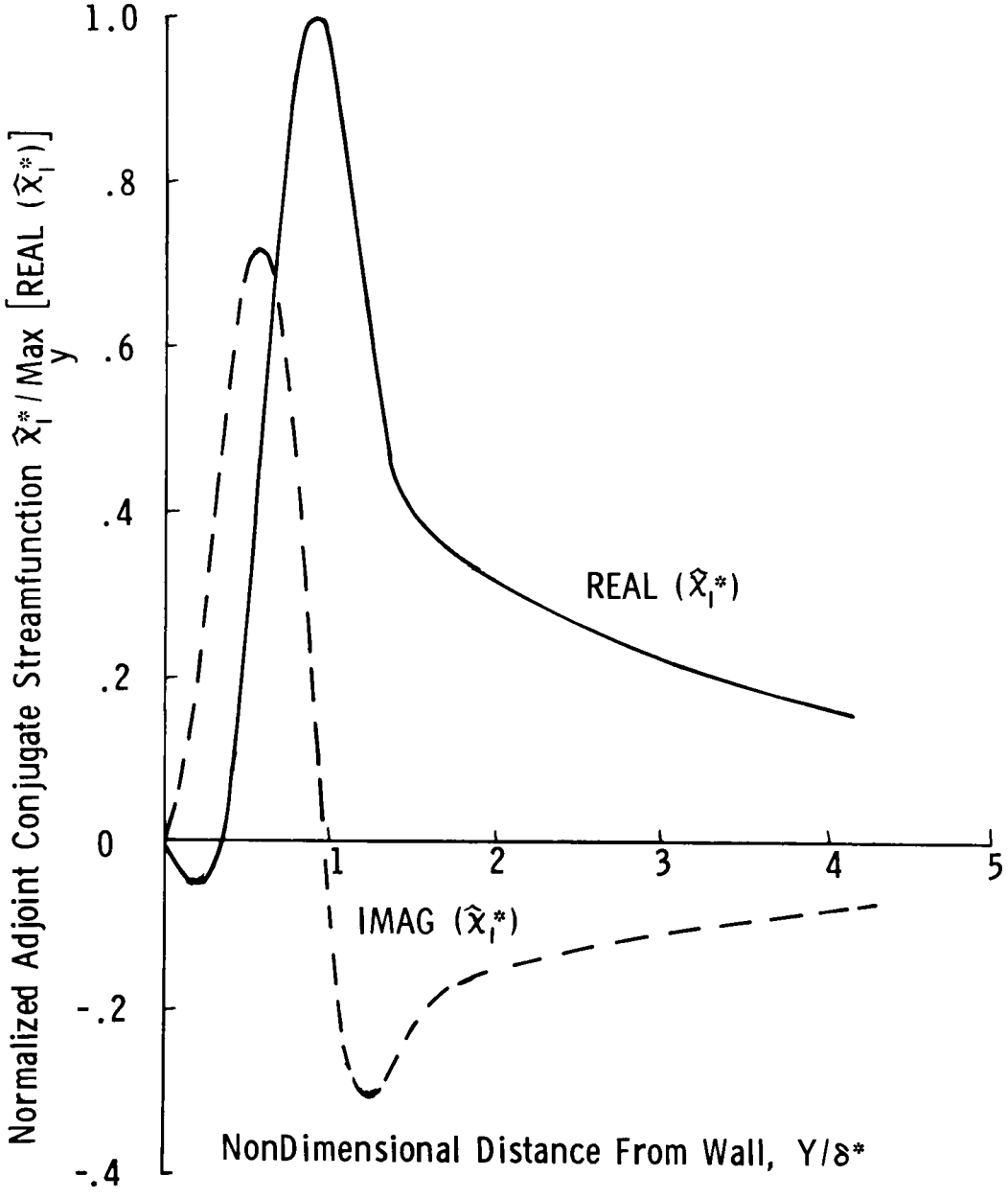

c. $\alpha^* = .308$, $R_{\delta^*} = 998$

Figure 5. (continued)



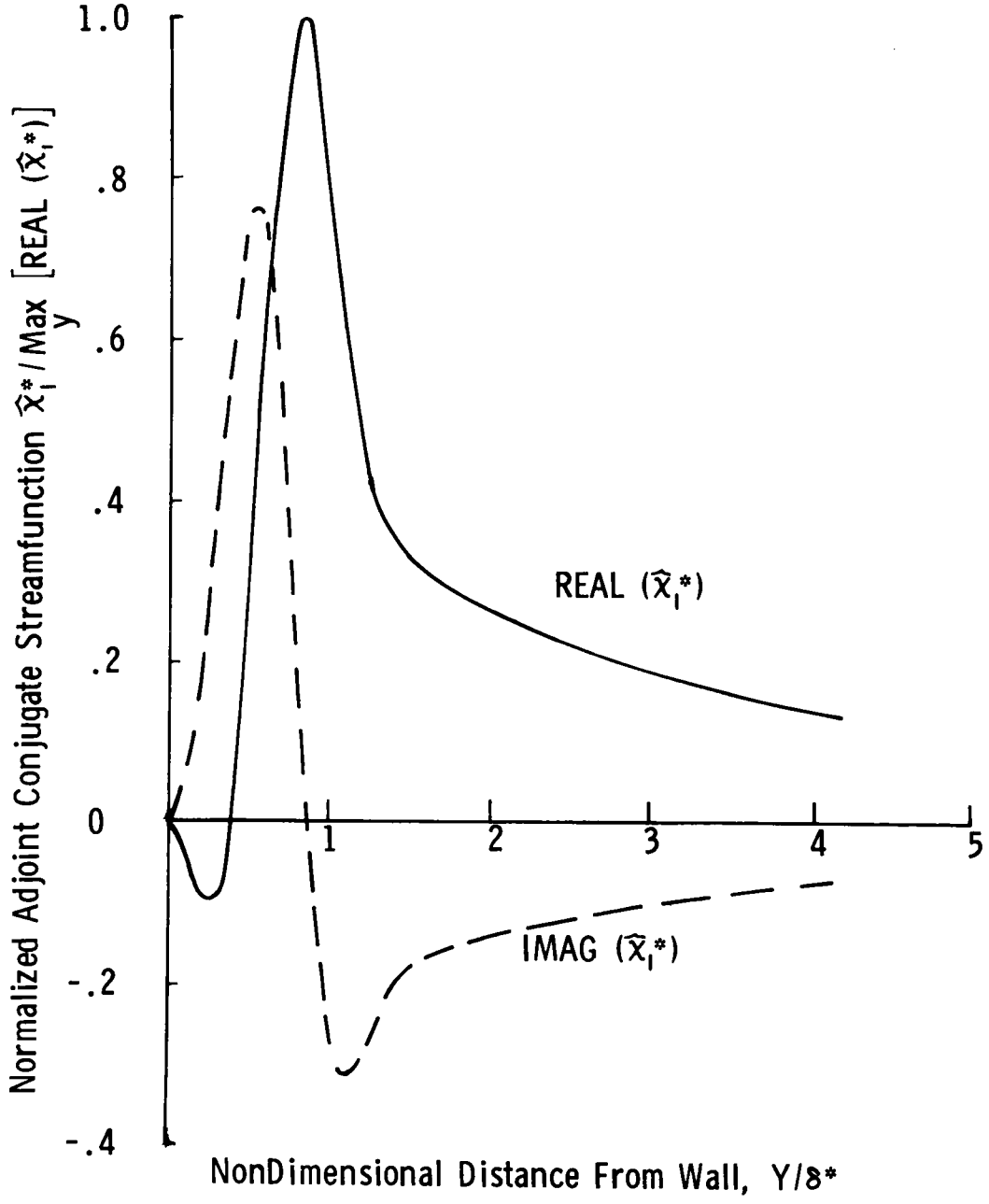

a. $\alpha^* = .308$, $R_{\delta^*} = 336$

Figure 6. Calculations of the adjoint conjugate streamfunctions for the three sample cases of Kurtz.



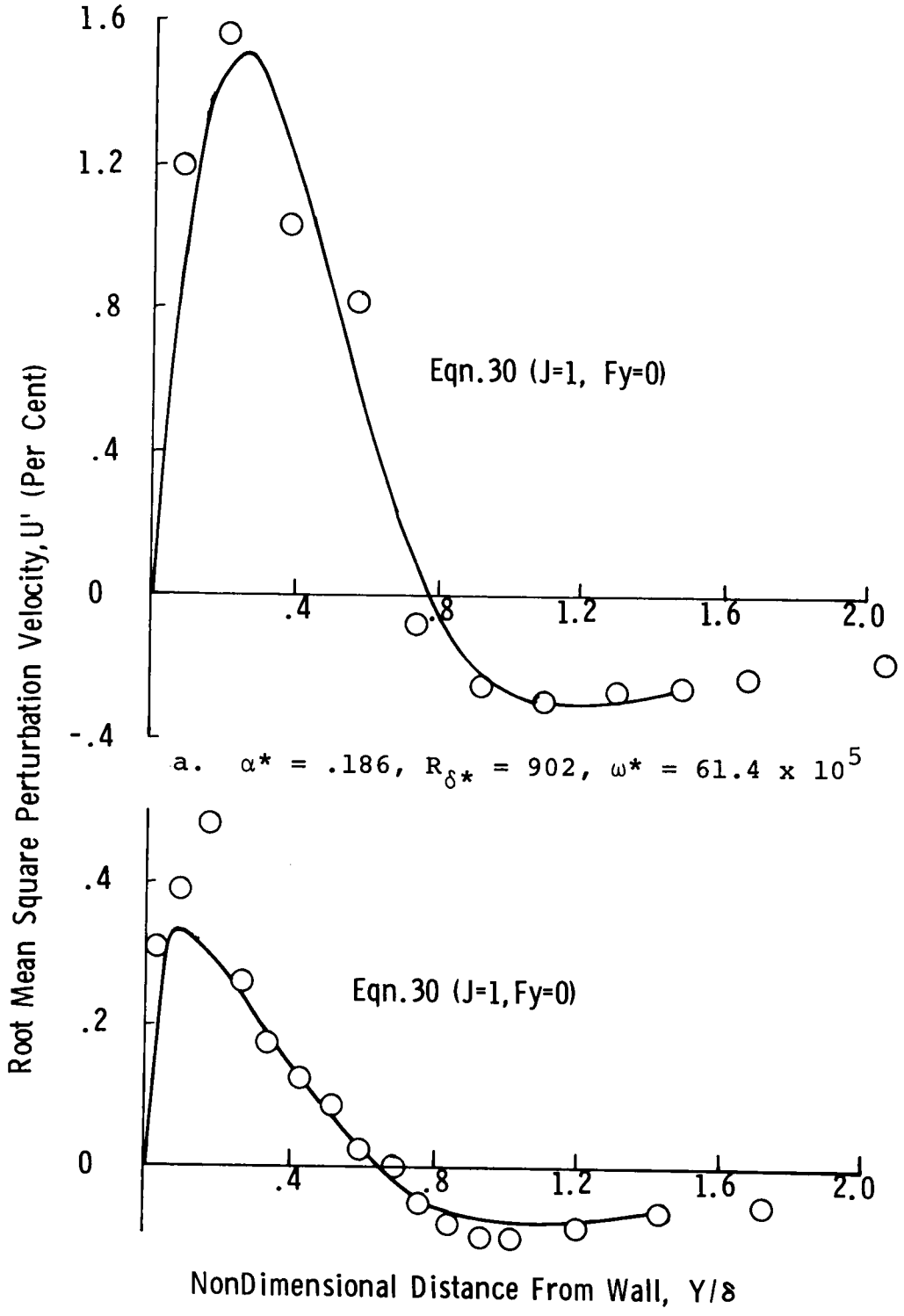

b. $\alpha^* = .308$, $R_{\delta^*} = 598$

Figure 6. (continued)




c. $\alpha^* = .308$, $R_{\delta^*} = 998$

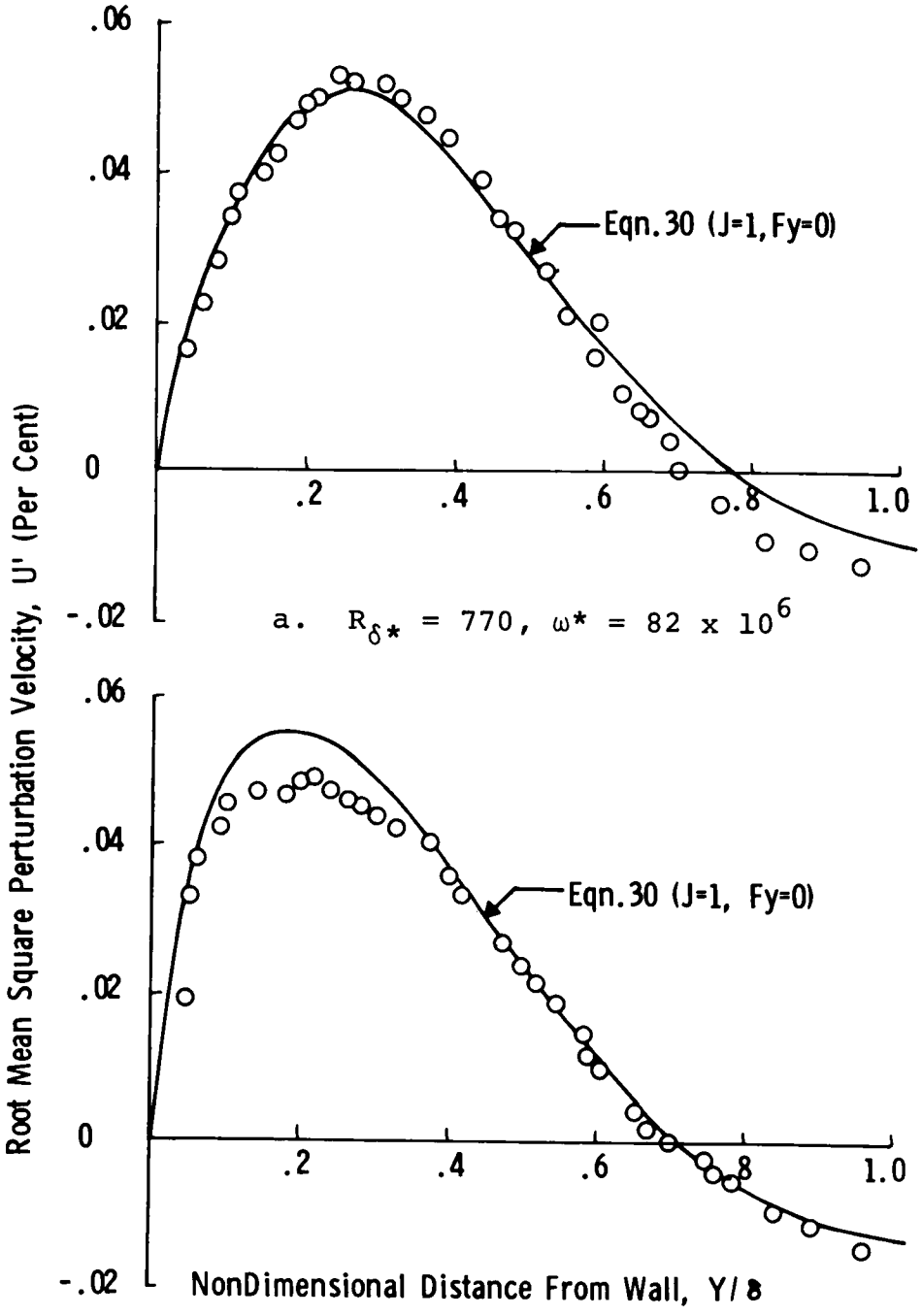
Figure 6. (continued)




a. $\alpha^* = .186$, $R_{\delta^*} = 902$, $\omega^* = 61.4 \times 10^{5}$

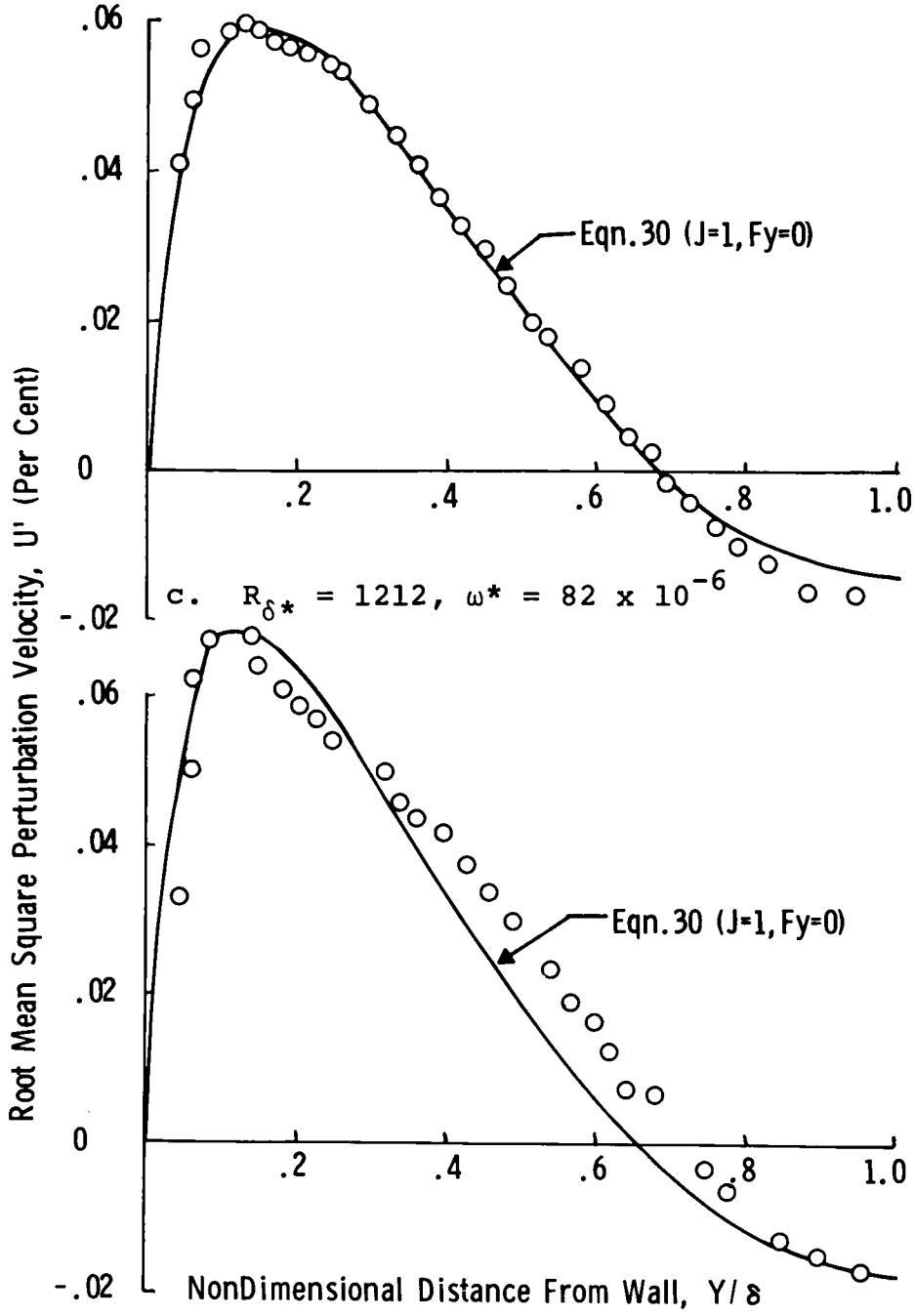
b. $\alpha^* = .315$, $R_{\delta^*} = 2080$, $\omega^* = 40.6 \times 10^{-6}$

Figure 7. Comparison of theory with rms velocity profiles of Schubauer and Skramstad (Ref. 1).




b. $R_{\delta*}$ = 1073, $\omega^*$ = 82 x $10^6$

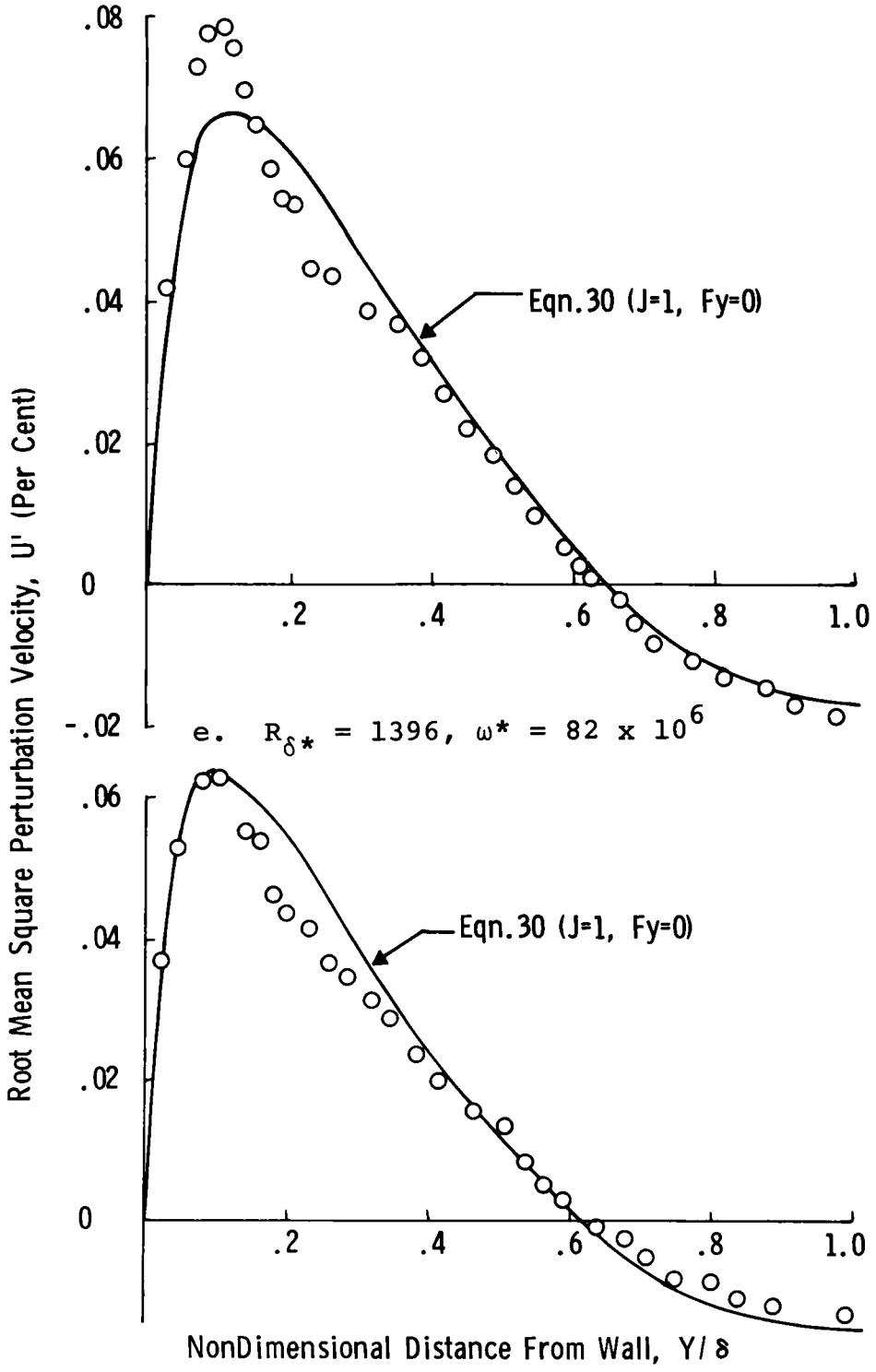
Figure 8. Comparison of theory with rms velocity profiles of Ross, et al. (Ref. 29).




c. $R_{\delta *} = 1212$, $\omega^* = 82 \times 10^{-6}$

d. $R_{\delta *} = 1363$, $\omega^* = 82 \times 10^{-6}$

Figure 8. (continued)




e. $R_{\delta*} = 1396$, $\omega^* = 82 \times 10^6$

f. $R_{\delta*} = 1555$, $\omega^* = 82 \times 10^6$

Figure 8. (continued)

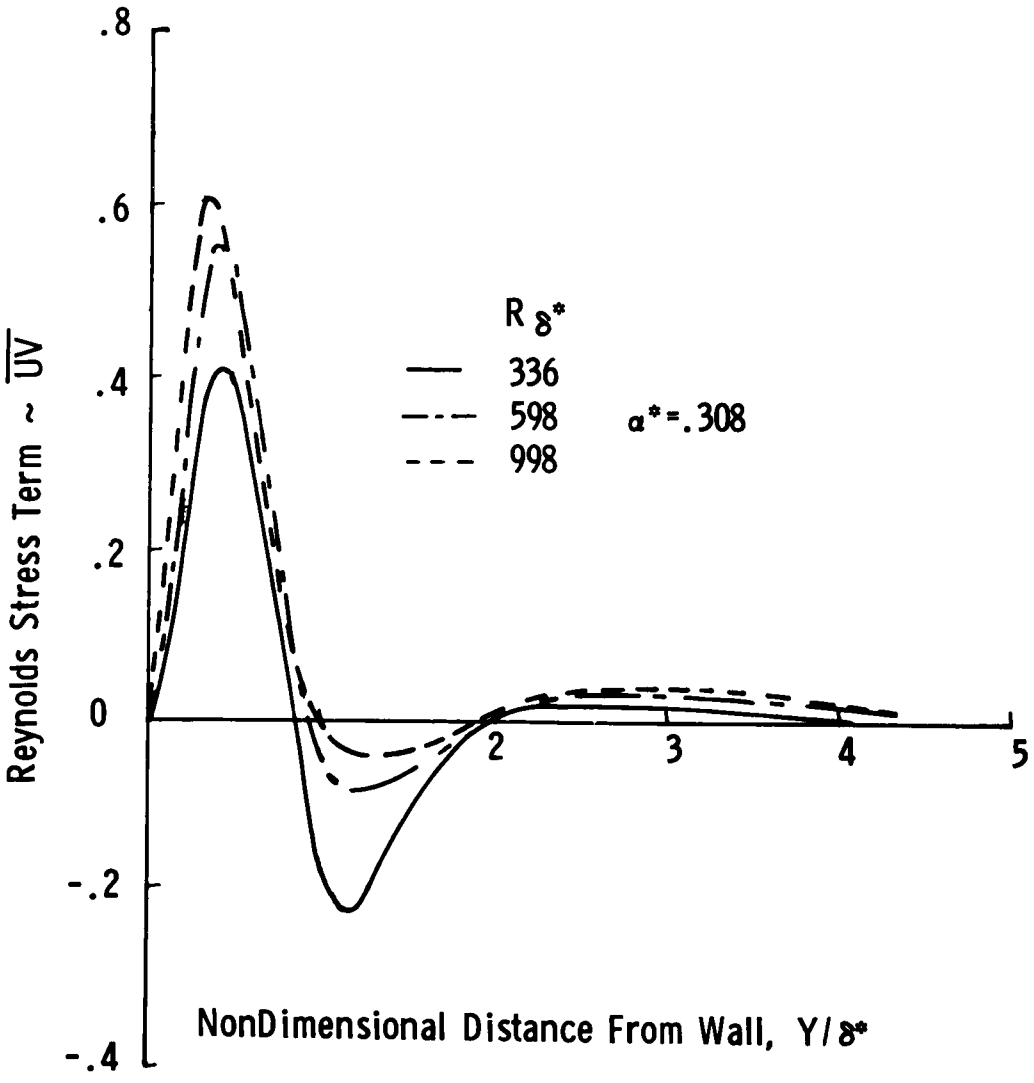
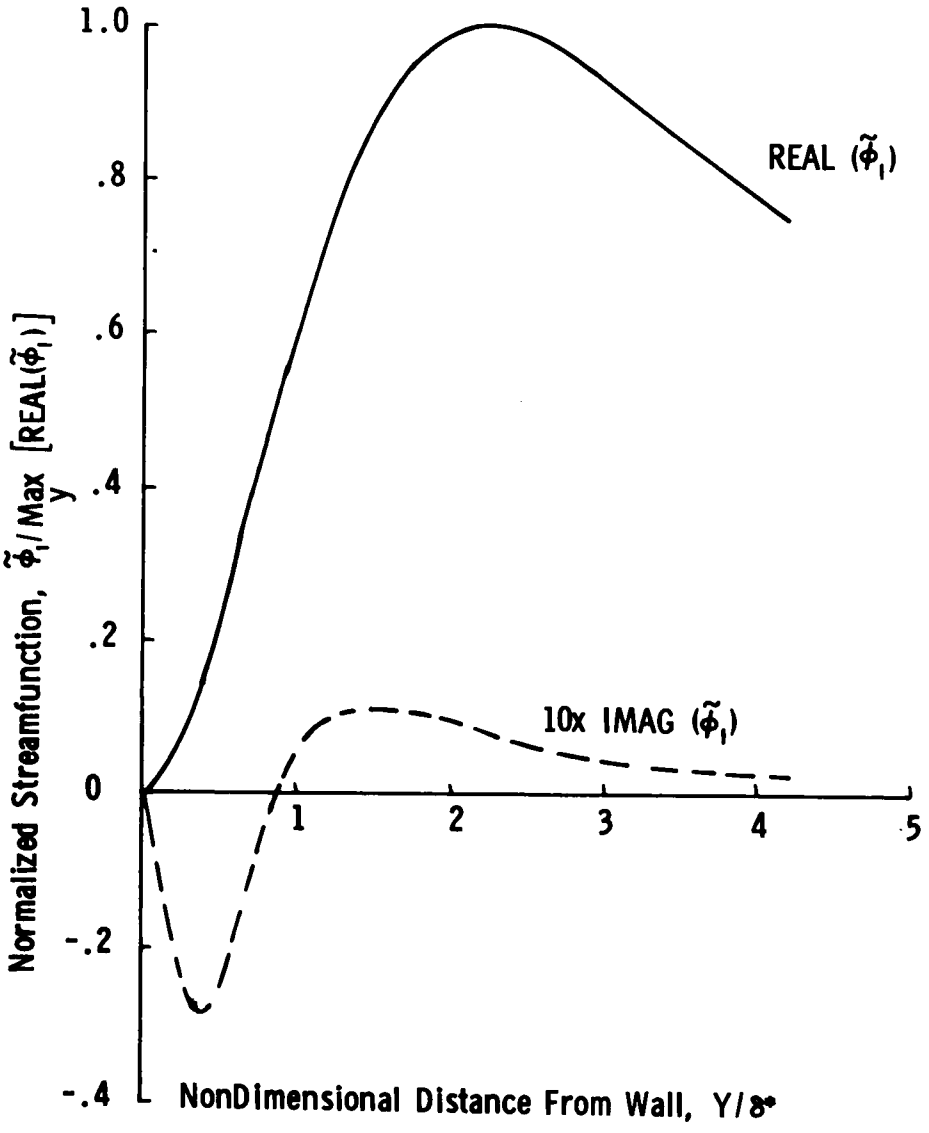
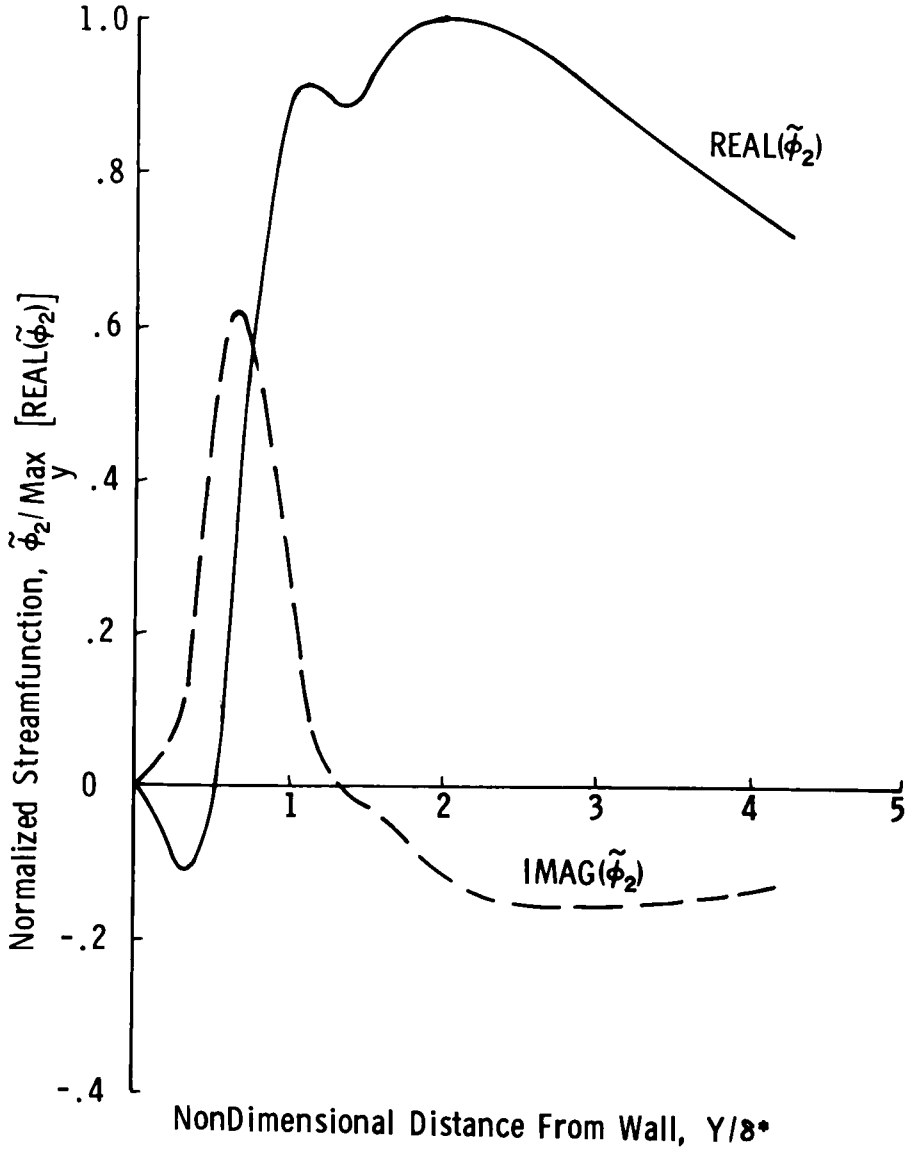



Figure 9. The Reynolds stress distribution across the boundary layer for the three sample cases of Kurtz.



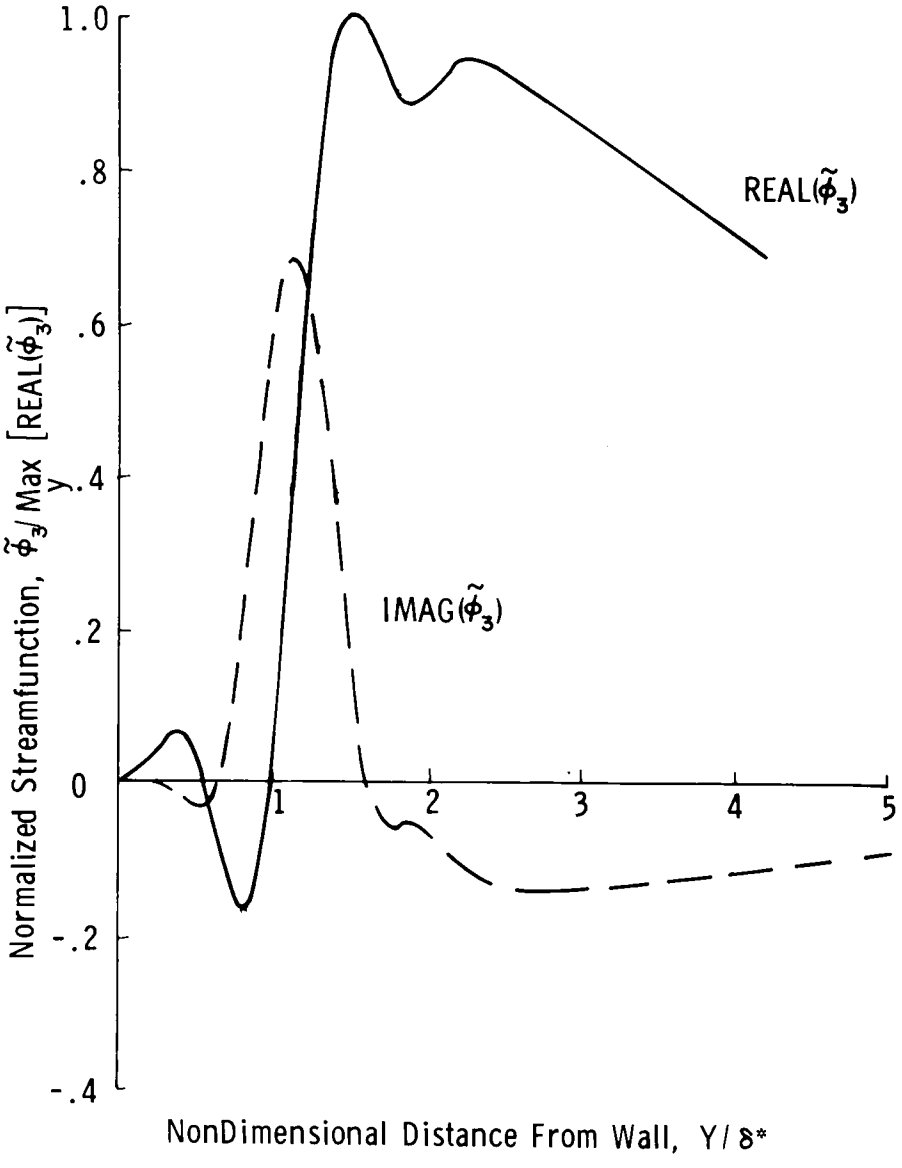

a. $R_{\delta^*} = 770$, $\alpha^* = .186$, $\lambda_1^* = 6.33 \times 10^{-2} \quad -7.21 \times 10^{-4}$ i

Figure 10. The higher eigenfunctions



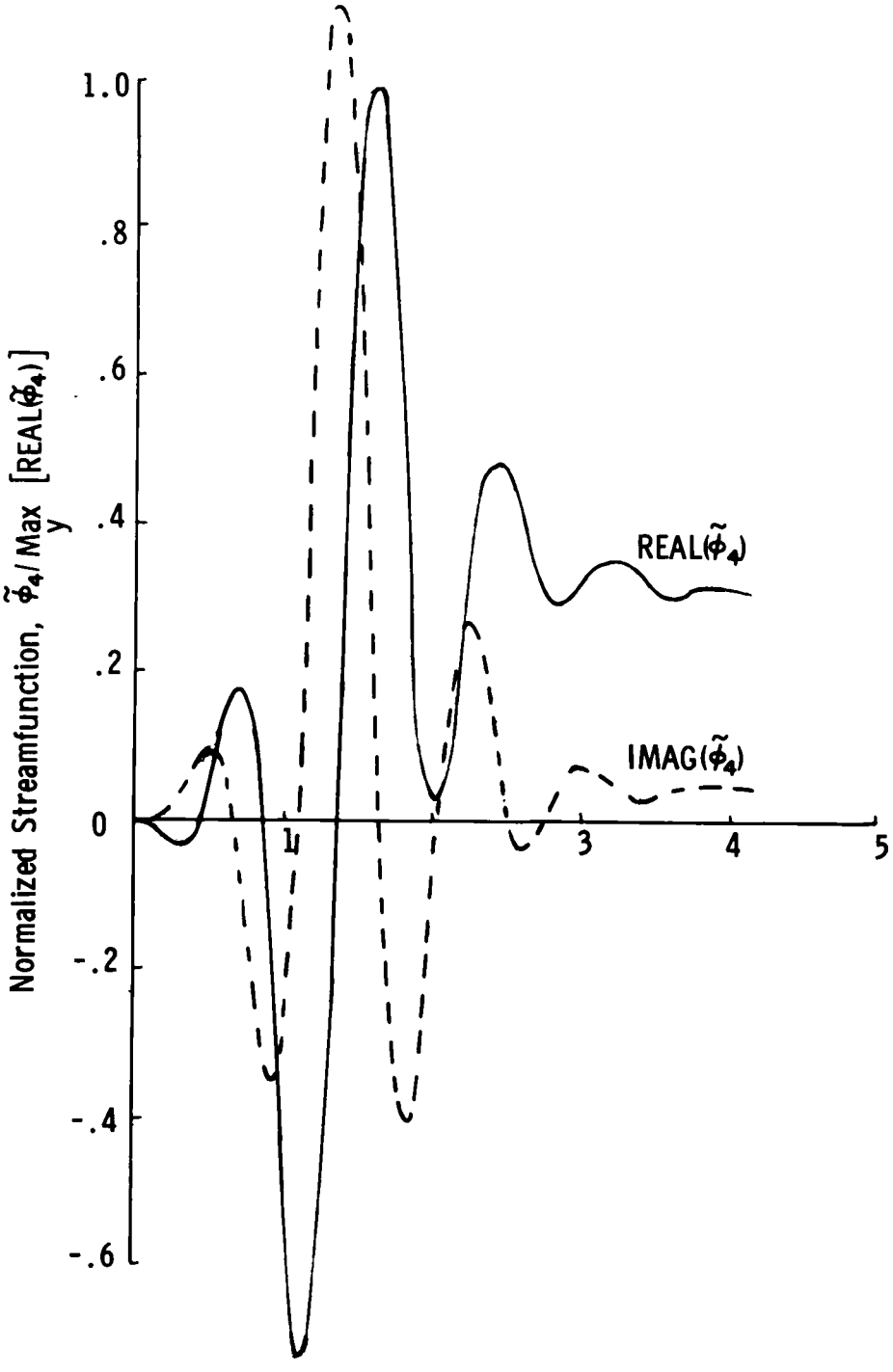

b. $R_{\delta^*} = 770$, $\alpha^* = .186$, $\lambda^* = 6.67 \times 10^{-2} - 5.79 \times 10^{-2}$ i

Figure 10. (continued)



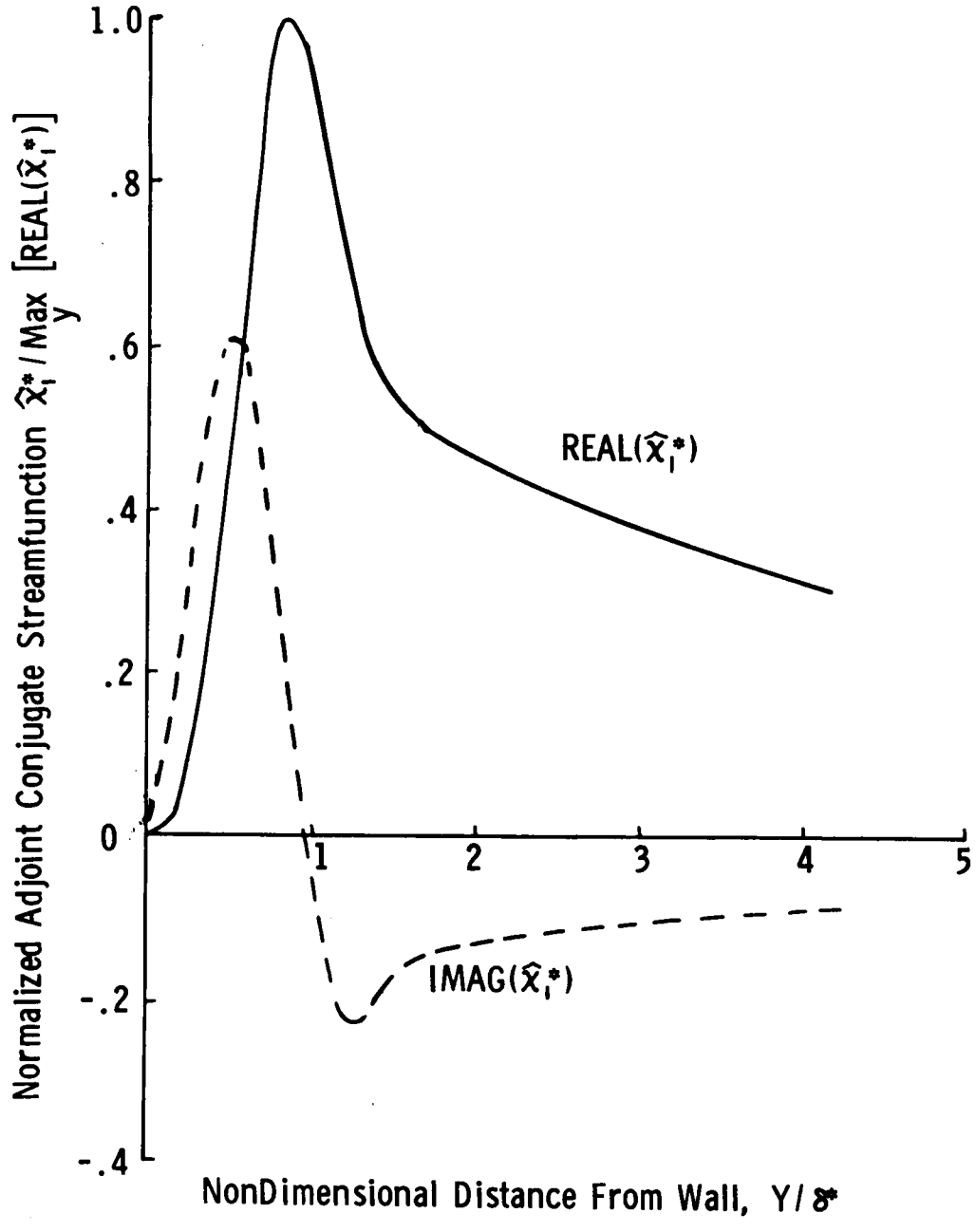

c. $R_{\delta^*} = 770$, $\alpha^* = .186$, $\lambda_3^* = 1.10 \times 10^{-1} - 5.35 \times 10^{-2}$ i

Figure 10. (continued)



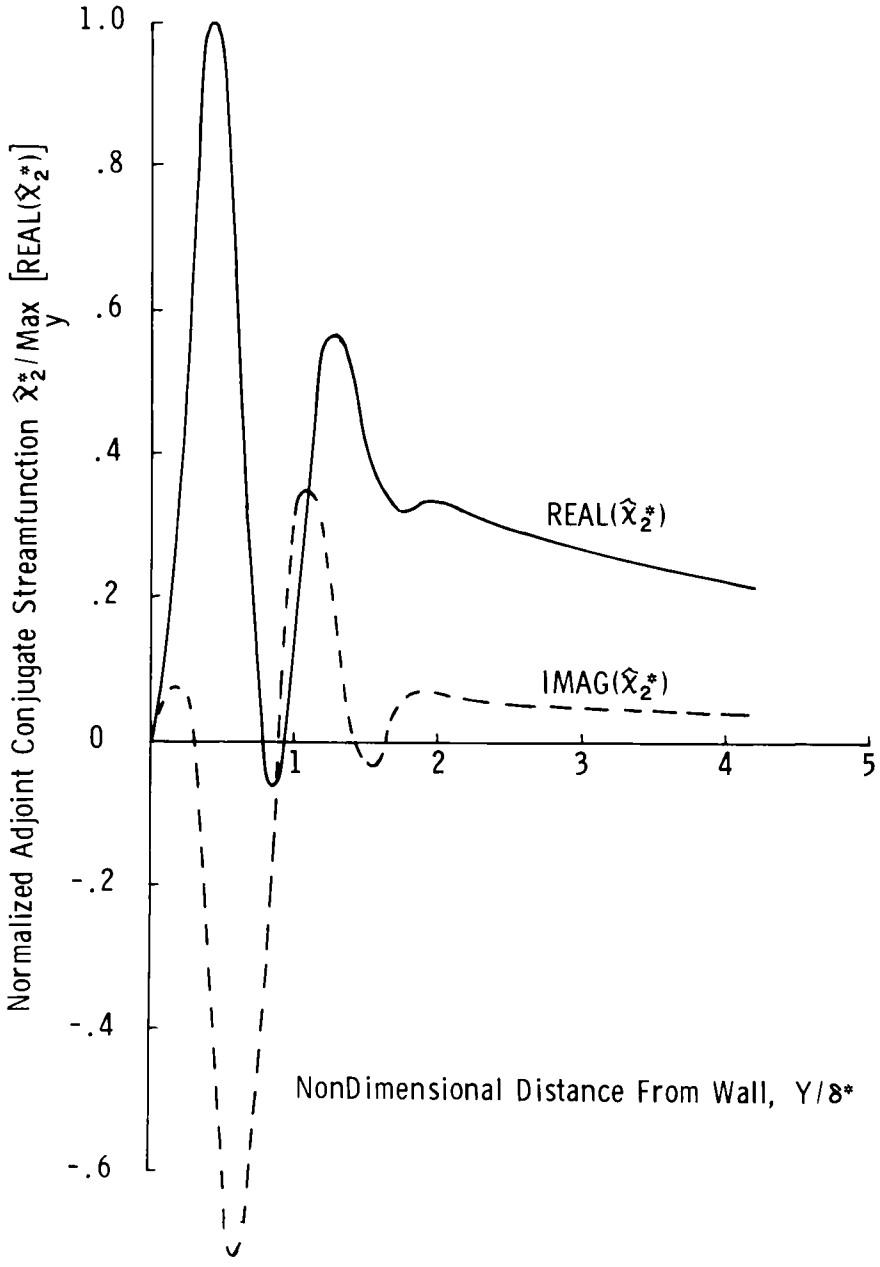

d. $R_{\delta^*} = 770$, $\alpha^* = .186$, $\lambda_4 = 1.35 \times 10^{-1} - 7.7 \times 10^{-2}$ i

Figure 10. (continued)



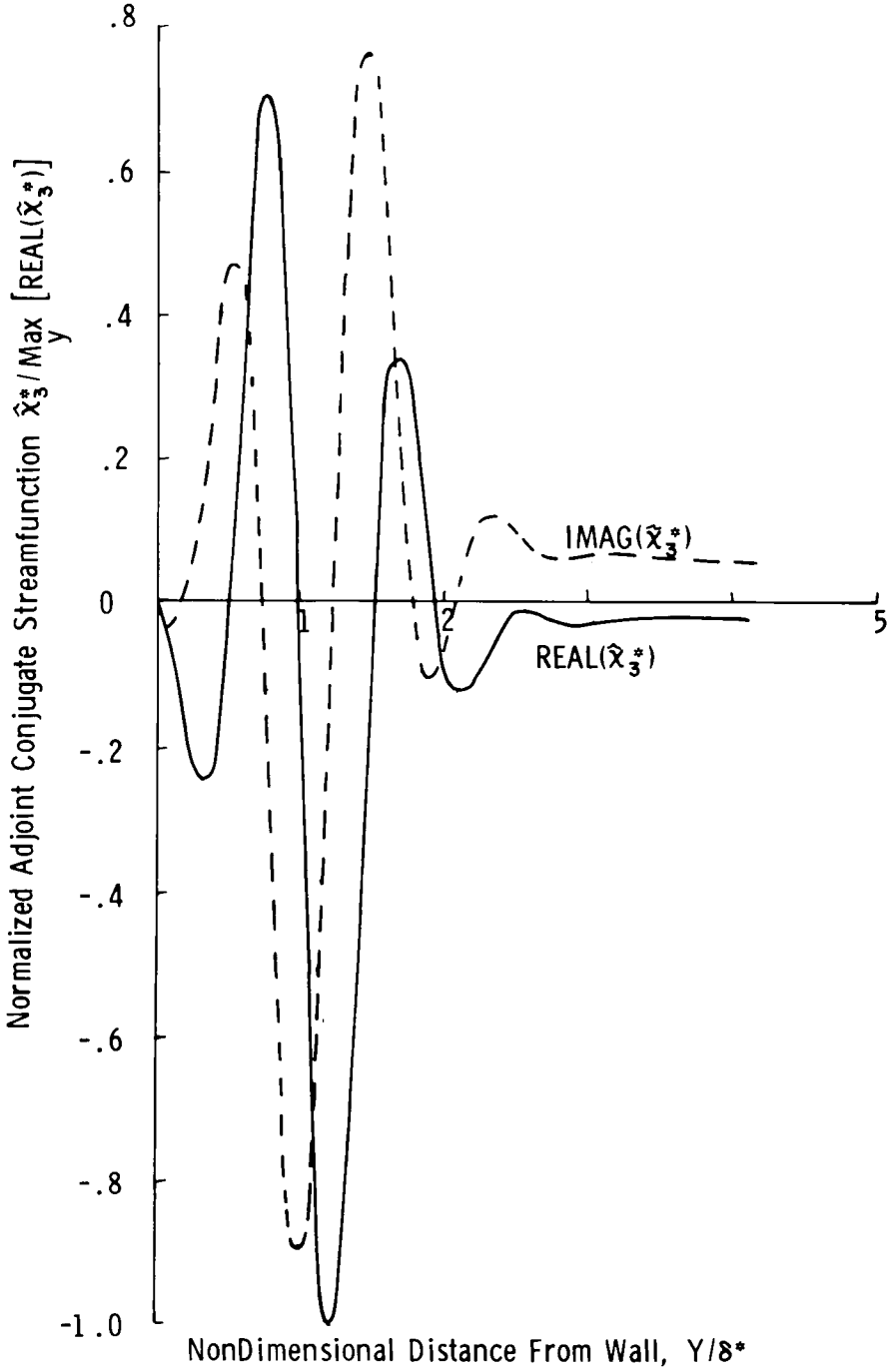

a. $R_{\delta^*} = 770$, $\alpha^* = .186$, $\lambda_1^* = 6.33 \times 10^{-2} - 7.2 \times 10^{-2}$ i

Figure 11. The higher adjoint streamfunction.



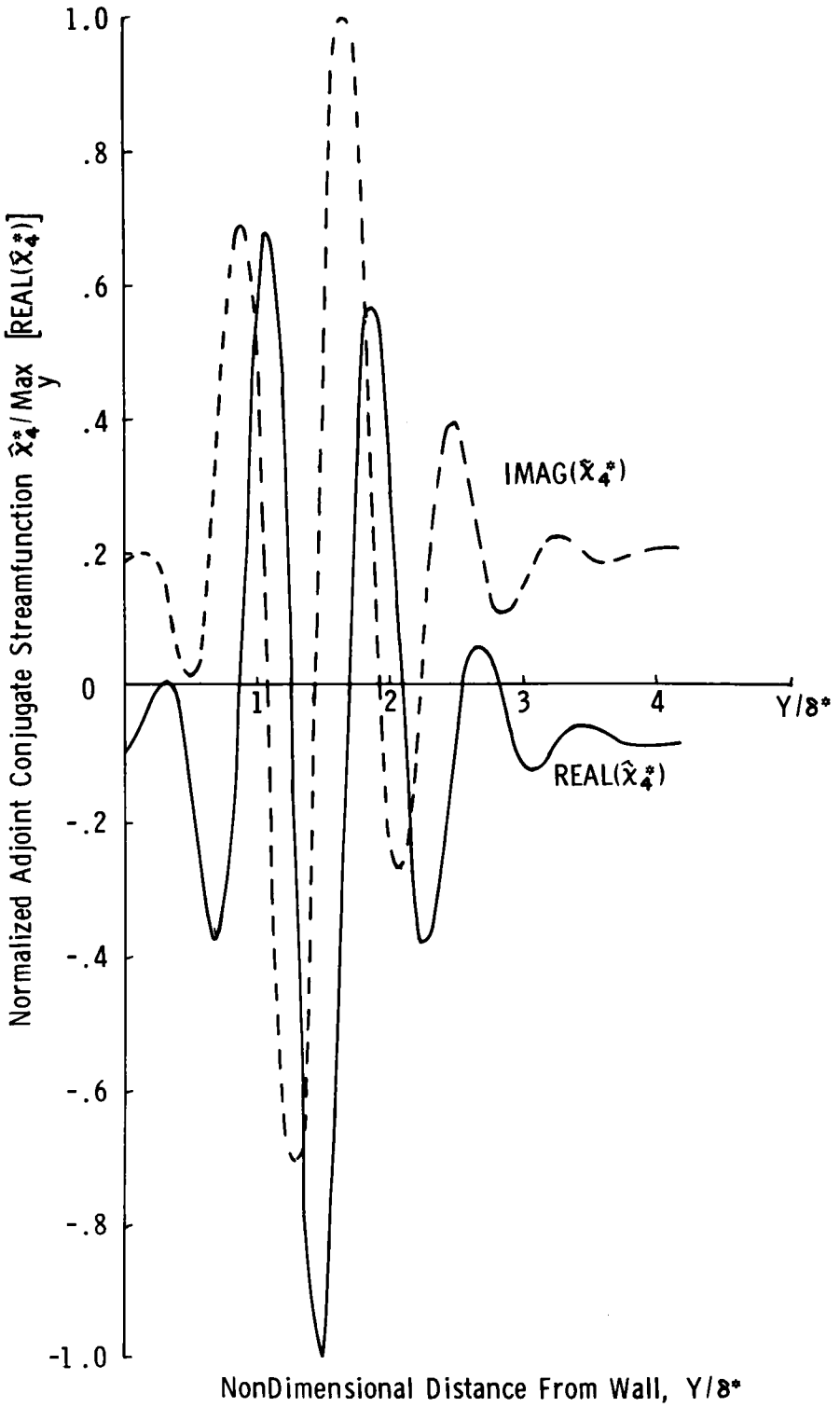

b. $R_{\delta^*} = 770$, $\alpha^* = .186$, $\lambda_2^* = 6.67 \times 10^{-2} - 5.76 \times 10^{-2}\, i$

Figure 11. (continued)



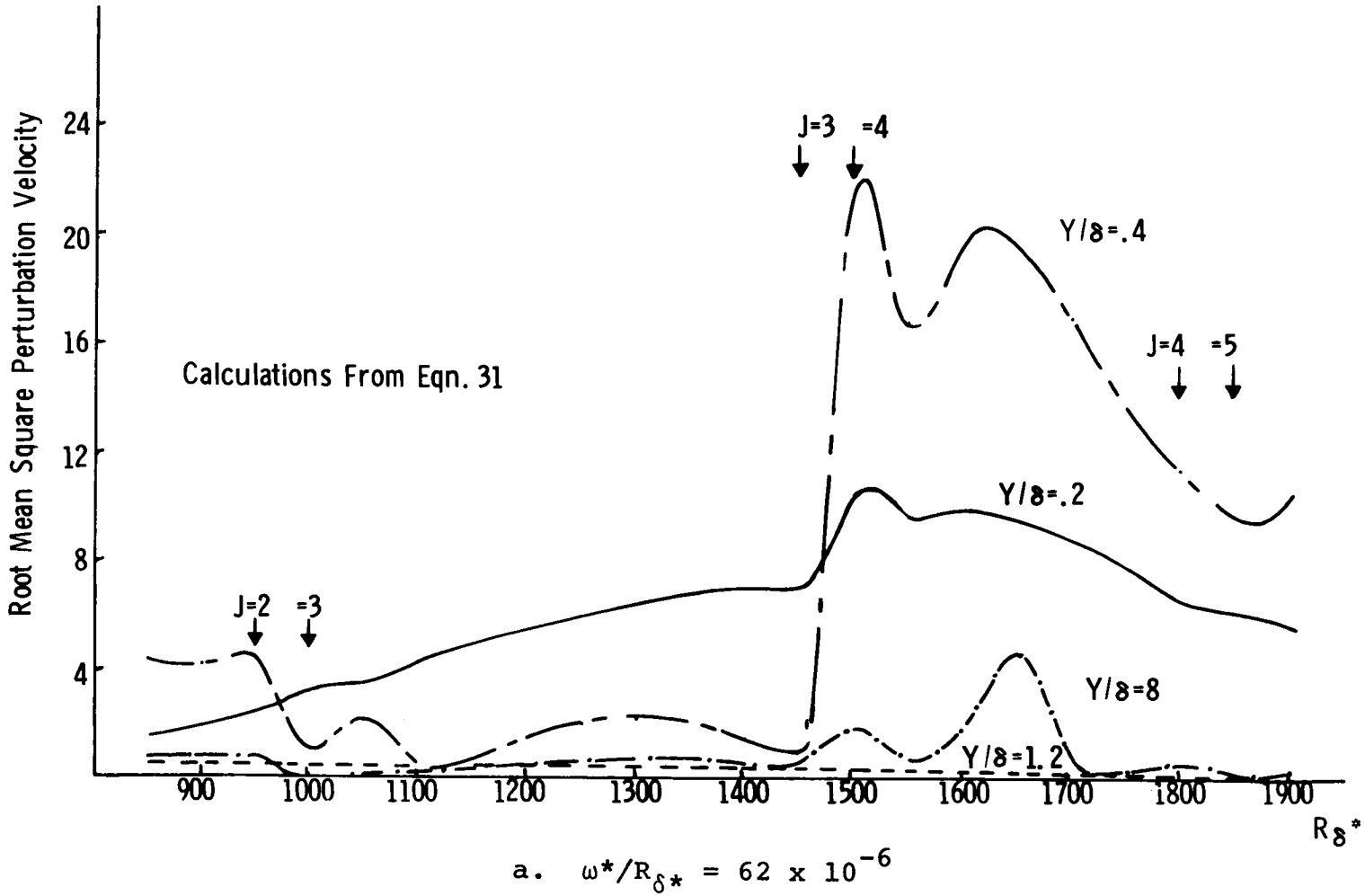

c. $R_{\delta^*} = 770$, $\alpha^* = .186$, $\lambda_3^* = 1.09 \times 10^{-1} - 5.34 \times 10^{-2}\, i$

Figure 11. (continued)



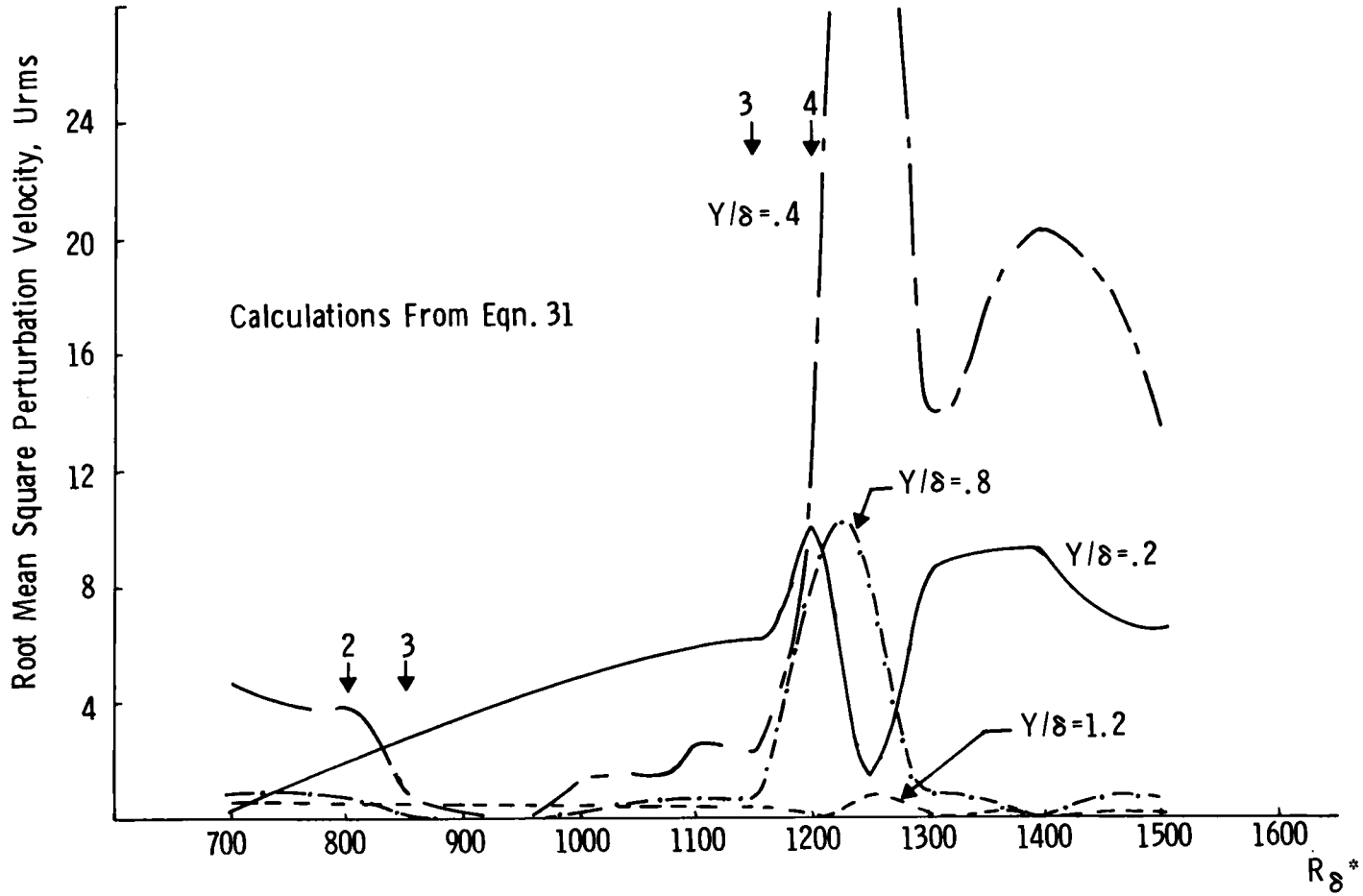

d. $R_{\delta^*} = 770$, $\alpha^* = .186$, $\lambda_4^* = 1.35 \times 10^{-1} - 7.70 \times 10^{-2}$ i

Figure 11. (continued)



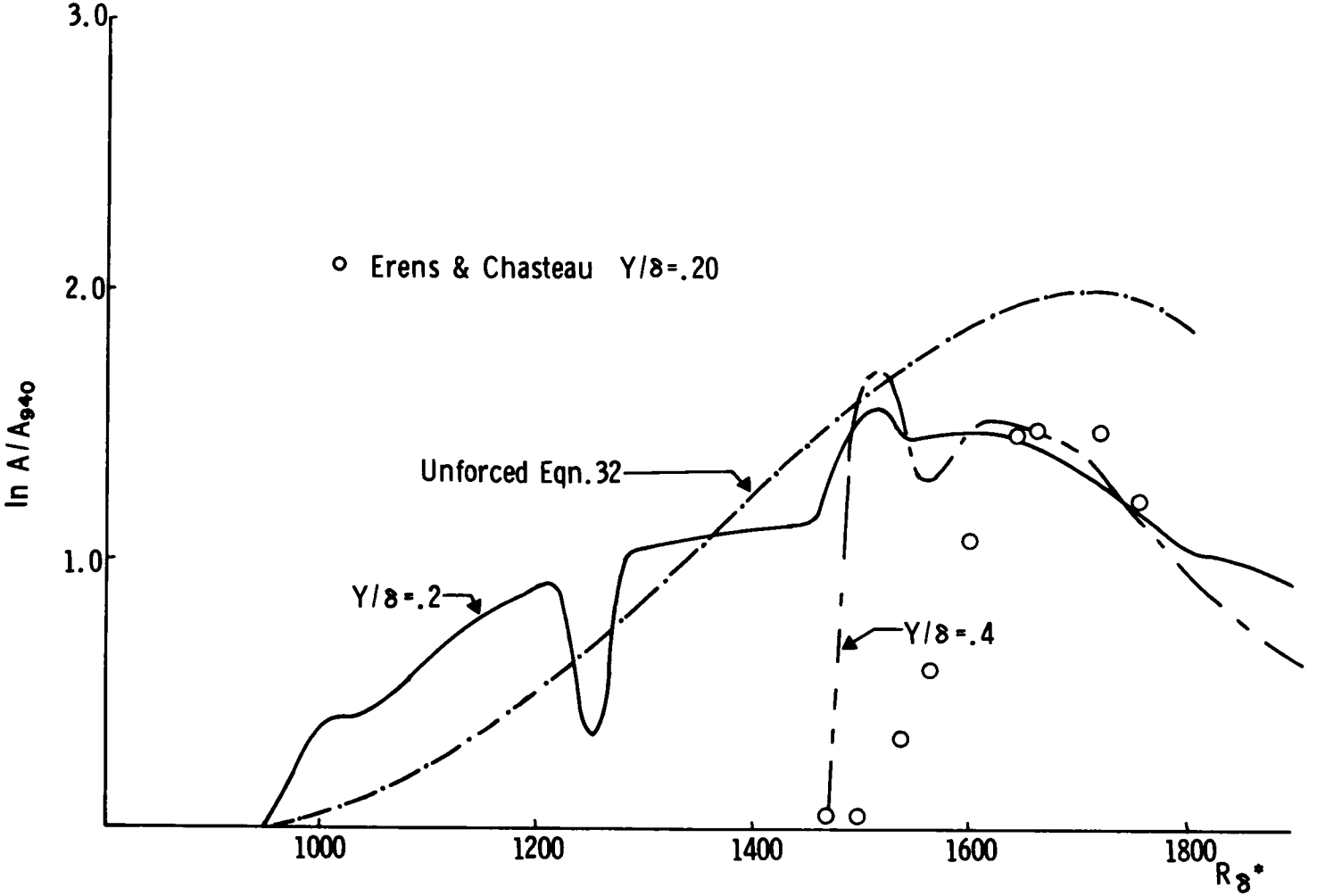

a. $\omega^*/R_{\delta^*} = 62 \times 10^{-6}$

Figure 12. Variation of root mean square fluctuating velocity with increasing streamwise distance at several points in the layer.



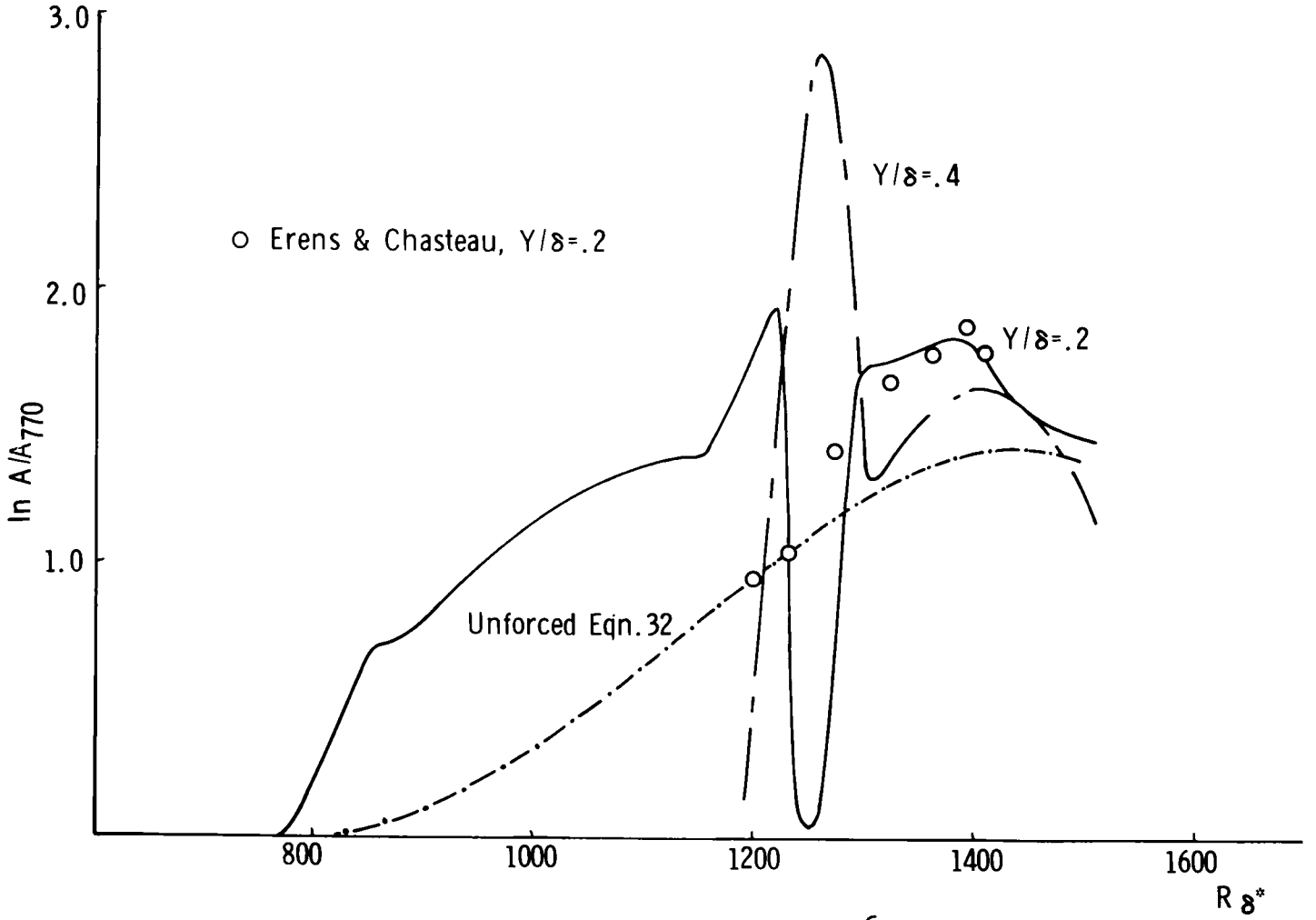

b. $\omega^*/R_{\delta^*} = 83.5 \times 10^{-6}$

Figure 12. (continued)



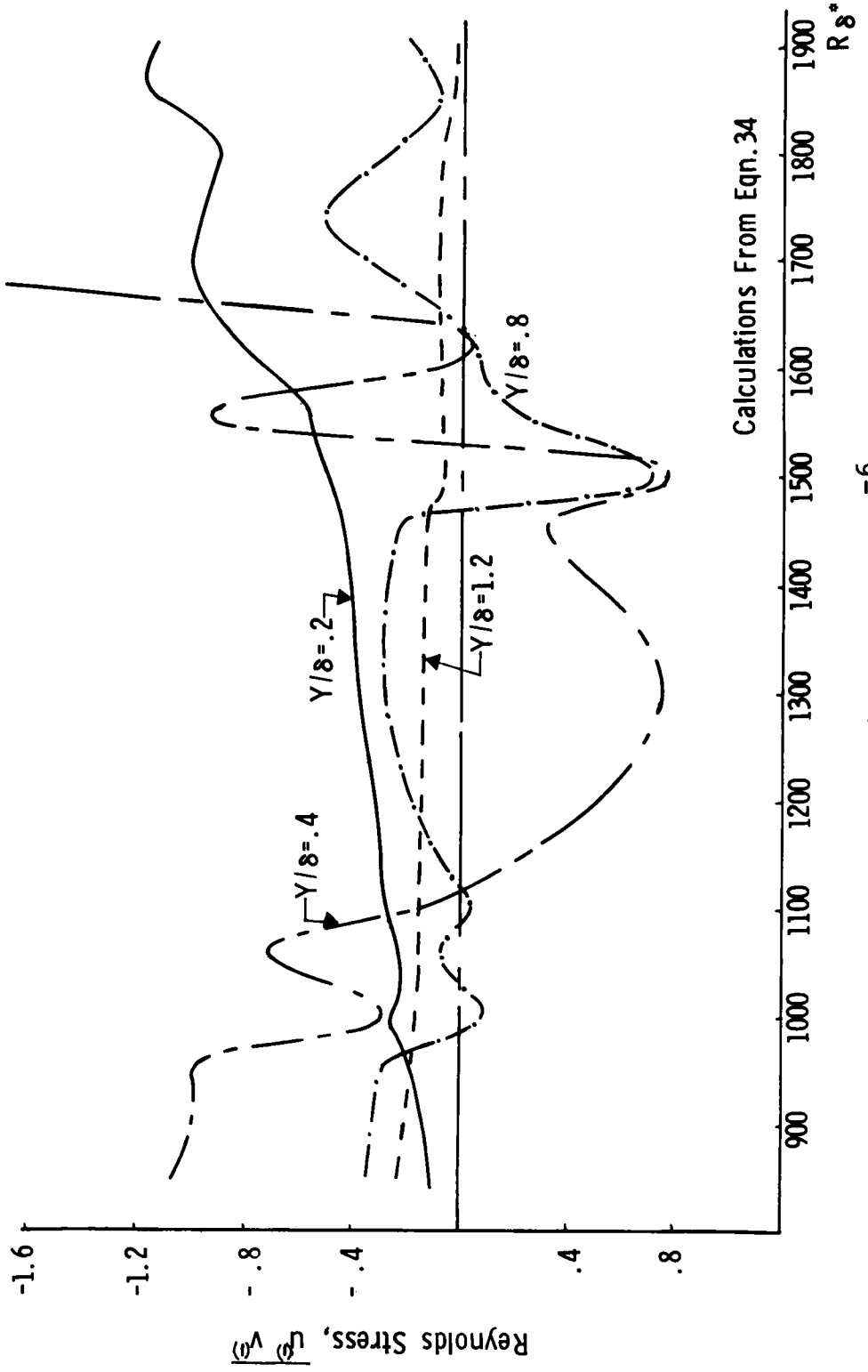

a. $\omega^*/R_{\delta^*} = 62 \times 10^{-6}$

Figure 13. Comparison of forced and unforced growth rates.



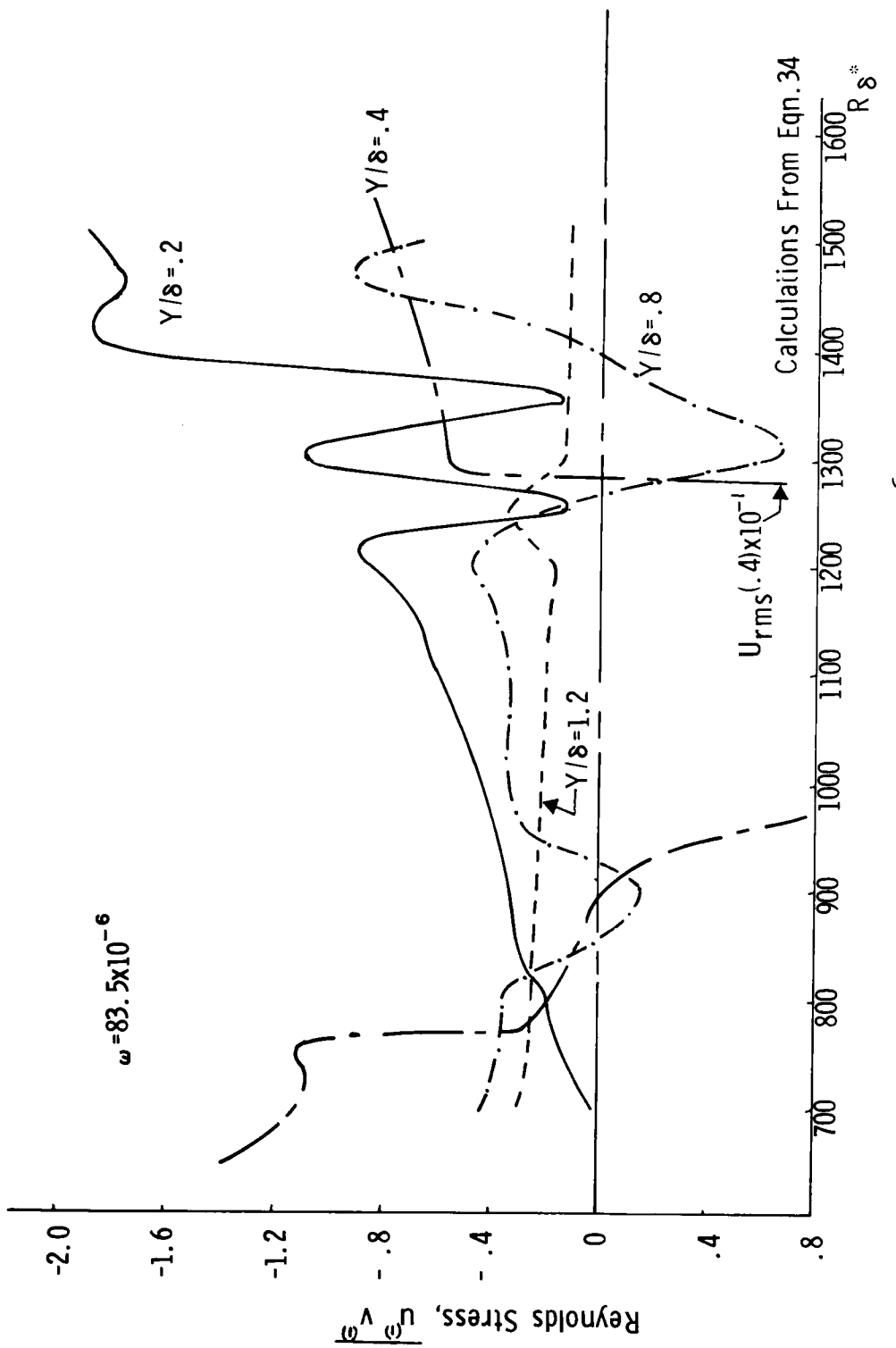

b. $\omega^*/R_{\delta^*} = 83.5 \times 10^{-6}$

Figure 13. (continued)



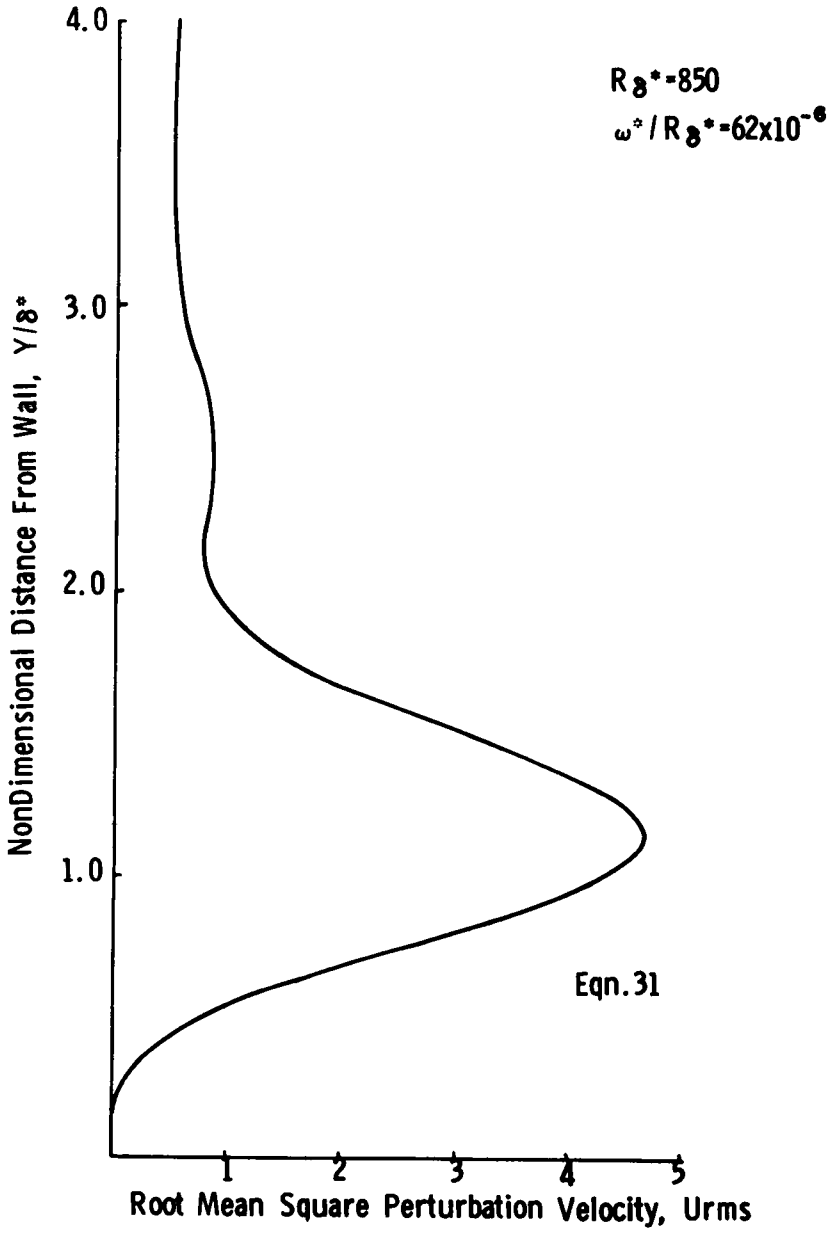

a. $\omega^*/R_{\delta^*} = 62 \times 10^{-6}$

Figure 14. Reynolds stress as a function of streamline distance.



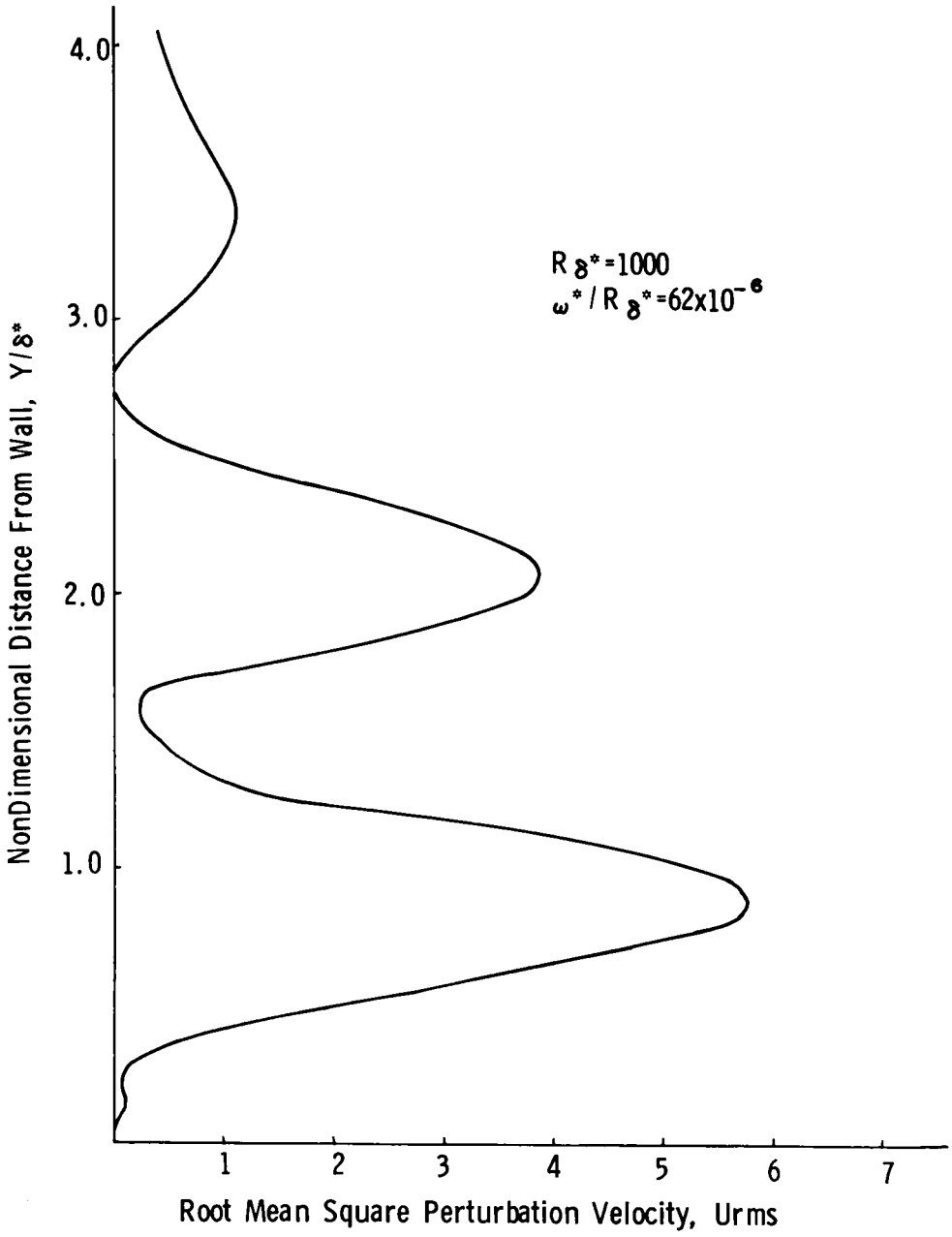

b. $\omega^*/R_{\delta^*} = 83.5 \times 10^{-6}$

Figure 14. (continued)



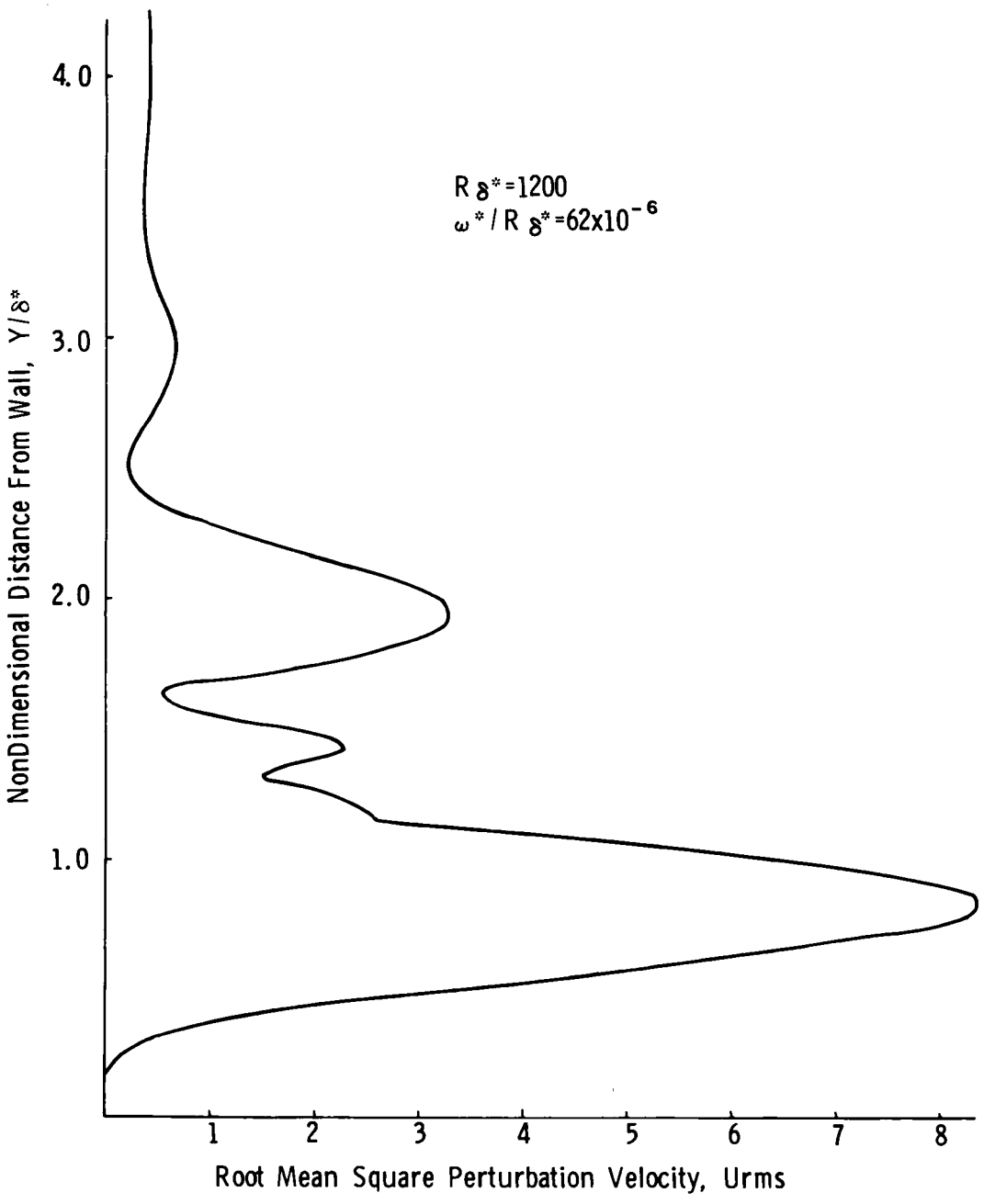

a. $R_{\delta*} = 850$

Figure 15. Development of the rms velocity profiles at $\omega^*/R_{\delta*} = 62 \times 10^{-6}$ with $R_{\delta*}$.



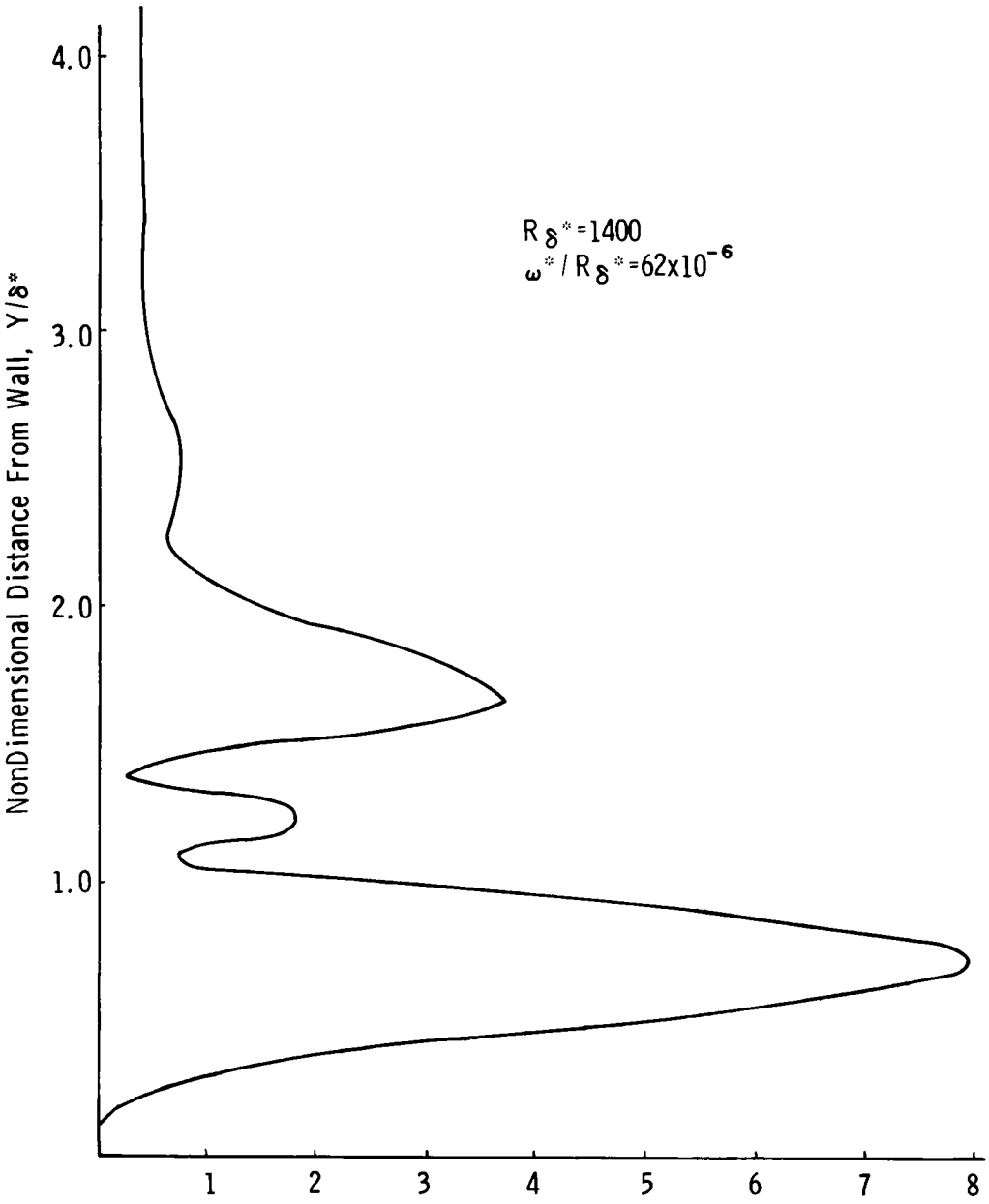

b. $R_{\delta *} = 1000$

Figure 15. (continued)



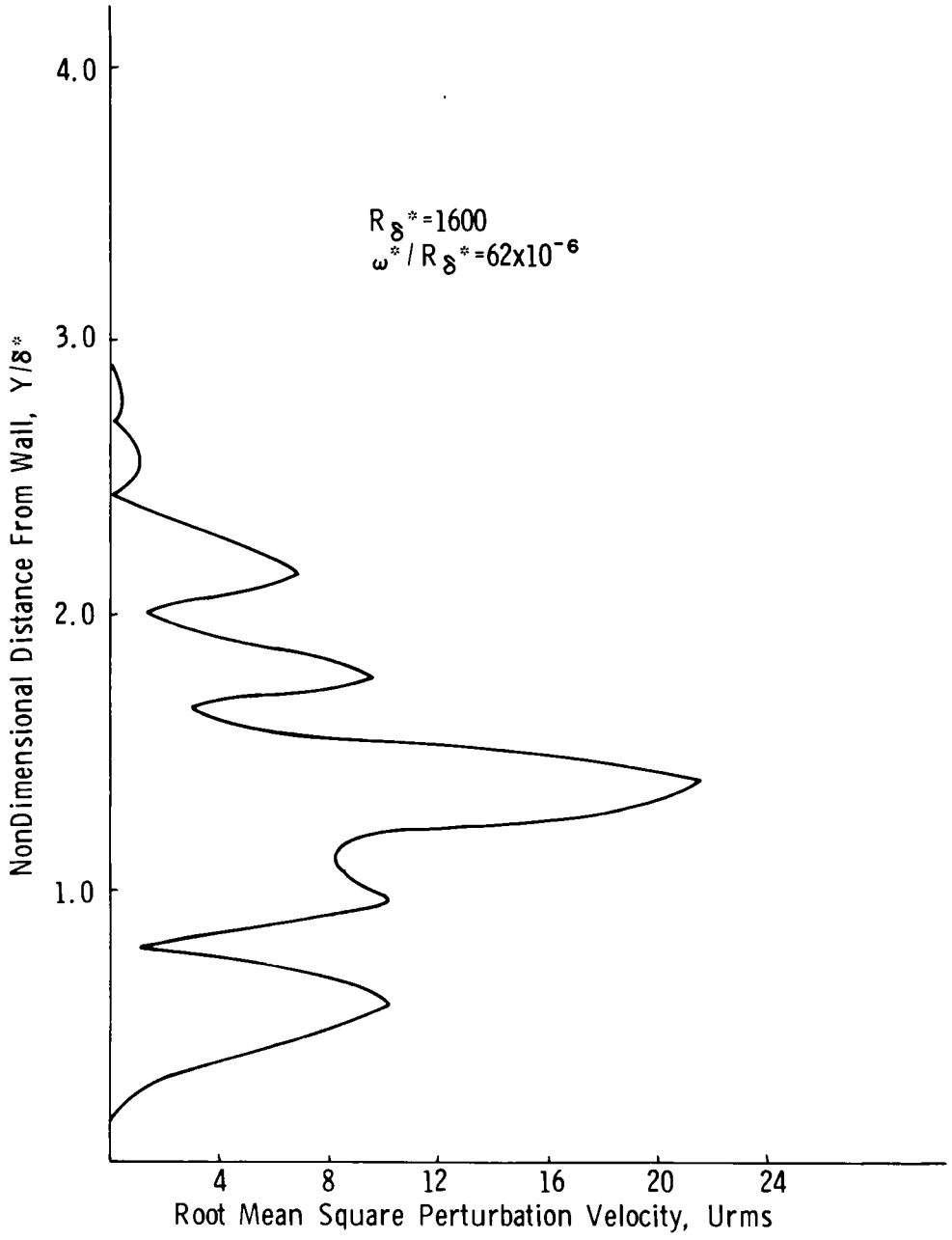

c. $R_{\delta *} = 1200$

Figure 15. (continued)



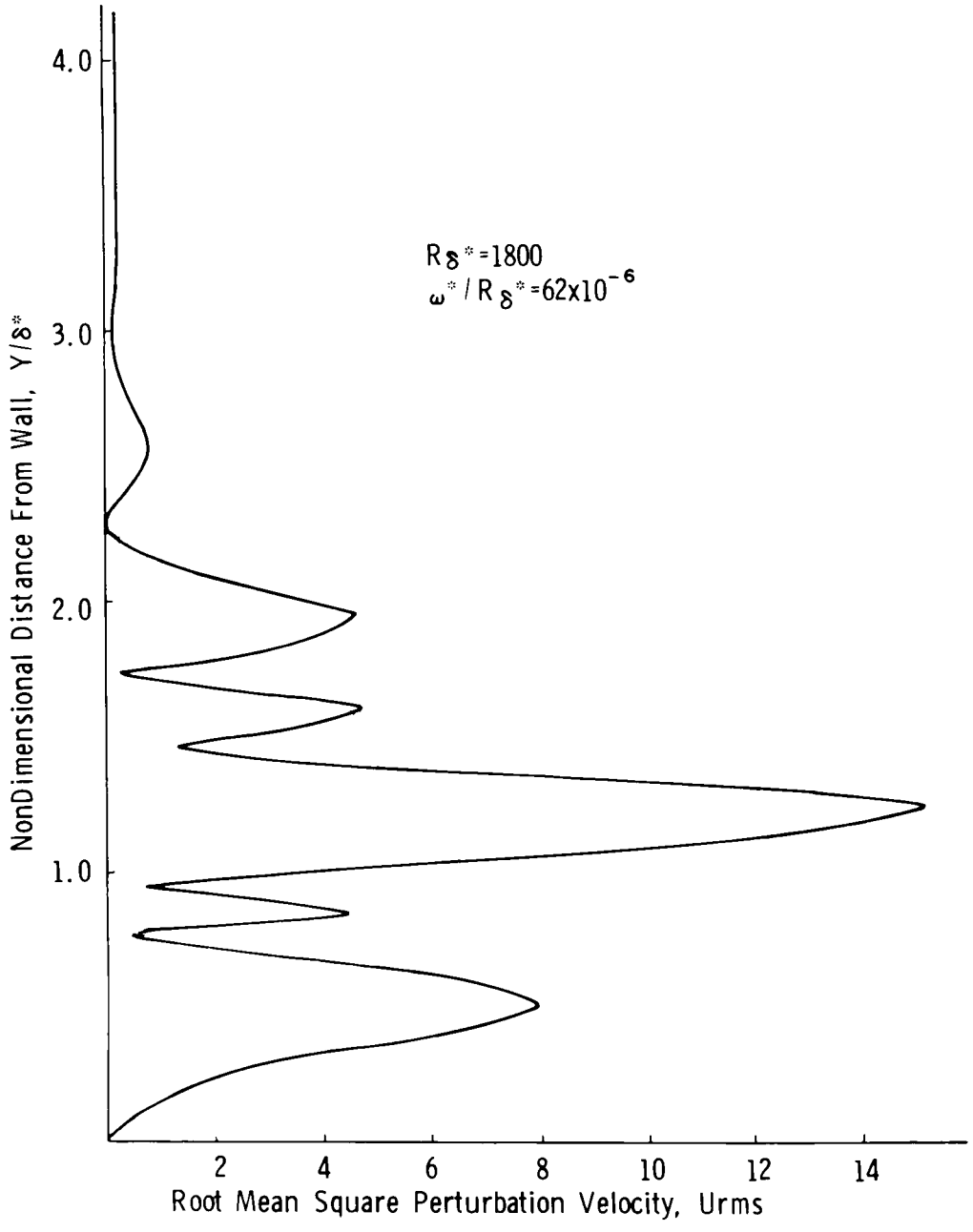

d. $R_{\delta^*}$ = 1400

Figure 15. (continued)



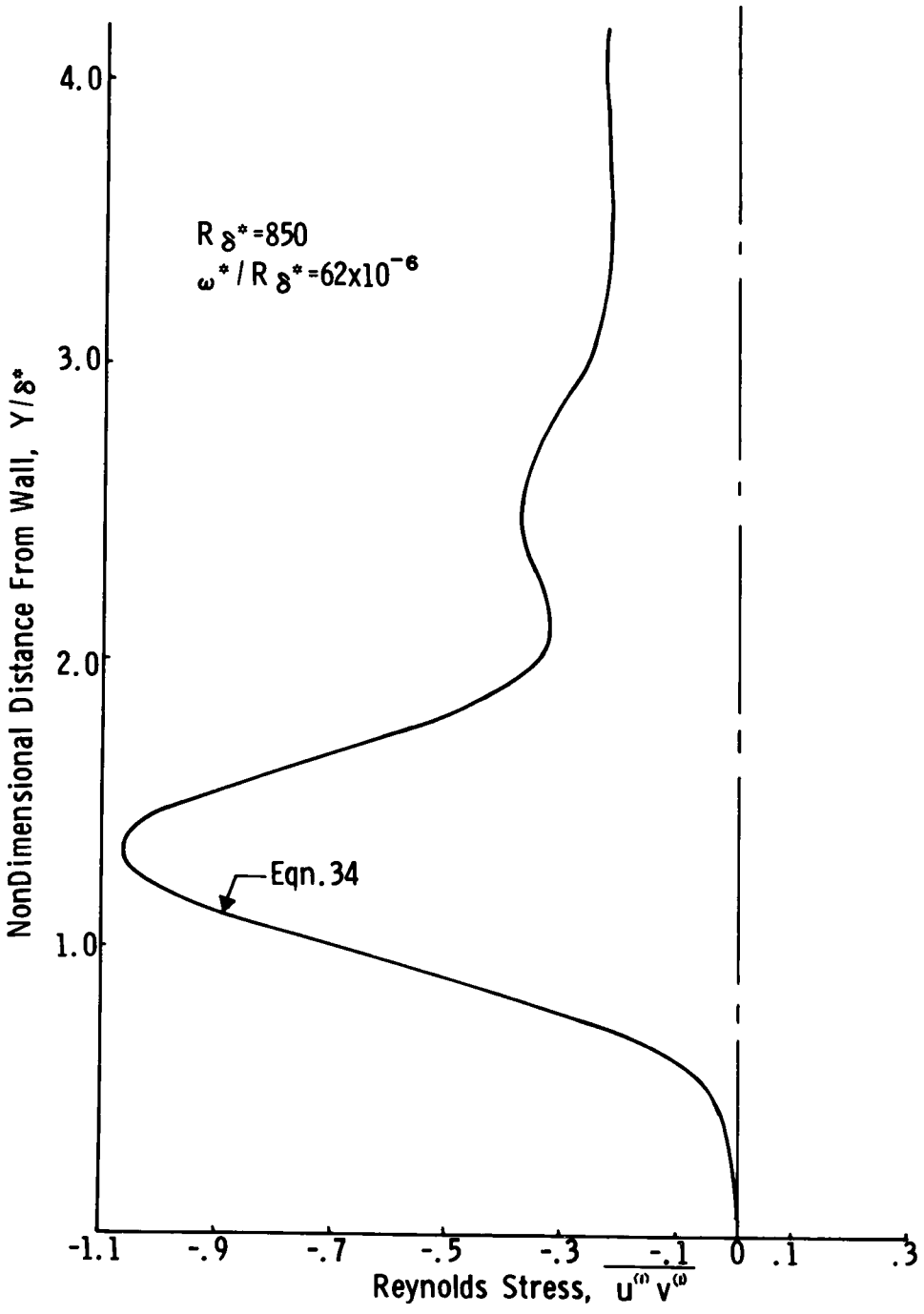

e. $R_{\delta^*}$ = 1600

Figure 15. (continued)



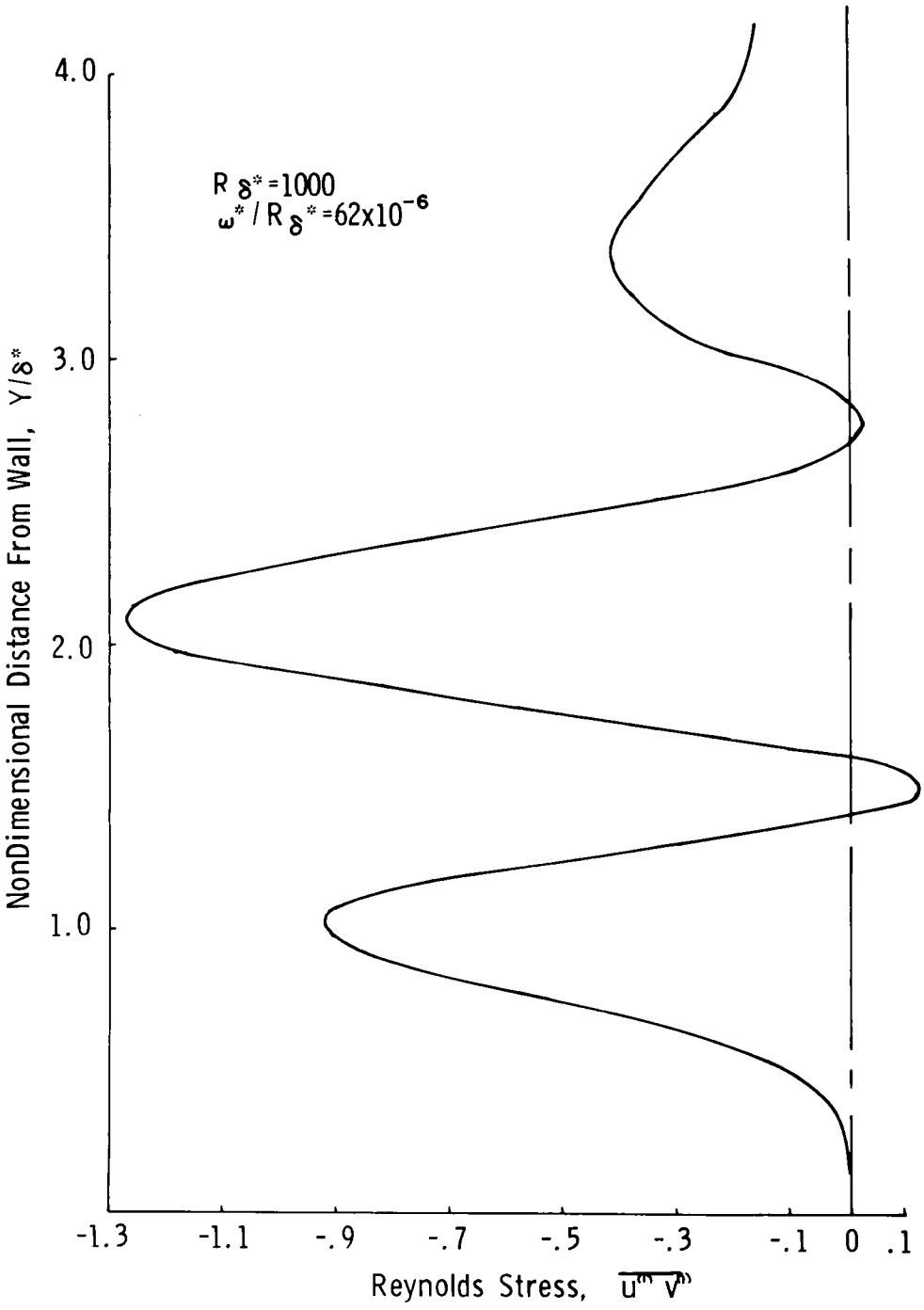

f. $R_{\delta^*}$ = 1800

Figure 15. (continued)



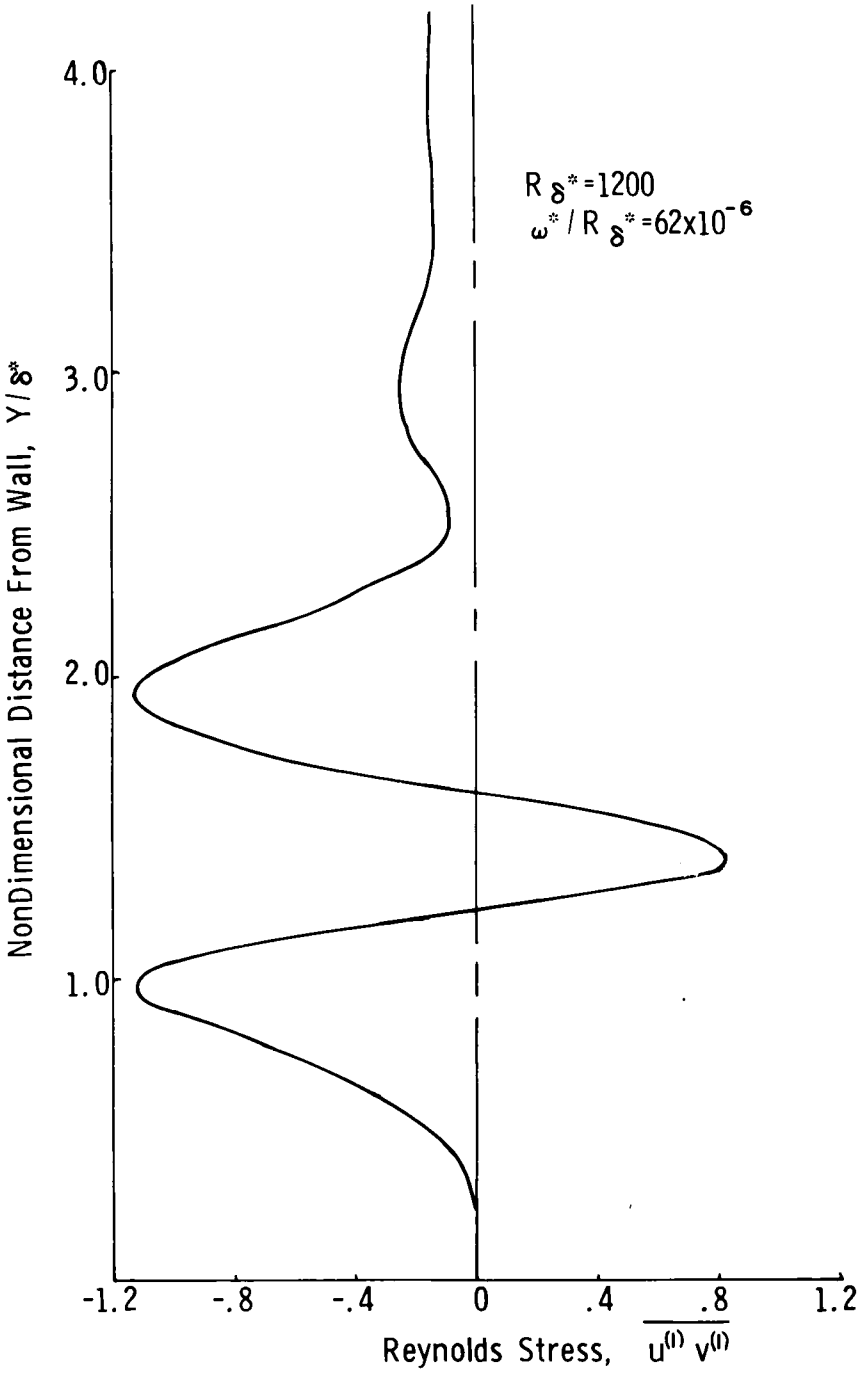

a. $R_{\delta *} = 850$

Figure 16. Development of the Reynolds stress profiles at $\omega^*/R_{\delta *} = 62 \times 10^{-6}$ with $R_{\delta *}$.



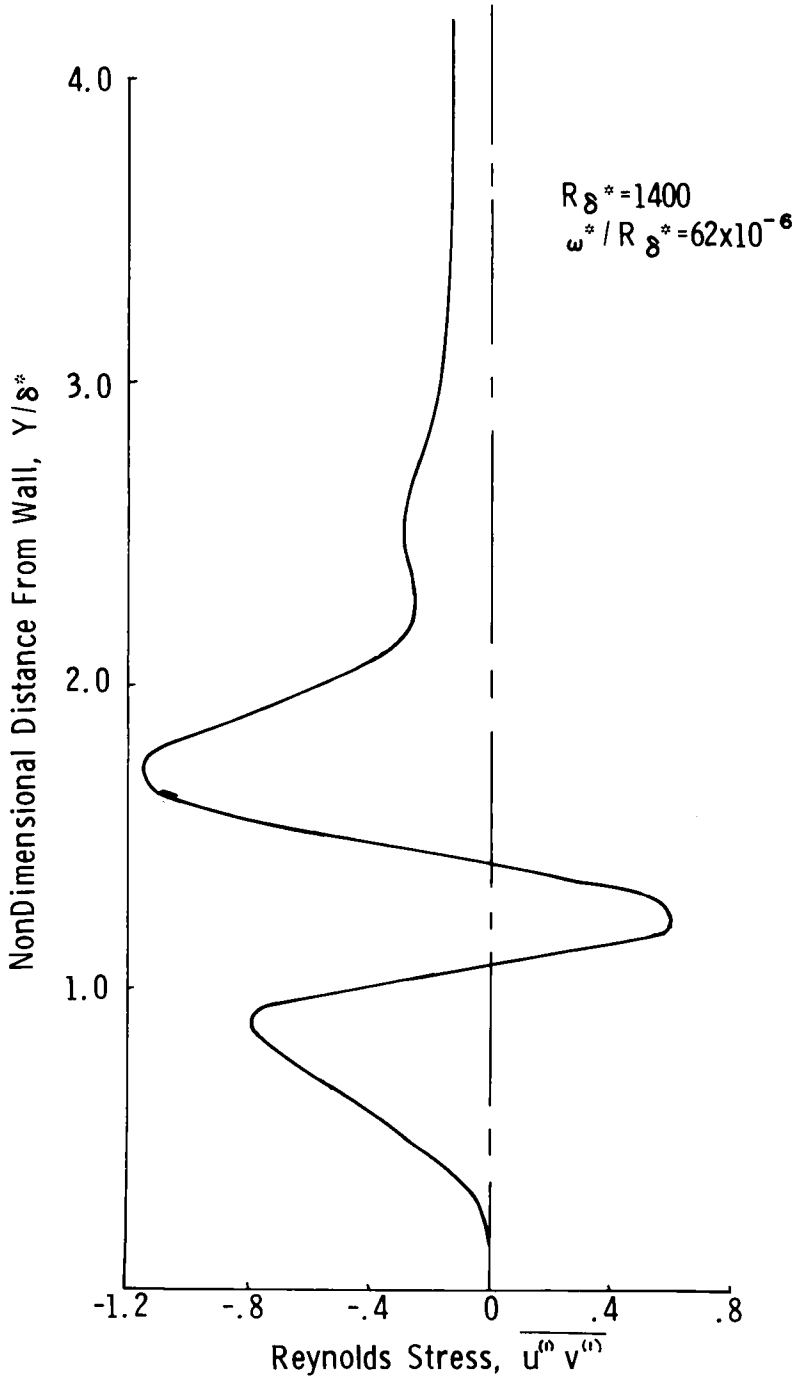

b. $R_{\delta^*} = 1000$

Figure 16. (continued)



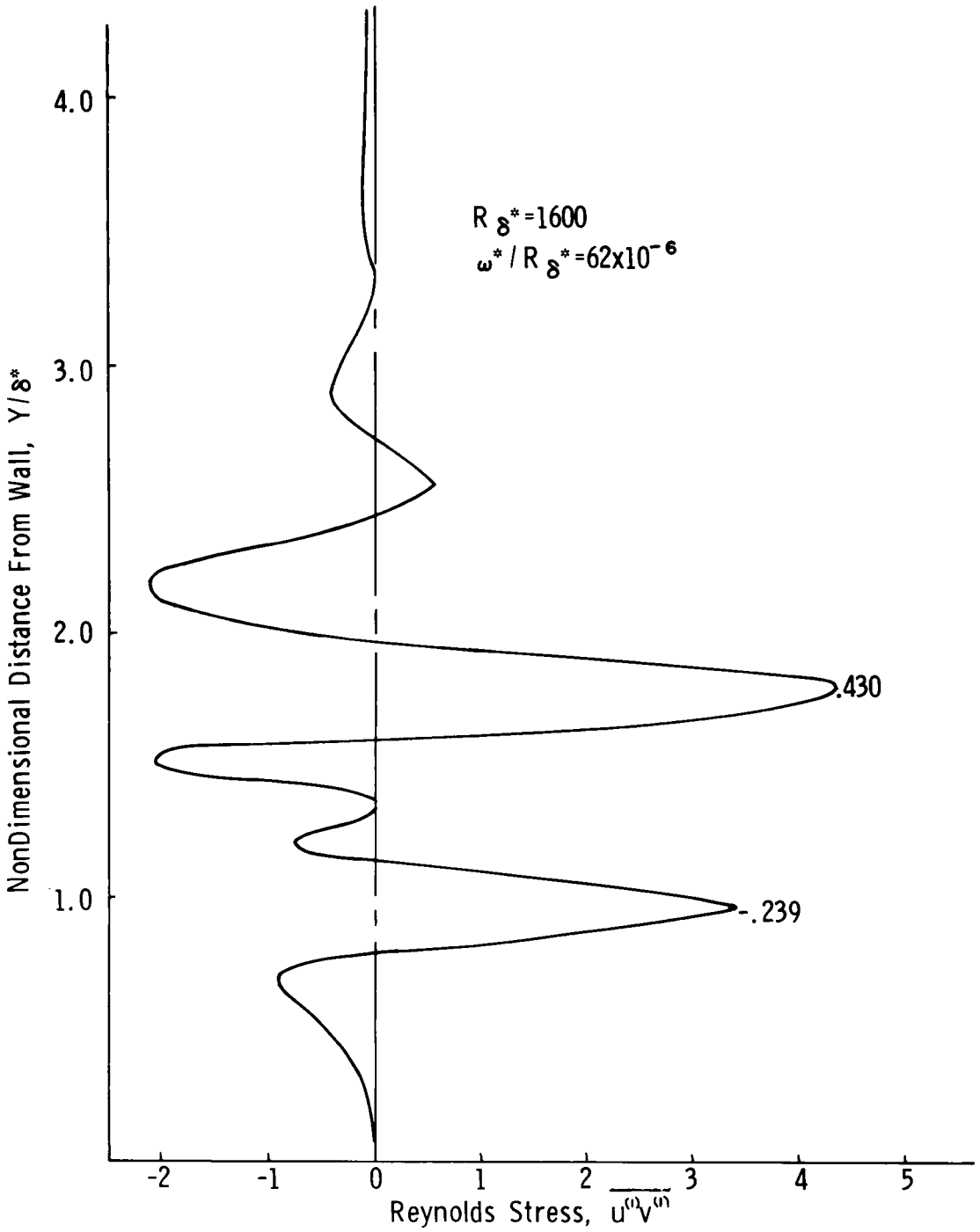

c. $R_{\delta^*} = 1200$

Figure 16. (continued)



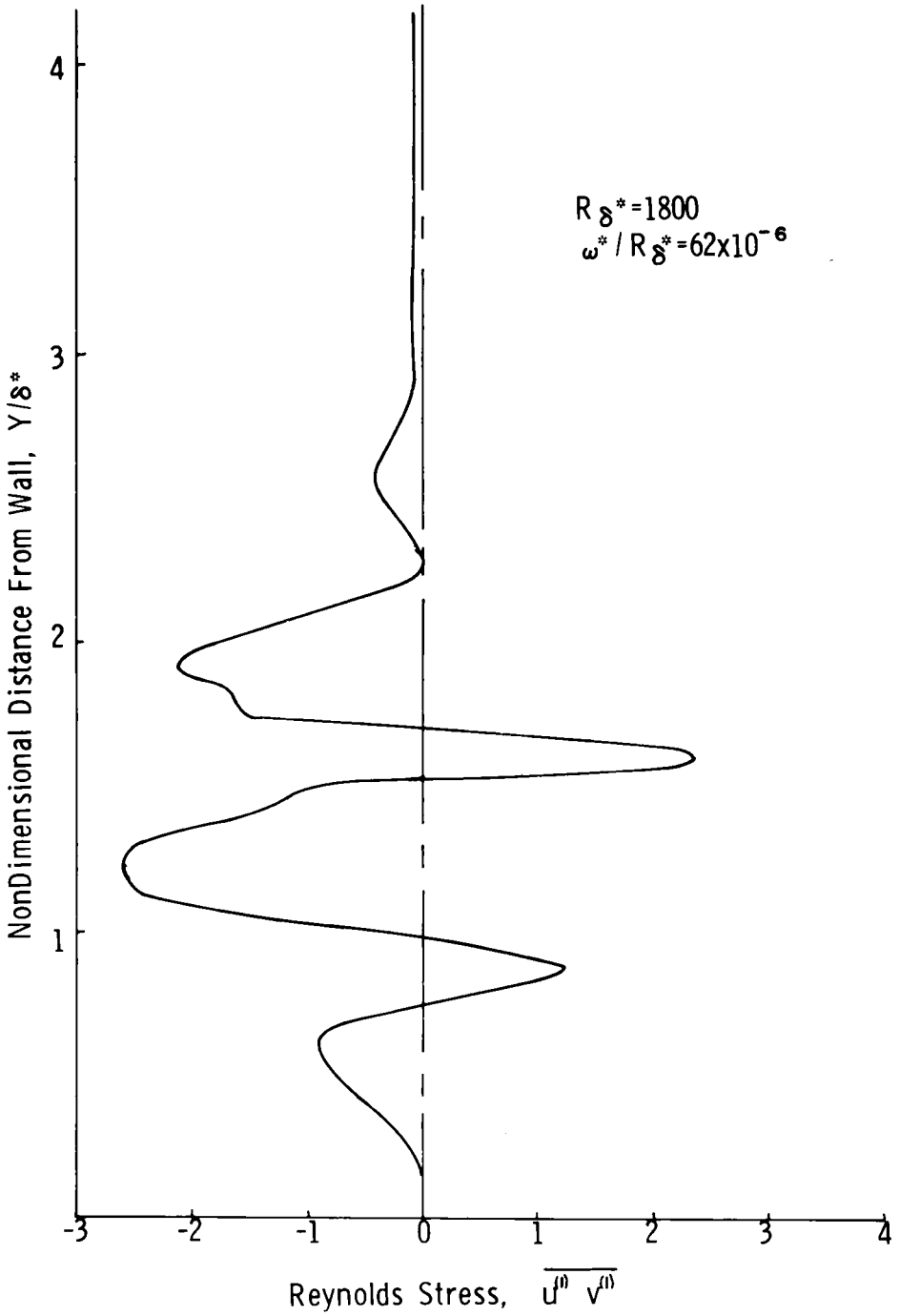

d. $R_{\delta*}$ = 1400

Figure 16. (continued)



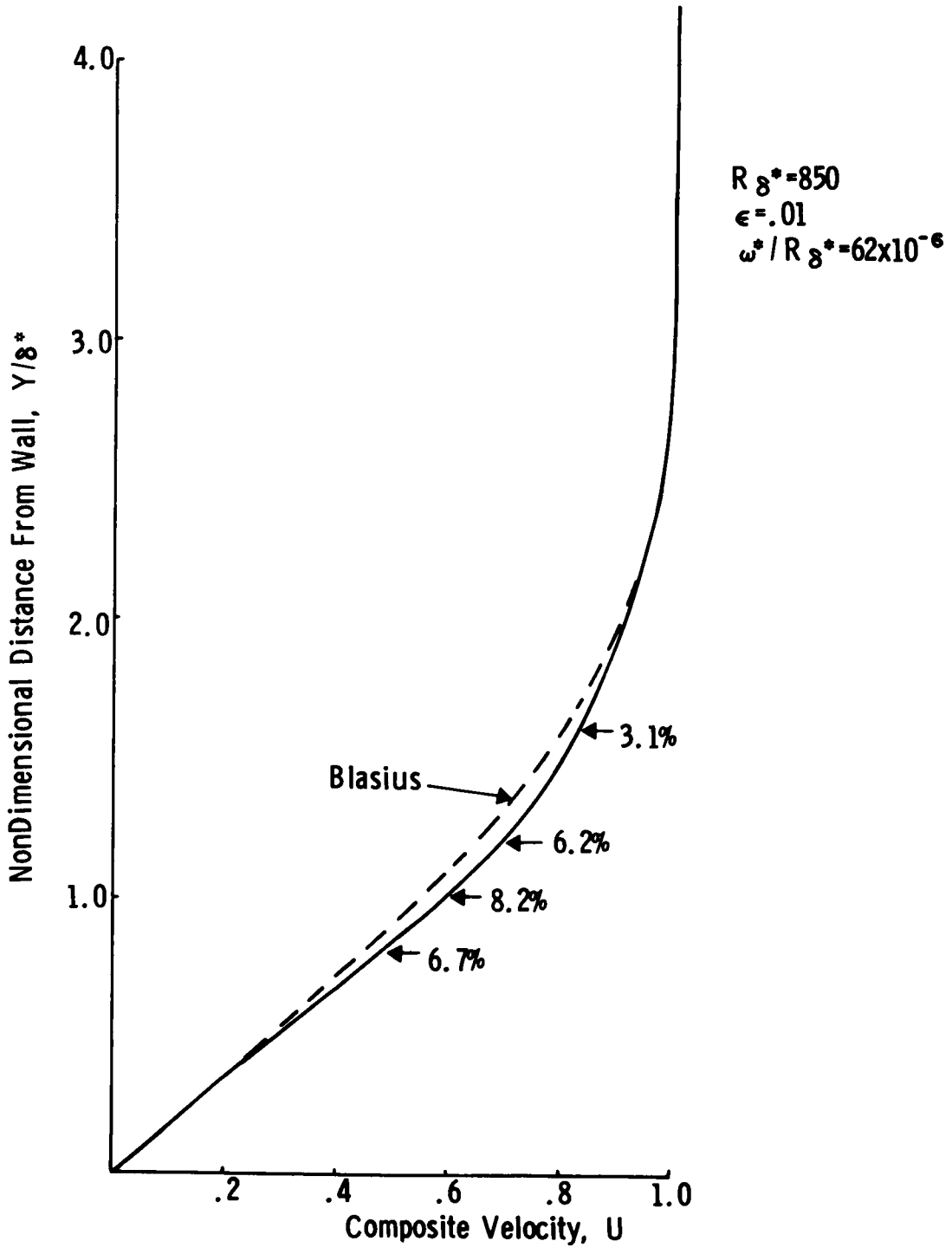

e. $R_{\delta *}$ = 1600

Figure 16. (continued)



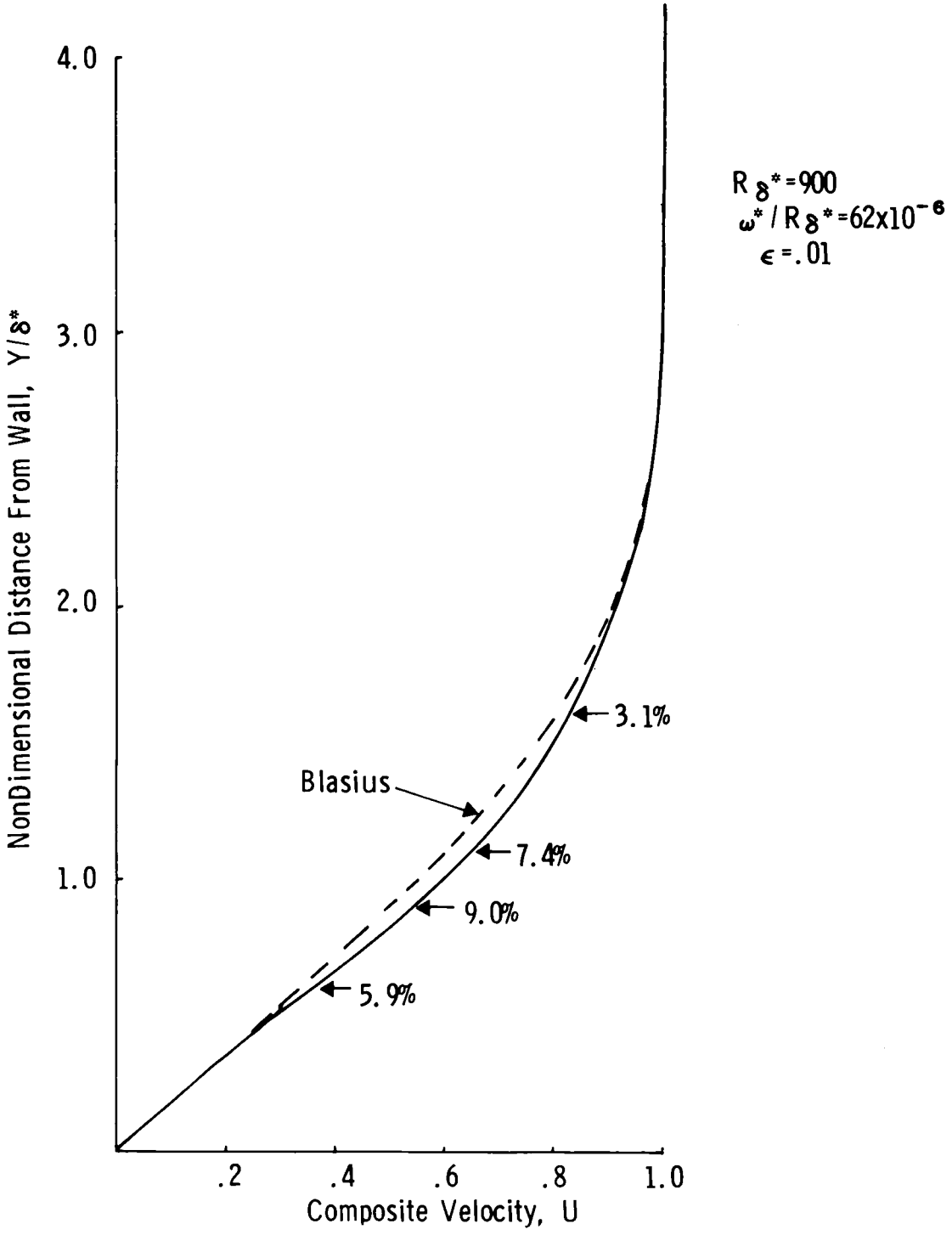

f. $R_{\delta^*}$ = 1800

Figure 16. (continued)



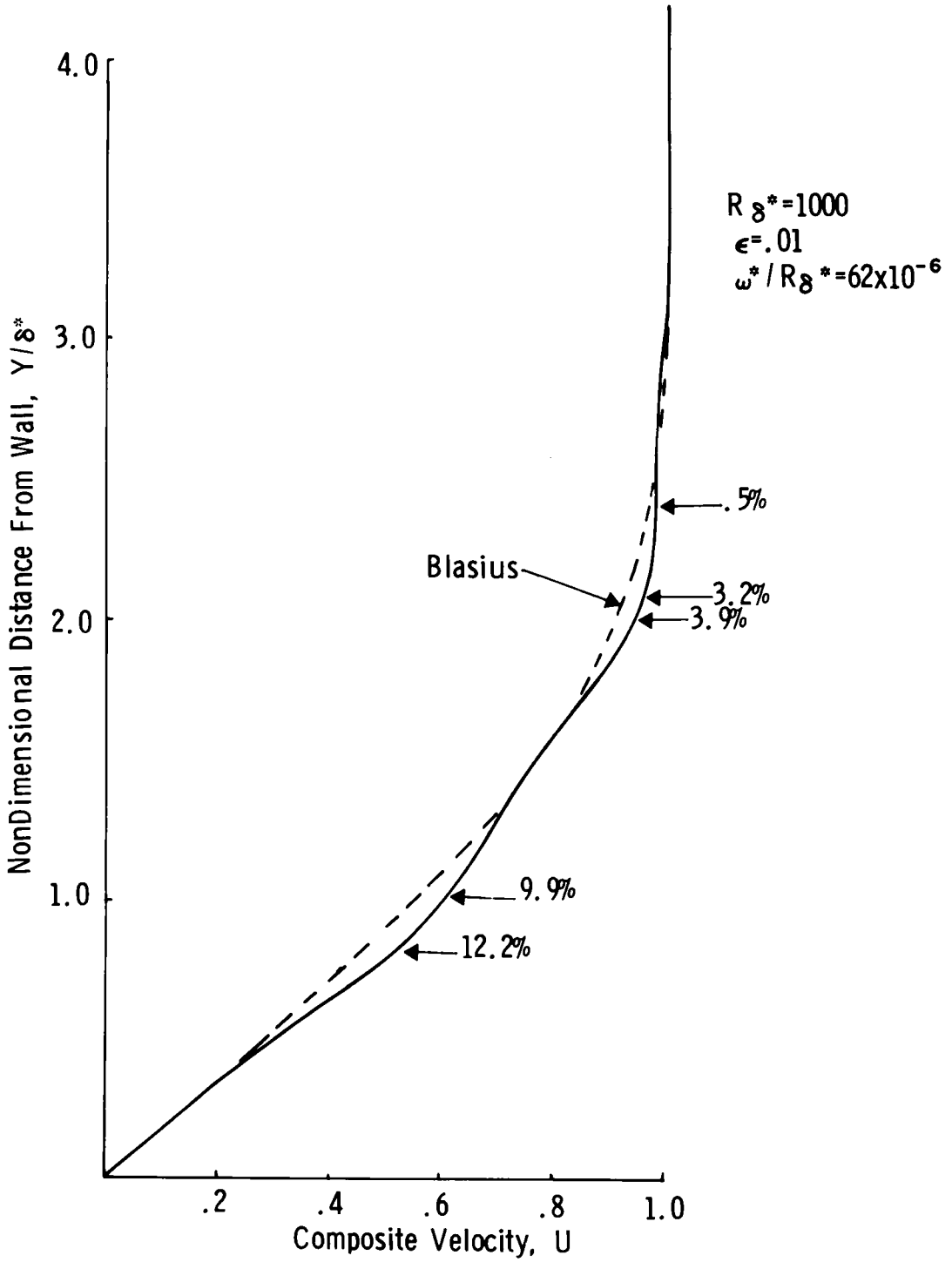

a. $R_{\delta *} = 850$

Figure 17. Composite velocity profiles for $\omega^*/R_{\delta *} = 62 \times 10^{-6}$ and $\varepsilon = .01$.



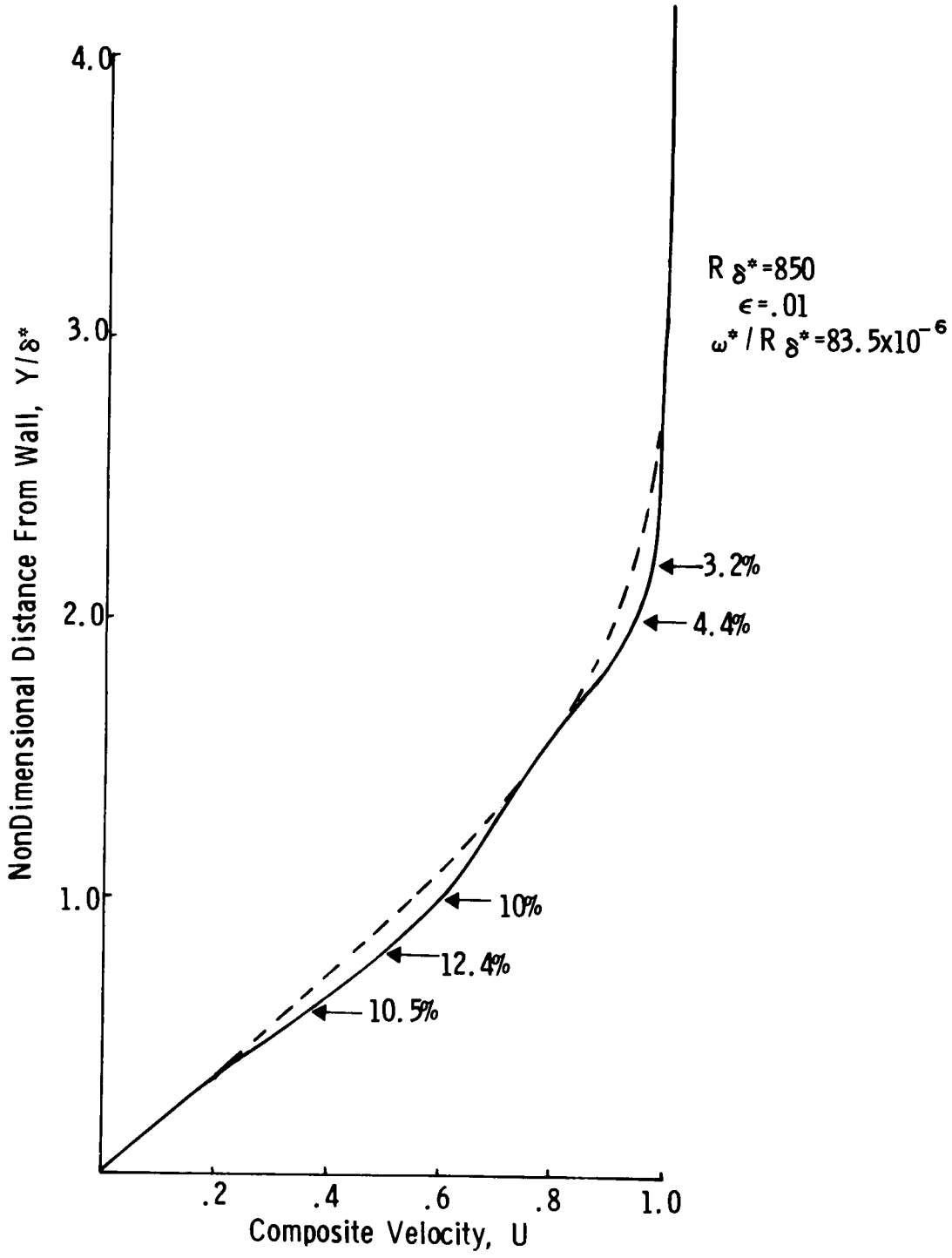

b. $R_{\delta *}$ = 900

Figure 17. (continued)



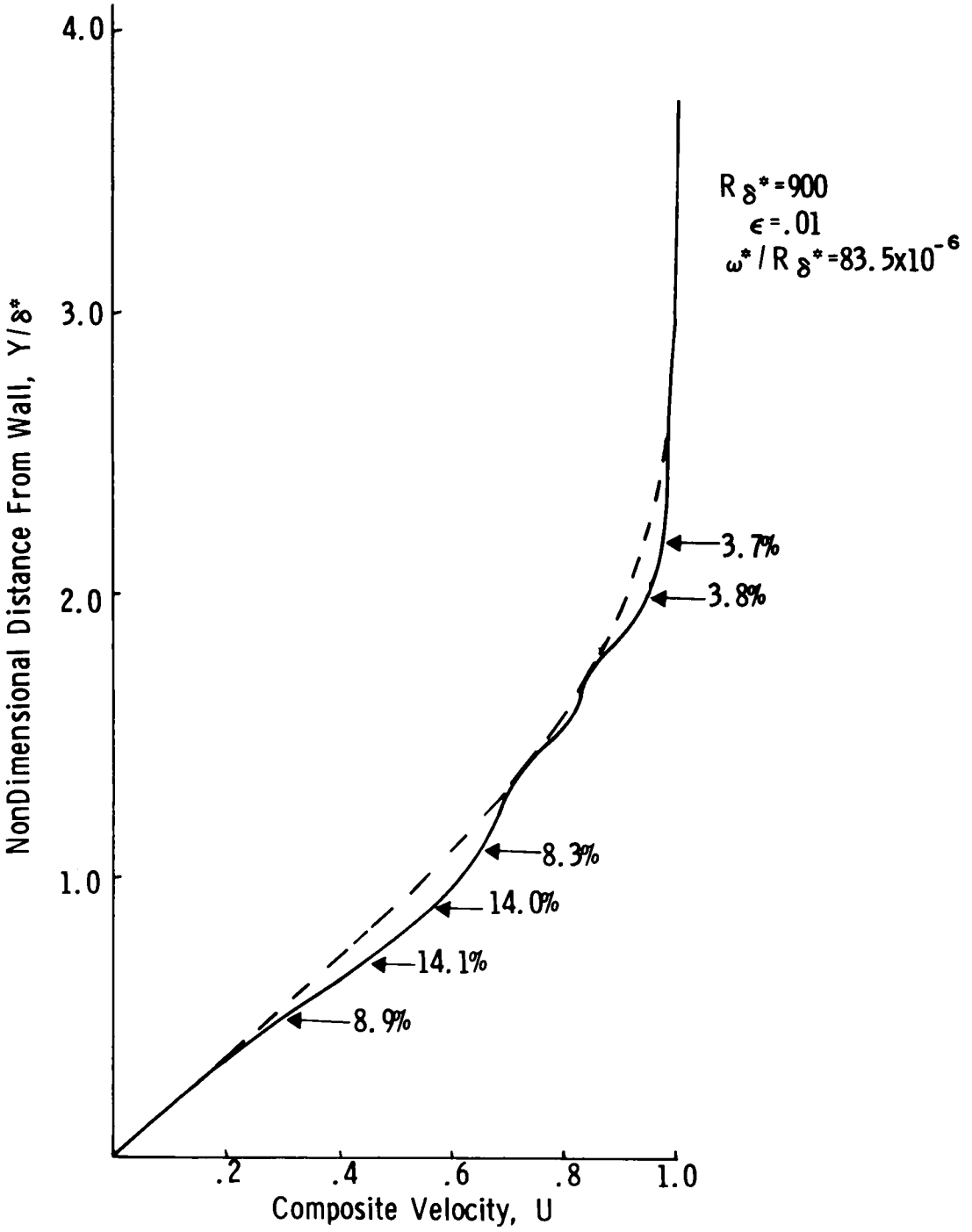

c. $R_{\delta *}$ = 1000

Figure 17. (continued)



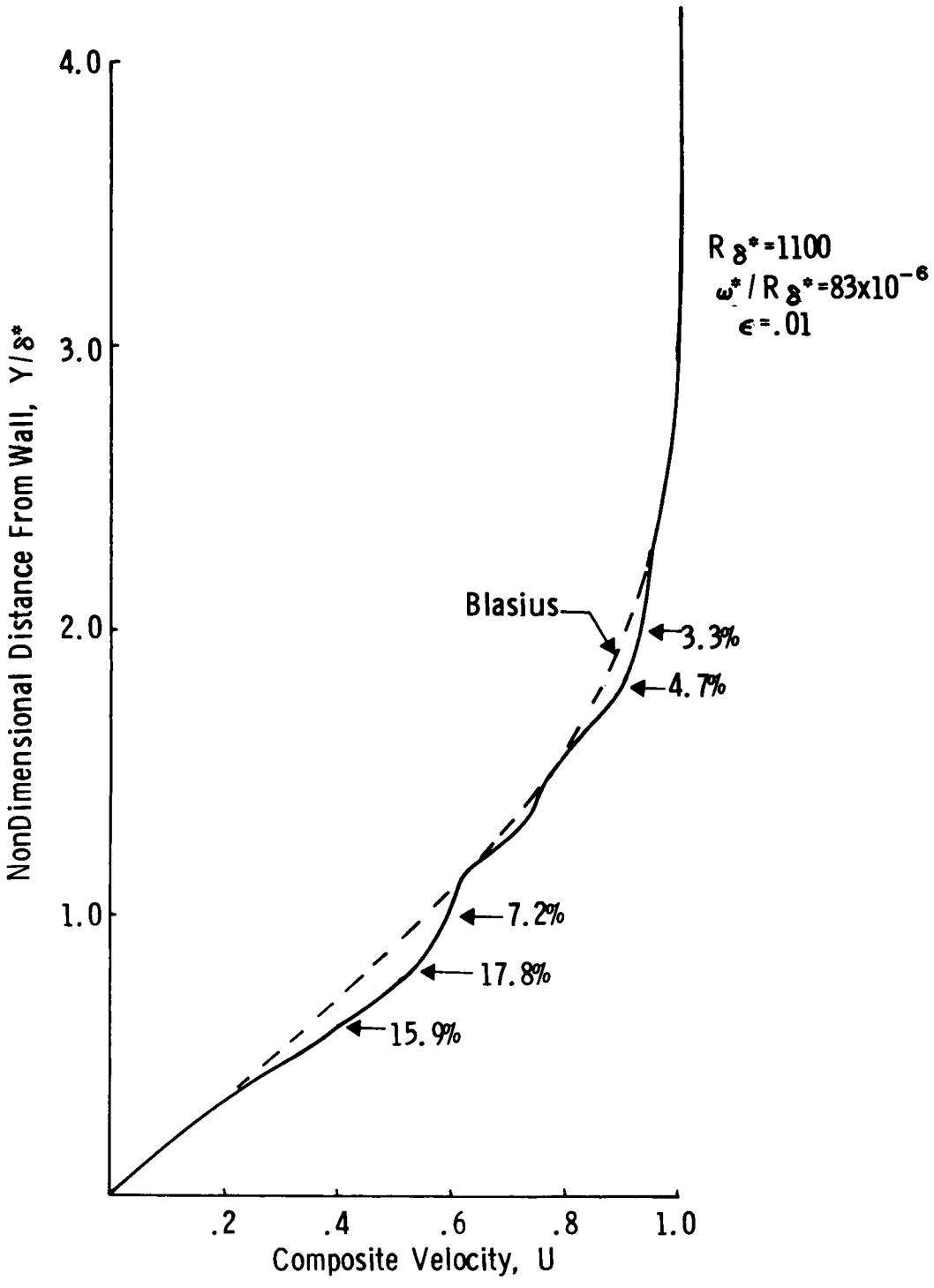

a. $R_{\delta *} = 850$

Figure 18. Composite velocity profiles for $\omega^*/R_{\delta *} = 83.5 \times 10^{-6}$ and $\epsilon = .01$.



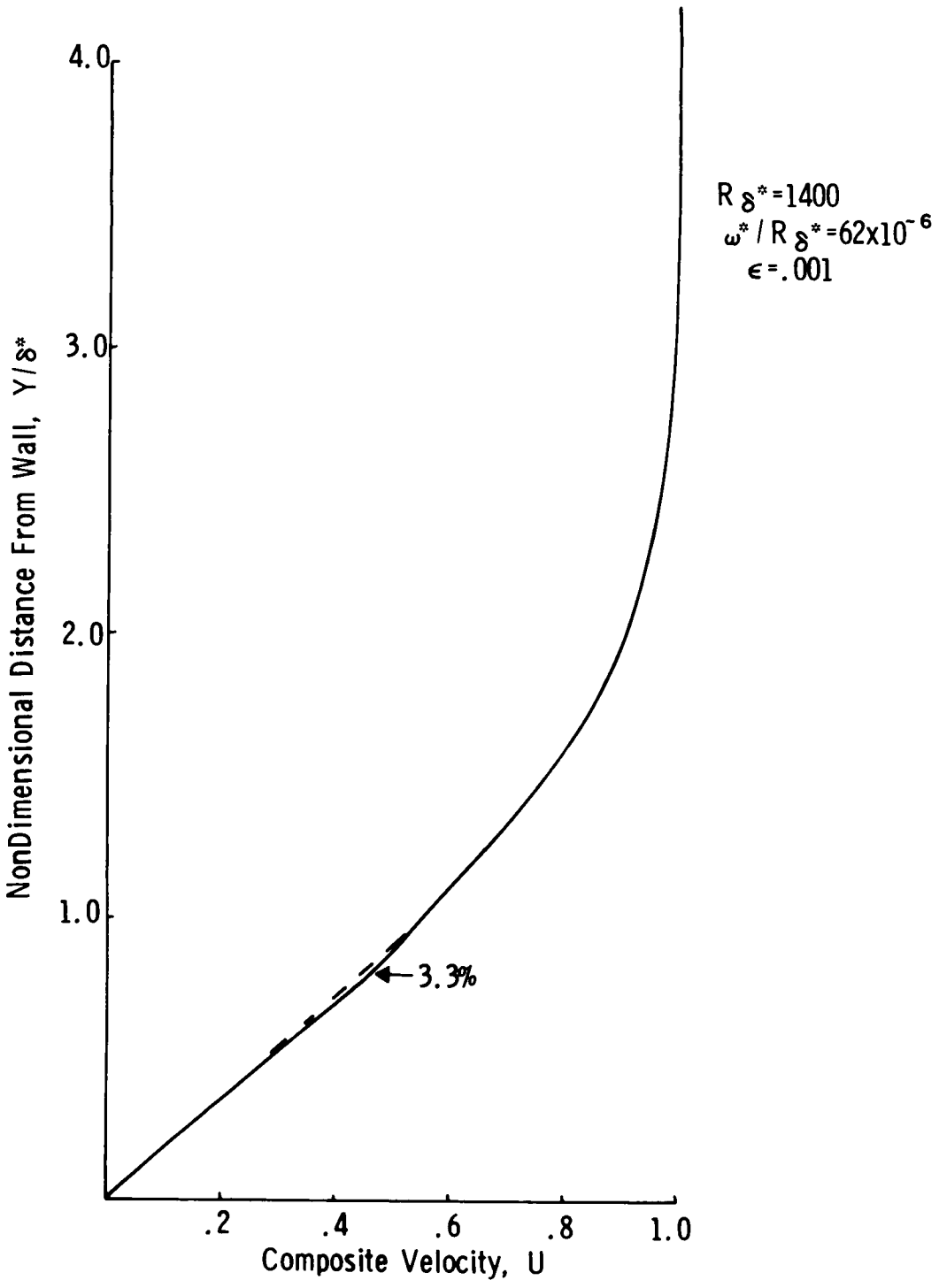

b. $R_{\delta*}$ = 900

Figure 18. (continued)



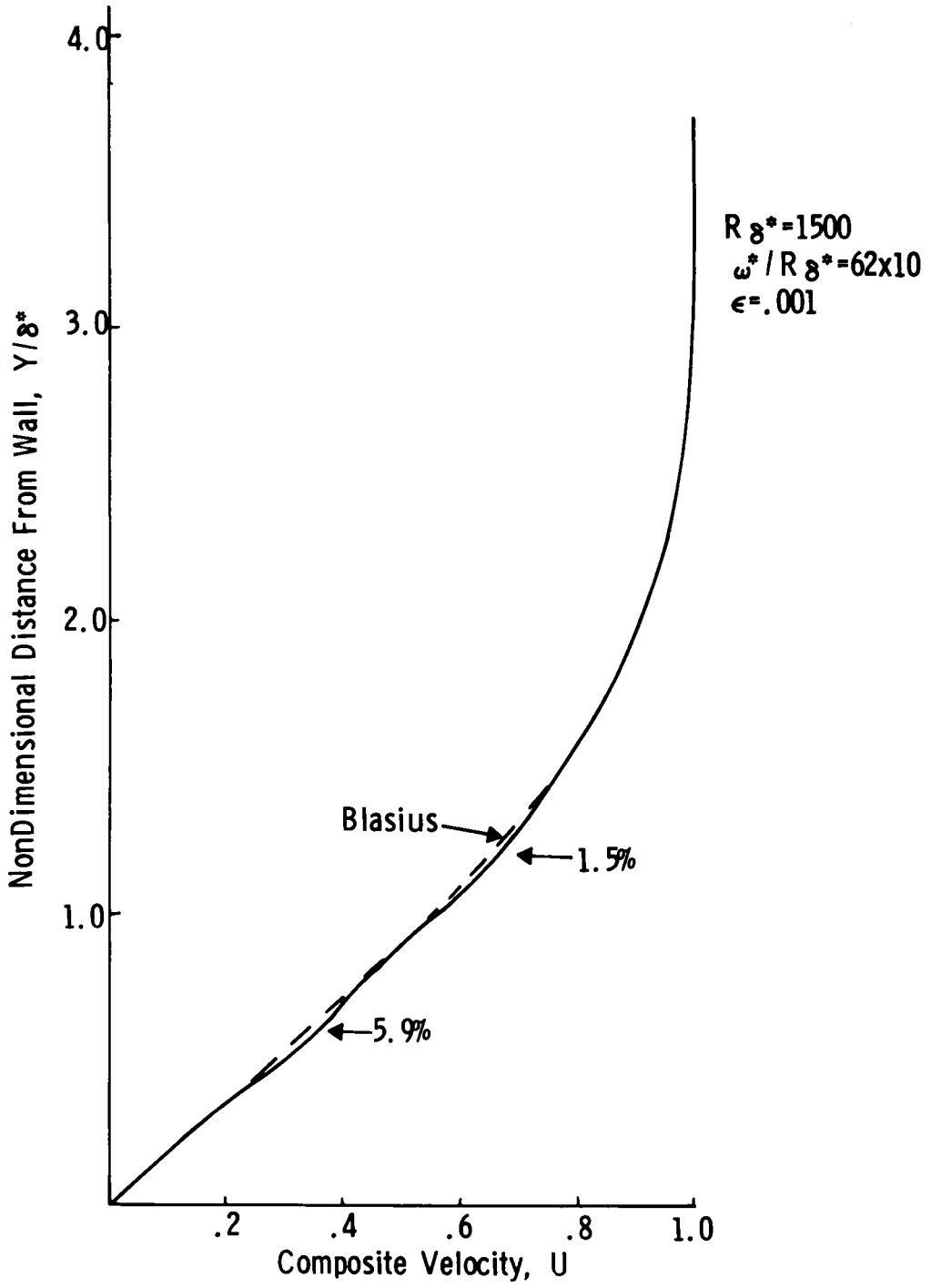

c. $R_{\delta *}$ = 1100

Figure 18. (continued)



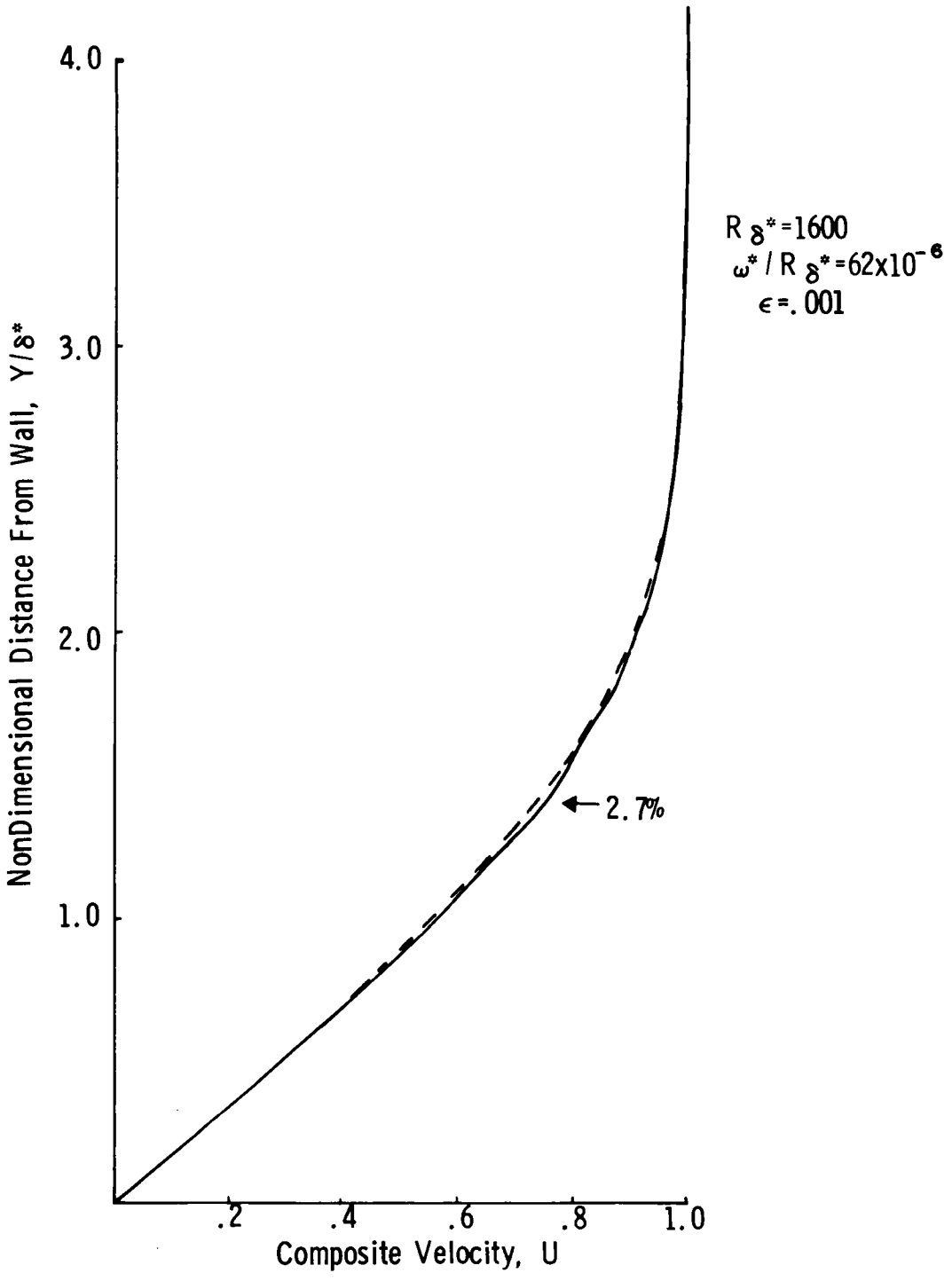

a. $R_{\delta *} = 1400$

Figure 19. Composite velocity profiles for $\omega^*/R_{\delta *} = 62 \times 10^{-6}$ and $\varepsilon = .001$.



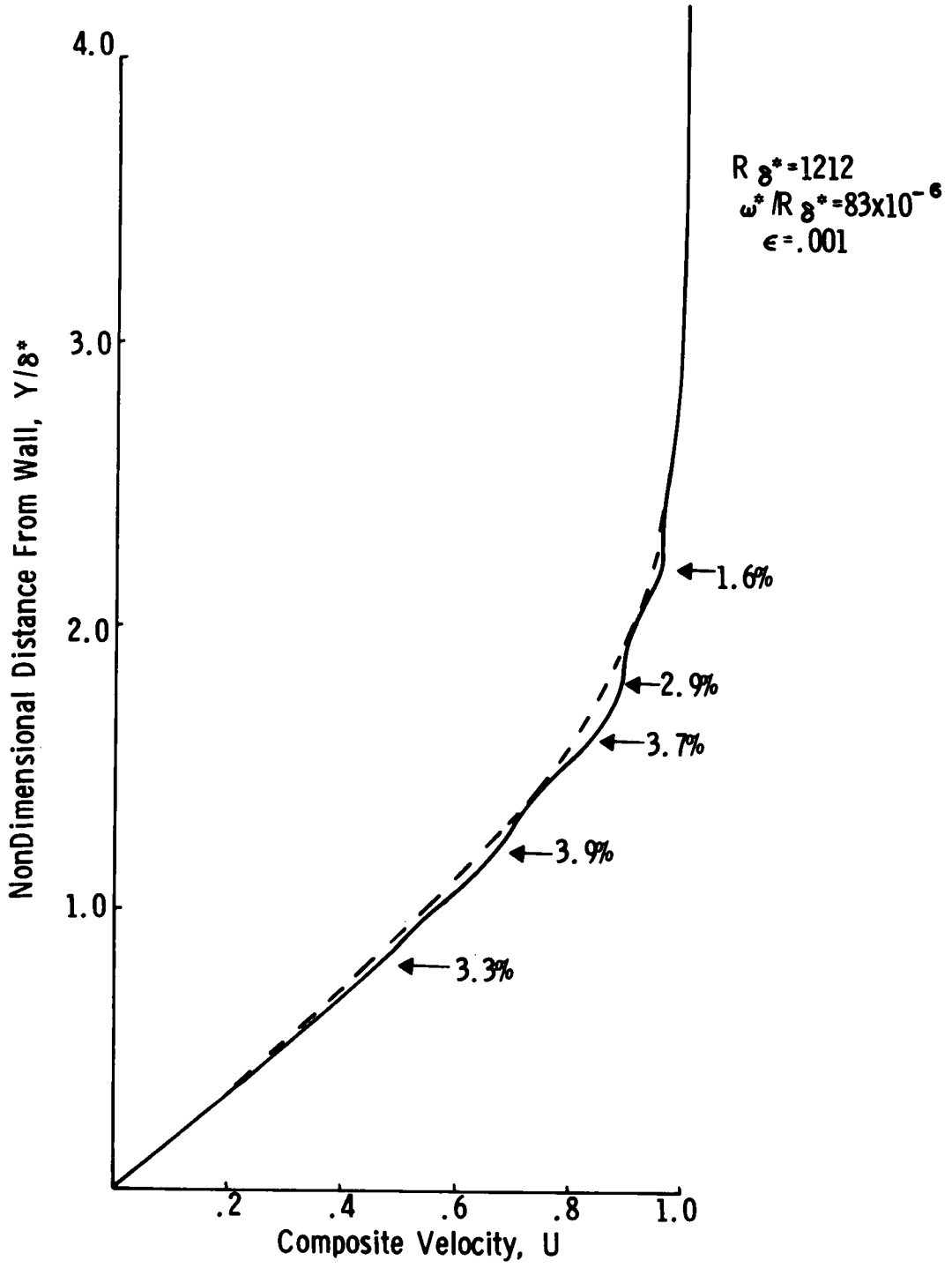

b. $R_{\delta^*}$ = 1500

Figure 19. (continued)



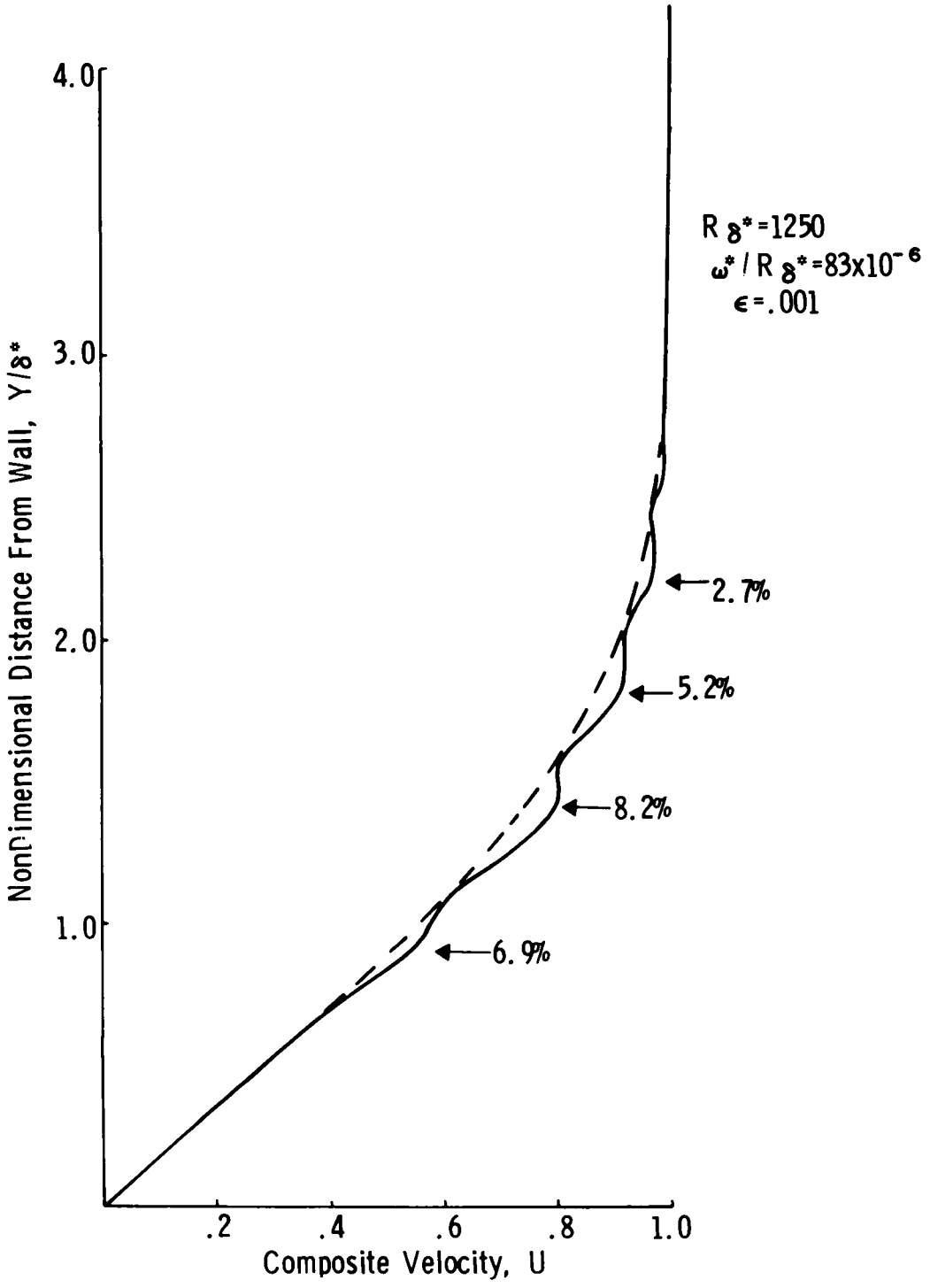

c. $R_{\delta *}$ = 1600

Figure 19. (continued)



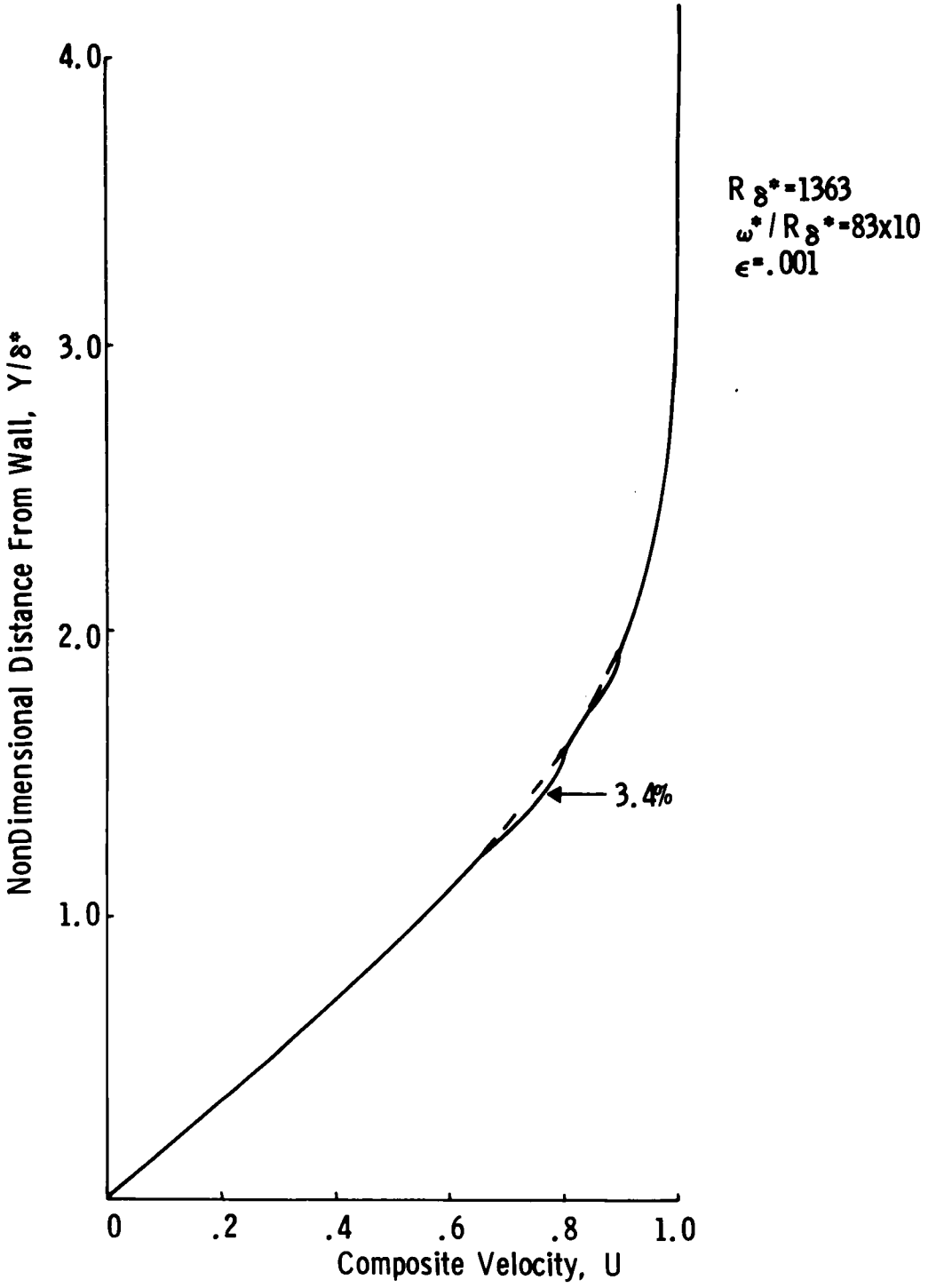

a. $R_{\delta *} = 1212$

Figure 20. Composite velocity profiles for $\omega^*/R_{\delta *} = 83.5 \times 10^{-6}$ and $\varepsilon = .001$.




b. $R_{\delta *}$ = 1250

Figure 20. (continued)




c. $R_{\delta*}$ = 1363

Figure 20. (continued)

## APPENDIX B

## THE PARALLEL FLOW APPROXIMATION

In the classical treatment of hydrodynamic stability, the perturbation equation (Eqn. (5)) subject to homogeneous boundary conditions is reduced to a separable form by removing the x dependence from the coefficients of the operator $L(x,y)$ (see Eqn. (8)). The parallel flow assumption is employed for this purpose as it requires that $v^{(0)}(x,y) = 0$, $\partial/\partial x = 0$, and $u^{(0)}(x,y) = u(y)$. It is in essence a restricted "local" approximation. Under the parallel flow assumption $L(x,y)\,\tilde{\psi} = 0$ gives

$$\left\{ i\alpha \left[ u - R^{-1} (D^2 - \alpha^2) \right] (D^2 - \alpha^2) - i\alpha D^2 u - i\lambda (D^2 - \alpha^2) \right\} \tilde{\phi}(y) = 0 \qquad \text{(B-1)}$$

where

$$\tilde{\psi} = \phi(y) e^{i\alpha x}, \text{ and } D = \partial/\partial y.$$

The first investigator to consider the implication of the nonparallelness of a real boundary layer flow was Reid (31). He obtained a model nonparallel flow equation by consideration of the asymptotic suction profile where $u(y) = 1 - e^{-y}$ and $v = -1/R$. In this case $L\tilde{\phi}$ takes the form

$$\left\{ \left[ i\alpha\, u^{(0)} - R^{-1}\, D - R^{-1}\, (D^2-\alpha^2) \right] (D^2-\alpha^2) - \alpha D^2\, u - i\lambda\, (D^2-\alpha^2) \right\} \tilde{\phi} = 0 \qquad \text{(B-2)}$$

Equation (B-2) is exact only for the asymptotic suction profile and has not been employed for a general nonparallel flow.

It has not been until relatively recently that a deliberate analysis of the case of nonparallel flow has been attempted. Barry and Ross (25) propose a model which accounts for boundary layer growth. They perform an order of magnitude analysis based upon the Prandtl boundary layer assumptions to obtain

$$\left\{ \left[ i\alpha u + v\, D - R^{-1}\, (D^2-\alpha^2) \right] (D^2-\alpha^2) - i\alpha D^2 u - (D^2 v) D - i\lambda\, (D^2-\alpha^2) \right\} \tilde{\phi} = 0 \qquad \text{(B-3)}$$

where v is the transverse velocity component and u and v and their derivatives are evaluated locally. Their results demonstrated a marked improvement in agreement with experiment, especially at the lower Reynolds numbers, for the case of the Blasius profile.

Wazzen, et al. (32) have extended the approach of Barry and Ross (25) to include all the terms of the operator $L(x,y)$. The zeroth order velocity components and their derivatives are evaluated "locally," as in Eqn. (8). They determined the change in the critical Reynolds number, $R_{\delta^* c}$

for the Falkner-Skan family of profiles caused by inclusion of various combinations of the additional terms. Their results for the smallest values of $R_{\delta *}$ for which amplification of any wave is possible, show variations of the order of 10% between the various approximations. The particular approximations they studied consisted of addition of terms to Eqn. (B-1); these are addition of the v terms only (Eqn. (B-2)), addition of the term $\partial^2 u/\partial x \partial y$ only, and the complete linearized equation, Eqn. (8).

There is a second group of investigators who propose to correct the parallel flow solutions by employing various expansion techniques. Ling and Reynolds (28) propose an expansion in powers of 1/R with the zeroth order being Eqn. (B-1). Subsequent orders provide the nonparallel correction. The major departure from formulation (25) is in the importance of the transverse velocity terms. Barry and Ross (25) argue that $V \sim 0(R^{-1})$ for the boundary layer and must be retained with the terms $R^{-1} \nabla^4 \tilde{\phi}$. Ling and Reynolds (28) observe that the viscous terms near the critical layer (i.e., where $u = \lambda/\alpha$) are $0(R^{1/3})$, while the terms $v \nabla^2 \tilde{\phi} \sim 0(1)$. Therefore, these latter terms may be safely neglected. The results of Ling and Reynolds are within 1% of the parallel flow results for the Blasius profile, whereas those of Barry and Ross differ on the order of 10% in the same range.

Gaster (33) employs a similar approach to that of Ling and Reynolds (28) but has included changes in the vertical structure of the disturbance. His formulation includes an iteration procedure to compute the nonparallel correction term. His calculation of the neutral curve of the Blasius profile is in general agreement with that of Barry and Ross (25).

The most rigorous approach of this second group is that taken by Bouthier (34,35). He implements the method of multiple scales in his perturbation analysis. Although this method differs formally from that used (28,33), his results are quite similar. However, he is able to identify three separate effects stemming from the nonparallelness of the flow. These are: (1) modifications of the velocity profile due to the nonparallel flow, (2) the effect of the transverse velocity, and (3) growth of the velocity profile with increasing distance downstream.

Thus, there are a number of results utilizing various types of formulation. In general, they indicate that some correction for the nonparallelness of boundary layer flow should be made to stability calculations at the lower Reynolds numbers. Because the easiest to implement in a temporal formulation is that of Wazzen, et al. (32), the fully linearized equation was adopted for the initial computations. However, it was found that for $R_{\delta^*} > 600$ no difference

was obtained in the solutions (a result verified by all of the above), whereas a savings in computer was obtained without them. Therefore, the forced solutions were computed using the operator given by Eqn. (8a) with no loss of generality.

## APPENDIX C

## THE ORTHOGONALITY RELATION

Consider a general, nonhermitian operator, $O$, defined on a space, S. The adjoint operator, $\hat{O}$, is related to $O$ through the generalized Green's theorem:

$$\int_S (g^* \, Of - f \, \hat{O}^* \, g^*) dS$$

$$= \int_\Gamma \nabla P \, ds = \int_\Gamma \vec{n} \cdot \vec{P} \, d\Gamma \qquad \text{(C-1)}$$

where P is the concomitant of $O$ and $\hat{O}$, $\Gamma$ is the boundary of S and where f and g are defined in S. Following the definition of the adjoint problem, $Of = 0$ and $\hat{O}g = 0$ and g satisfies the adjoint form of the boundary conditions and $\vec{n} \cdot \vec{P} = 0$. The above may be reduced to the inner product form

$$\langle g, \, Of \rangle - \langle \hat{O}g, f \rangle = 0 \qquad \text{(C-2)}$$

(For a more detailed discussion of nonhermitian operators, see Morse and Feshbach (36).)

We have written the general Orr-Sommerfeld operator of Eqn. (8) in the form

$$L \, \overset{\gamma}{\phi}_n - i \, \lambda_n \, \nabla^2 \, \overset{\gamma}{\phi}_n = 0 \qquad \text{(C-3a)}$$

and from Reference (37, p. 121), its adjoint is

$$\hat{L}\,\tilde{\chi}_m + i\,\mu_m^*\,\nabla^2\,\tilde{\chi}_m = 0 \qquad \text{(C-3b)}$$

where it is assumed that $\lambda_n \neq \mu_n$ when $n \neq m$. Further, it is assumed that the spectrum of $L$ is infinite but discrete and single valued. If we note that the generator operator $L(x,y)$ is comprised of two separate linear operators and take Eqn. (C-2) as the definition of the adjoint property a relation between the eigenvalues, $\lambda_n$ of $L$ and the eigenvalues, $\mu_m^*$ of $L$ may be obtained.

Formation of the inner product of Eqn. (C-3a) with $\tilde{\chi}_m$ and Eqn. (C-3b) with $\tilde{\phi}_m$ and subtraction of the conjugates of inner products of Eqn. (C-3b) from Eqn. (C-3a) yields, after some manipulation

$$\langle \tilde{\chi}_m,\, L\tilde{\phi}_n \rangle - \langle \hat{L}\,\tilde{\chi}_m,\, \tilde{\phi}_n \rangle + (i\mu_m)\,\langle \nabla^2\,\tilde{\chi}_m,\, \tilde{\phi}_n \rangle - i\,\lambda_n\,\langle \tilde{\chi}_m,\, \nabla^2\,\tilde{\phi}_n \rangle = 0 \qquad \text{(C-4)}$$

Using the definition of the adjoint property of Eqn. (C-2), Eqn. (C-4) reduces to

$$(\mu_m - \lambda_n)\,\langle \tilde{\chi}_m,\, \nabla^2\,\tilde{\phi}_n \rangle = 0 \qquad \text{(C-4b)}$$

where the self-adjoint property of the Laplacian operator has been used. Clearly, if $n \neq m$,

$$\langle \tilde{\chi}_m,\, \nabla^2\,\tilde{\phi}_n \rangle = 0 \qquad \text{(C-5)}$$

as $\lambda_n \neq \mu_m$ by assumption. This is the orthogonality relation

for the binormal system formed by $\{\tilde{\psi}_m\}$ and $\{\tilde{\chi}_m\}$.

If m = n, then Eqn. (C-4b) becomes

$$(\mu_n - \lambda_n) < \tilde{\chi}_n, \nabla^2 \tilde{\phi}_n > = 0$$

It must be shown that the inner product is not zero in this case. To do this we form the inner product of Eqn. (C-3a) with $\tilde{\chi}_n$ and Eqn. (C-3b) with $\tilde{\phi}_n$, add the conjugates of the inner products of Eqn. (C-3b) to Eqn. (C-3a) and obtain after some manipulation

$$< \tilde{\chi}_n, L\tilde{\phi}_n > + < \hat{\hat{L}}\chi_n, \tilde{\phi}_n > - i (\mu_n + \lambda_n) < \tilde{\chi}_n, \nabla^2 \tilde{\phi}_n > = 0$$

Suppose $< \tilde{\chi}_n, \nabla^2 \tilde{\phi} > = 0$. Then

$$< \tilde{\chi}_n, L \tilde{\phi}_n > + < \hat{L} \hat{\chi}_n, \tilde{\phi} > = 0$$

which violates the definition of the adjoint operator given by Eqn. (C-2). Thus, when n = m $< \tilde{\chi}_n, \nabla^2 \phi_n > \neq 0$. A similar result is obtained if $\mu_n = - \lambda_n$. Therefore, the condition

$$(\mu_n - \lambda_n) < \tilde{\chi}_n, \nabla^2 \tilde{\phi}_n > = 0$$

requires that

$$\mu_n = \lambda_n \qquad \text{(C-6)}$$

as the inner product is non-zero. That is, the eigenvalues of the adjoint conjugate operator are the same as those of the original operator. This is a significant development and is discussed at some length by Reid (31). A detailed discussion

of the adjoint operator, $\hat{L}$, is given in Appendix D.

The results of this appendix are used in obtaining the expansion coefficients, $C_j$ of $\phi^{(H)}$. Equation (12) shows the final expression for the $C_j$ containing the inner product of Eqn. (C-5).

## APPENDIX D

## SPECIAL PROPERTIES OF THE CHEBYSHEV EXPANSION

The shifted Chebyshev polynomials of the first kind, $T_n^*$, are defined as an interval 0,1 as

$$T_n^*(y) = \frac{n}{2} \sum_{m=0}^{\left[n/2\right]_I} (-1)^m \frac{(n-m-1)!}{m!(n-2m)!} (4y-2)^{n-2m}, n > 0$$

$$= 1, \; n = 0$$

where $\left[x\right]_I$ indicates the closest integer, I, such that $I \leq x$. The Chebyshev polynomials are orthogonal with weight $(y - y^2)^{-1/2}$ and form a complete set over the interval $\left[0,1\right]$.

Part I: The Derivatives

A piecewise continuous function, f, may be approximated in the interval $y \in \left[0,1\right]$ by an expansion in shifted Chebyshev polynomials of the first kind

$$f(y) = \sum a_n T_n^*(y)$$

where the coefficients $a_n$ have the form

$$a_n = \int_0^1 \langle f, T_n^* \rangle \Big/ \sqrt{y^2 - y^2} \; dy$$

Unfortunately, derivatives of f are not directly obtainable as the $d T_n^*/dy$ have no expression solely in terms of Chebyshev polynomials. Therefore, after Fox (18) and Fox

and Parker (19), an expansion of the form

$$\frac{d^m f}{dy^m} = f^{(m)} = \sum a_n^{(m)} T_n^*(y)$$

can be taken for the $m^{th}$ derivative of f. The difficulty, then, is to obtain a relation between the coefficients $a_n^{(m)}$ and $a_n$. This is accomplished by using identities involving the Chebyshev polynomials (18,19), in particular

$$T_n^* = \frac{1}{4} \frac{d}{dy} \left[ \frac{\gamma_n T_{n+1}^*}{n+1} - \frac{\Gamma_{n-2} T_{n-1}^*}{n-1} \right]$$

$\gamma_n = \Gamma_n = 0$, $n < 0$; $\gamma_o = 2$, $\Gamma_o = 1$, $\gamma_n = \Gamma_n = 1$, $n > 0$.

The expansion for df/dy and f show the $n^{th}$ coefficients to be related as

$$\frac{1}{4} a_n^{(1)} \left[ \frac{\gamma_n T_{n+1}^*}{n+1} - \frac{\Gamma_{n-2} T_{n-1}^*}{n-1} \right] = a_n T_n^* \qquad \text{(D-1)}$$

Equation (D-1) shows the relation between the $a_n^{(1)}$ and $a_n$ for n = N to be

$$4N\, a_n = a_{N-1}^{(1)}$$

n = N-1

$$4(N-1)\, a_{N-1} = a_{N-2}^{(1)} - a_N^{(1)}$$

and so on. This leads to the general expression

$$\gamma_n a_n^{(1)} = 4 \sum_{i=n+1,2}^{N} i\, a_i \qquad \text{(D-2)}$$

where the n+1,2 means i = n+1, n+3, n+5, etc. Similarly, an expression for $a_n^{(2)}$, $a_n^{(3)}$, and $a_n^{(4)}$ may be obtained by using Eqns. (D-1) and (D-2), and after some manipulation, we have:

$$\gamma_n \, a_n^{(2)} = 4^2 \sum_{i=n+2,2}^{N} i \, a_i \sum_{j=N+1}^{i-1} j$$

$$\gamma_n \, a_n^{(3)} = 4^3 \sum_{i=n+3,2}^{N} i \, a_i \sum_{j=n+2,2}^{i-1} j \sum_{k=n+1,2}^{j-1} k$$

$$\gamma_n \, a_n^{(4)} = 4^4 \sum_{i=n+4,2}^{N} i \, a_i \sum_{j=n+3,2}^{i-1} j \sum_{k=n+1,2}^{j-1} k \sum_{\ell=n+1,2}^{k-1} \ell \qquad \text{(D-3)}$$

Equations (D-3) are not convenient expressions with which to work, whereas Eqn. (D-2) does have a simple form. Simplifications to Eqns. (D-3) may be obtained by finding expressions for the sums appearing as coefficients of $a_i$ in terms of i and n. After progressively lengthy algebra, the results for the first four derivatives may be written as

$$\gamma_n \, a_n^{(j)} \sum_{i=N+j,2} \ell_j(i,n) \, a_i \qquad \text{(D-4)}$$

where

$$\ell_1(i) = 4i$$

$$\ell_2(i,n) = 4i^2 \, (i^2-n^2)$$

$$\ell_3(i,n) = 2i \left[(i^2-n^2) - 2(i^2+n^2) + 1\right]$$

$$\ell_4(i,n) = \frac{2}{3}\, i \left[ i^2(i^2-4) - 3i^4\, n^4 + 3i^2\, n^4 - n^2\, (n^2-4)^2 \right]$$

Part II: The Product Terms

The convection terms give rise to products of the expansion coefficients and the stream function expansion. Therefore, we are interested in expansions of the form

$$\sum_{n=0}^{N} a_n\, T_n^* \sum_{m=0}^{M} b_m\, T_m^* = \frac{1}{2} \sum^{N} \sum^{M} a_n b_m \left( T^*_{m+n} - T^*_{|m-n|} \right)$$

where the idenity

$$T_n^*\, T_m^* = \frac{1}{2} \left( T^*_{m+n} - T^*_{|m-n|} \right)$$

has been used. An alternate form is

$$\sum^{N} a_n T_n^* \sum^{M} b_m T_m^* = \frac{1}{2} \sum^{N} \sum_{-M}^{M} a_n\, b_{|m|}\, \gamma_{|m+n|}\, T^*_{|m+n|} \qquad \text{(D-5)}$$

where

$$\gamma_{|m+n|} = \begin{cases} 1, & |m+n| \neq 0 \\ 2, & |m+n| = 0 \end{cases}$$

Finally, if the compact form of Eqn. (D-5) is rearranged slightly it can be put in the more compact form

$$\frac{1}{2} \sum_{n=0}^{N+M} e_n\, T_n^*$$

where

$$e_n = \frac{1}{\gamma_n} \sum_{\substack{|j| \le N \\ |n-j| \le m}} \gamma_{|j|}\, a_{|j|}\gamma_{|i-j|}\, b_{|i-j|}$$

Introduce the notation $\overline{a_j} = \gamma_{|j|}\, a_{|j|}$. The product relation is

$$\sum_{n=0}^{N} a_n T_n^* \sum_{m=0}^{M} b_m T_m^* = \frac{1}{2} \sum_{n=0}^{M+N} \frac{1}{\gamma_n} \left( \sum_{|m| \le N} \bar{a}_m\, \bar{b}_{n-m} \right) T_n^* \qquad \text{(D-6)}$$

There are other product terms arising from products involving derivatives of the stream function. These may be expressed in a form similar to Eqn. (D-6) as

$$\sum_{n=0}^{N} a_n^{(j)}\, T_n^* \sum_{m=0}^{M} b_m\, T_m^*$$

$$= \frac{1}{2} \sum_{n=0}^{M+N-j} \frac{1}{\gamma_n} \left[ \sum_{k=j}^{N} a_k \left( \sum_{\substack{|m| \le k-j,2 \\ |n-m| \le M}} \bar{\gamma}_m \bar{b}_{n-m} \ell_j(k,m) \right) \right] T_n^* \qquad \text{(D-7)}$$

Equations (D-4), (D-6), and (D-7) are used in the reduction of Eqn. (16) in Section II.

An example of the notation of Eqn. (D-7) for N = 2, M = 1, and j = 1 is given below

$$\frac{1}{2} \sum_{n=0}^{2+l-1} \frac{1}{\gamma_n} \left[ \sum_{k=1}^{2} a_k \sum_{\substack{|m| \leq k-1,2 \\ |n-m| \leq 1}} \bar{\gamma}_m \bar{b}_{n-m} \ell_1(k_1) \right] T_n^*$$

$$= \frac{1}{2} \left\{ \frac{1}{\gamma_o} \left[ a_1 \, (\gamma_o \, \bar{b}_o \, \ell_1(1_1)) + a_2 \, (\gamma_1 \, \bar{b}_1 \, \ell_1 \, (2_1)) \right] T_o^* \right.$$

$$+ \frac{1}{\gamma_1} \left[ a_1 \, (\gamma_o \, \bar{b}_1 \, \ell_1 \, (1)) + a_2 \, (\gamma_1 \, \bar{b}_o \, \ell_1 \, (2_1)) \right] T_1^*$$

$$\left. + \frac{1}{\gamma_2} \left[ a_1 \, (0) + a_2 \, (\gamma_1 \, \bar{b}_1 \, \ell_1 \, (2_1)) \right] T_2^* \right\} .$$

## APPENDIX E

## THE ADJOINT OPERATOR

The adjoint generalized Orr-Sommerfeld operator may be written as (see Morse and Feshbach (36), and Collitaz (37))

$$\hat{L} = -\left( \frac{\partial}{\partial x} \nabla^2 \psi_y^{(0)} - \frac{\partial}{\partial y} \nabla^2 \psi_x^{(0)} \right) - \nabla^2 \psi_x^{(0)} \frac{\partial}{\partial y}$$

$$+ \nabla^2 \psi_y^{(0)} \frac{\partial}{\partial x} - R^{-1} \nabla^4 + i \mu^* \nabla^2 \qquad \text{(E-1)}$$

Simplifications can be made to Eqn. (E-1) by expansion of the terms and use of the first order continuity equation, i.e.

$$u_x^{(0)} + v_y^{(0)} = 0$$

In order to simplify the following let $\psi_y^{(0)} = u(x,y)$, $-\psi_x^{(0)} = v(x,y)$, and $\nabla^2 \psi^{(0)} = z^{(0)}$. The first term in brackets gives

$$\frac{\partial}{\partial x} \nabla^2 u^{(0)} + \frac{\partial}{\partial x} \nabla^2 v^{(0)} = \left( \nabla^2 u^{(0)} \frac{\partial}{\partial x} + \nabla^2 v^{(0)} \frac{\partial}{\partial y} \right)$$

$$+ \left( u^{(0)} \frac{\partial}{\partial x} + v^{(0)} \frac{\partial}{\partial y} \right) \nabla^2$$

$$+ 2 \left[ u_x^{(0)} \frac{\partial^2}{\partial x^2} + \left( u_y^{(0)} + v_x^{(0)} \right) \frac{\partial^2}{\partial x \partial y} \right.$$

$$\left. + v_y^{(0)} \frac{\partial^2}{\partial x^2} \right] + \nabla^2 \left( u_x^{(0)} + v_y^{(0)} \right) \qquad \text{(E-2)}$$

The last term in Eqn. (E-2) is clearly zero. The terms involving the vorticity may be expanded as

$$- \frac{\partial}{\partial y} z_x^{(0)} + \frac{\partial}{\partial x} z_y^{(0)} = -z_{xy}^{(0)} + z_{xy}^{(0)} - z_x^{(0)} \frac{\partial}{\partial y} + z_y^{(0)} \frac{\partial}{\partial x}$$

$$= \left( -u_{xy}^{(0)} + v_{xx} \right) \frac{\partial}{\partial y} + \left( u_{yy}^{(0)} - v_{xy}^{(0)} \right) \frac{\partial}{\partial x} \qquad \text{(E-3)}$$

Combining Eqns. (E-1), (E-2), and (E-3) yields, after some rearrangement

$$\hat{L} = - \left( u^{(0)} \frac{\partial}{\partial x} + v^{(0)} \frac{\partial}{\partial y} \right) \nabla^2$$

$$- 2 \left[ u_x^{(0)} \frac{\partial^2}{\partial y^2} + \hat{z} \frac{\partial^2}{\partial x \partial y} + v_y^{(0)} \frac{\partial^2}{\partial y^2} \right]$$

$$- R^{-1} \nabla^4 + i \mu^* \nabla^2$$

where $\hat{z}^{(0)} = u_y + v_x$ and where Eqn. (D-6) has been used. Equation (E-4) is used in Section II to obtain the adjoint conjugate stream function, $\tilde{\chi}^*$.

## APPENDIX F

## SOME PROPERTIES OF THE GENERAL ALGEBRAIC EIGENVALUE PROBLEM: det $(A-\lambda B) = 0$

Consider the two general complex square matrices of order N, A, and B. These matrices may be written as row vectors, the elements of which are column vectors, i.e.

$$A = \left[A_1, A_2, \ldots, A_n\right], \qquad B = \left[B_1, B_2, \ldots, B_n\right]$$

The general eigenvalue problem,

$$\det\left[A - \lambda B\right] = 0 \tag{F-1}$$

may then be written as

$$\det\left[(A_1 - \lambda B_1), (A_2 - \lambda B_2), \ldots (A_n - \lambda B_n)\right] = 0 \tag{F-2}$$

The characteristic equation corresponding to Eqn. (F-2) may be found with the aid of the following theorem from determinant theory.

TH: If each element of the $k^{th}$ column of a matrix A is expressed as the sum of m terms, then det A may be expressed as the sum of m determinants, the elements of which have their $k^{th}$ columns made up of the first, second, ..., $m^{th}$ terms of the corresponding elements of the $k^{th}$ column of A. All other elements are unchanged throughout.

Examination of Eqn. (F-2) shows that each of the columns of

the matrix $A - \lambda B$ is made up of a sum of terms, the $k^{th}$ being $(A_k - \lambda B_k)$. Thus, repeated application of the theorem will lead to the characteristic equation. Thus,

$$\det\left[A - \lambda B\right] = \det\left[(A_1 - \lambda B_1), (A_2 - \lambda B_2), \ldots, (A_n - \lambda B_n)\right] = \det\left[A_1, (A_2 - \lambda B_2), \ldots, (A_n - \lambda B_n)\right] - \det\left[B_1, (A_2 - \lambda B_2), \ldots (A_n - \lambda B_n)\right]$$

and

$$= \det\left[A_1, A_2, (A_3 - \lambda B_3), \ldots, (A_n - \lambda B_n)\right] - \lambda\left\{\det\left[A_1, B_2, (A_3 - \lambda B_3), \ldots, (A_n - \lambda B_n)\right] + \det\left[B_1, A_2, (A_3 - \lambda B_3), \ldots, (A_n - \lambda B_n)\right]\right\} + \lambda^2\left\{\det\left[B_1, B_2, (A_3 - \lambda B_3), \ldots, (A_n - \lambda B_n)\right]\right\}$$

Clearly, the expansion has the form

$$(-\lambda)^N \det B + (-\lambda)^{N-1} \sum_{j}^{J_1} M_{AB_j}^{(1)} + \ldots + (-\lambda) \sum_{j}^{J_{N-1}} M_{AB_j}^{(N-1)} + \det A = 0 \qquad \text{(F-3)}$$

where the $M_{AB}^{(i)}$ are determinants formed by successively replacing columns of the B matrix by the corresponding columns of the A matrix i at a time, e.g.

$$M_{AB_1}^{(1)} = A_1, B_2, B_3, \ldots, B_n \;,\; M_{AB_2}^{(1)} = B_1, A_2, B_3, \ldots, B_n \;, \text{ etc.}$$

and similarly,

$$M^{(2)}_{AB_1} = \left[A_1, A_2, B_3, \ldots, B_n\right], \quad M^{(2)}_{AB_2} = \left[B_1, A_2, A_3, \ldots B_n\right], \text{etc.}$$

The summations indicate that the replacements extend over all possible combinations of the columns of A and B, taken i and N-i at a time, respectively, hence the $i^{th}$ summation gives

$$J_i = N! \Big/ \left[i!\ (N-i)!\right] \tag{F-4}$$

terms. In the case where B is the idenity matrix, Eqn. (F-3) reduces to a polynomial in $\lambda$ whose coefficients are the principal minors of A.

The determinants of the $M^{i}_{AB_j}$ may be expanded in terms of their minors. If this expansion is restricted to the minors of A, then

$$\det M^{N-i}_{AB_j} = \sum_{k} {}_{B}C^{N-i,j}_{k}\ M^{N-i}_{A_j}$$

where the ${}_{B}C^{N-i,j}_{k}$ are products of the elements of B and the $M_{A_j}$ are the minors of A of order N-i which are contained in $M^{N-i}_{AB_j}$. Equation (F-3) now has the form

$$(-\lambda)^N \det B + (-\lambda)^{N-1} \left[ \sum_{j=1}^{J_1} \sum_{k=1}^{K_1} {}_{B}C^{1,j}_{k}\ M^{N-1}_{A_k} \right]$$

$$+ (-\lambda)^{N-2} \left[ \sum_{j=1}^{J_2} \sum_{k=1}^{K_2} {}_{B}C^{2,j}_{k}\ M^{N-2}_{A_k} \right] + \ldots$$

$$+ \sum_{k=1}^{k_n} M^{1}_{A_k} = 0 \tag{F-5}$$

where the $K_i$ have the same form as the $J_i$ (Eqn. (F-4)). A similar expansion can be written in the minors of B with ${}_AC_k^{i,j}$ as the products of the elements of A.

Equation (F-5) shows that if the rank of A, $r_A$, is such that $r_A < N$ while the rank of B, $r_B$, is N, then there are $N - r_A$ nonzero roots. However, if $r_B < N$ while $r_A = N$, there are only $N - r_B$ solutions. If $r_A$, $r_B < N$ simultaneously then $r_A + r_B \geq N$ for solutions to exist, $N - r_A$ of which are zero.

In the case when det $B \neq 0$, the eigenvalue problem of Eqn. (F-1) may be reduced to standard form by multiplying by $B^{-1}$, i.e. det $(B^{-1} A - \lambda I) = 0$. However, when B is singular as in Eqn. (24) the expansion procedure of Eqn. (F-5) can be utilized to obtain solutions. If $r_B < N$, then Eqn. (F-5) becomes

$$(-\lambda)^{N-r_B}\left[\sum_{j}^{J_{N-r_B}}\ \sum_{k}^{K_{N-r_B}} {}_BC_j^{N-r_B,j}\ M_{A_k}^{r_B}\right]$$

$$+\ (-\lambda)^{N-r_B-1}\left[\sum_{j}^{J_{N-r_B-1}}\ \sum_{k}^{K_{N-r_B-1}} {}_BC_j^{n-r_B-1}\ M_{A_k}^{r_B-1}\right] \qquad \text{(F-6)}$$

$$+\ \ldots\ +\ \sum_{k=1}^{K_N} M_{A_k}^{(1)} = 0$$

As it is simplest to expand the determinant of a triangular matrix by minors, apply suitable transforms to A and B such that

$$\begin{pmatrix} a & a & a & \dots & a \\ o & a & a & \dots & a \\ o & o & a & \dots & a \\ o & o & a & \dots & . \\ \circ & & & & \circ \\ . & & & & a \end{pmatrix} \qquad \begin{pmatrix} b & b & b & \dots & b \\ b & b & b & \dots & b \\ \circ & & & & \\ b & b & b & b & . \; b \\ o & . & \circ & . & \circ \; . \\ o & . & \circ & . & . \; o \end{pmatrix}$$

where the rows of $j > r_B$ will be zero in the B matrix reflecting its singular nature. Now, if these matrices and the associated det $(M^i_{AB_j})$ are expanded in minors about the rows N, N-1, ..., $N-r_B$ only the elements on the diagonal of A are involved. At this point it will be observed that only the last $N-r_B$ rows need to be triangularized. Thus, for example

$$\det A = \sum_{j}^{J^{N-r_B}} \prod_{i=N-r_{B+1}}^{N} a_{ii} \; M^{N-r_B}_{A_j}$$

where $\prod_{i=1}^{I} d_i = d_1 \cdot d_2 \cdot \ldots \cdot d_I$. It is observed that the expansion of $M^i_{AB_j}$, which contain columns to the right of the $r_B$th column will yield a zero element on the diagonal. Thus, the expansion in minors of det $M^i_{AB_j}$ about the N, N-1, ..., $N-r_B$ rows will be zero, the nonzero terms will all have the form

$$\prod_{k=N-r_{B+1}}^{N} a_{ii} \det \bar{M}^{i}_{AB_j}$$

where the $\bar{M}^{i}_{AB_j}$ have the order $N-r_B$. Thus, Eqn. (F-5) has the form

$$\prod_{k=N-r_{B+1}}^{N} a_{ii} \left\{ (-\lambda)^M \sum_{j=1}^{\bar{J}_1} \sum_{k=1}^{\bar{K}_1} {}_B C_j^{m,j} \, M_{A_k}^{r_B} + \ldots + \sum_{k=1}^{\bar{K}_N} M_{A_k}^{1} \right\} = 0 \qquad \text{(F-6)}$$

where $\bar{J}_i$, $\bar{K}_i = M! \Big/ \left[ i!(M-i)! \right]$. If the transforms are such that the $a_{ii}$, $N-r_{B+1} \leq i \leq N$ are nonzero, the terms in the braces must be zero. These terms can be seen to be a characteristic equation corresponding to an eigenvalue problem of the form of Eqn. (F-1) and order $N-r_B$

$$\det (\bar{A} - \lambda \bar{B}) = 0 \qquad \text{(F-7)}$$

where $\bar{A}$ and $\bar{B}$ are order $N-r_B$. Thus, Eqn. (F-1) has been reduced to an equivalent eigenvalue problem of order $N-r_B$. If $\bar{B}$ is nonsingular, Eqn. (F-7) may be reduced to standard form by multiplying by $\bar{B}^{-1}$. If $\bar{B}$ is singular, the above process may be repeated until a nonsingular $\bar{B}$ is obtained or until $r_B = 0$.

The previous development is essentially the algorithm of Gary and Helgason (20) discussed in Section II.

Their procedure may be briefly outlined as follows:

1. Diagonalize B by total pivoting, i.e., apply elementary transforms P and Q such that

$$\tilde{B} = PBQ = \beta_{ij} \qquad \beta_{ii} \neq 0,\ \beta_{ij} = 0,\ i \neq j$$

$$\tilde{A} = PAQ$$

2. Determine the rank of B, $r_B$ if $r_B = N$, stop.

3. Apply the column transform T which reduces the last $N-r_B$ rows of A to triangular form

$$\hat{A} = \tilde{A}T$$

$$\hat{B} = \tilde{B}T$$

4. The equivalent matrices are now located in the upper $r_B \times r_B$ submatrix of $\hat{A}$ and $\hat{B}$, respectively.

5. Reduce the order of A and B to $r_B$ by deleting the last $N-r_B$ rows and columns and go to step 1.

# VITA

John Addison Benek was born in Pittsburgh, Pennsylvania on October 5, 1945. He attended elementary schools in and around McDonald, Pennsylvania and was graduated from Fort Cherry High School in 1963. In September, 1963 he entered the University of Cincinnati, and in June, 1968, he received a Bachelor of Science degree in Aerospace Engineering. In the fall of 1968, he accepted a research assistantship at the University of Tennessee. In March, 1970 he received a Masters degree and has been employed by ARO, Inc. since November, 1969. Since this time he has worked to meet the requirements of the Doctor of Philosophy degree in Aerospace Engineering at the University of Tennessee. He received this latter degree in December, 1975.